MOLECULAR MECHANISMS OF CENTRIOLE ASSEMBLY

by

Tiffany McLamarrah

_____

A Dissertation Submitted to the Faculty of the

DEPARTMENT OF CELLULAR AND MOLECULAR MEDICINE

In Partial Fulfillment of the Requirements

For the Degree of

DOCTOR OF PHILOSOPHY

In the Graduate College

THE UNIVERSITY OF ARIZONA

2016

THE UNIVERSITY OF ARIZONA
GRADUATE COLLEGE

As members of the Dissertation Committee, we certify that we have read the dissertation prepared by Tiffany McLamarrah, titled Molecular Mechanisms of Centriole Assembly and recommend that it be accepted as fulfilling the dissertation requirement for the Degree of Doctor of Philosophy.

_____ Date: July 29, 2016
Gregory Rogers

_____ Date: July 29, 2016
Joyce Schroeder

_____ Date: July 29, 2016
Tom Doetschman

_____ Date: July 29, 2016
Ghassan Mouneimne

Final approval and acceptance of this dissertation is contingent upon the candidate's submission of the final copies of the dissertation to the Graduate College.

I hereby certify that I have read this dissertation prepared under my direction and recommend that it be accepted as fulfilling the dissertation requirement.

_____ Date: July 29, 2016
Dissertation Director: Gregory Rogers

STATEMENT BY AUTHOR

This dissertation has been submitted in partial fulfillment of the requirements for an advanced degree at the University of Arizona and is deposited in the University Library to be made available to borrowers under rules of the Library.

Brief quotations from this dissertation are allowable without special permission, provided that an accurate acknowledgement of the source is made. Requests for permission for extended quotation from or reproduction of this manuscript in whole or in part may be granted by the head of the major department or the Dean of the Graduate College when in his or her judgment the proposed use of the material is in the interests of scholarship. In all other instances, however, permission must be obtained from the author.

SIGNED: _____ Date: July 29, 2016

Tiffany McLamarrah

ACKNOWLEDGMENTS

I would like to thank my advisor Dr. Gregory Rogers for his mentorship and scientific support.

I would also like to thank the members of my committee: Dr. Joyce Schroeder, Dr. Tom Doetschman, Dr. Ghassan Mouneimne, and past members Dr. Christina Laukaitis and Dr. Patricia Thompson for their intellectual guidance.

Many thanks to the other members of the Rogers lab for their companionship and help with experiments.

Finally, a special thanks to my family and friends.

TABLE OF CONTENTS

PRIOR PUBLICATIONS

- Tiffany A. McLamarrah, Daniel W. Buster, Brian J. Galletta, Cody J. Boese, Natalie A. Hollingsworth, Naser M. Rusan and **Gregory C. Rogers**. Plk4 phosphorylation of Ana2 inhibits their association and suppresses centriole duplication. Submitted to J. Cell Biol.

- Brian J. Galletta, Carey J. Fagerstrom, Todd A. Schoborg, Tiffany A. McLamarrah, John M. Ryniawec, Daniel W. Buster, Kevin C. Slep, **Gregory C. Rogers**, Nasser M. Rusan. A detailed centrosome interactome provides insight into organelle assembly and human disease. In press at Nat. Comm.

- Klebba, J.E., Buster, D.W., McLamarrah, T.A., Rusan, N.M. and **Rogers, G.C.** An autoinhibition and relief mechanism for Polo-like kinase 4. Proc Natl Acad Sci U S A. 2015 Feb 17; 112(7) :E657-66

LIST OF FIGURES

LIST OF TABLES

ABSTRACT

Chromosomal Instability (CIN) occurs in over 90% of all sporadic tumors and manifests as whole chromosome loss or gain, gene deletions, amplifications, inversion, and translocations. CIN is not only a hallmark of cancer but promotes tumorigenesis. CIN is caused by errors during mitosis and one major CIN-promoting mechanism is centrosome over-duplication (amplification); another cancer hallmark. Centrosome amplification causes abnormal mitotic spindle assembly, directly promoting chromosome mis-segration with consequent aneuploidy and other forms of CIN. Central to controlling centrosome numbers and function are the Polo kinases, including Polo-like kinase 4 (Plk4). Plk4 is a component of centrosomes and recognized as the master-regulator of centrosome function and duplication.

Plk4 is a mitotic kinase whose levels increase throughout S-phase and G2 to peak in mitosis. During late mitosis, Plk4 localizes to a spot on parent centrioles, licensing this single site for future daughter centriole assembly. Plk4 activity initiates the hierarchial recruiment of two conserved essential centriole proteins: Ana2, followed by the cartwheel protein Sas6. By analysis in a yeast-2-hybrid screen, we identified several novel interactions of centriole proteins, including the interaction of Ana2 and Plk4. Plk4 phosphorylates Ana2 to both positively and negatively regulate centriole duplication. Our preliminary data suggests that Plk4 recruits Ana2 by phosphorylating a protein on the outer centriole surface, generating a phospho-landing platform, and that this Plk4 target is Sas4 (CPAP in humans). Notably, the Sas4 pattern on centrioles is complex, forming both a ring and an asymmetric spot during mitotic progression. Like Sas4, Ana2 is a Plk4 substrate, and when mixed with purified Ana2, Sas4 stimulates Ana2 hyperphosphorylation in vitro. Thus, Plk4 influences centriole assembly on multiple platforms.

CHAPTER ONE: BACKGROUND AND INTRODUCTION

1.1 Overview

Centrosome research has gained momentum over the past several years as high interest in the field has produced keen insights into the assembly of this important organelle. Centrosome assembly is an excellent model for organelle biogenesis, as the components required to form a functional centrosome range from 5 proteins (in *C. elegans*)[1] to 11 in Drosophila (unpublished data) and more in humans[2]. These tiny organelles are comprised of two centrioles surrounded by pericentriolar material forming the microtubule organizing center (MTOC) of the cell[3,4,5]. As the replicating elements of centrosomes, centriole duplication must remain tightly regulated so each cell has the correct number of centrosomes during cell division.[6] Too many, or too few centrosomes can lead to multipolar or monopolar spindle formation during mitosis, a process that often leads to chromosomal instability (CIN) and tumor formation.[7,8,9] Defects in centriole assembly result in a variety of human diseases, including primary microcephaly, dwarfism, ciliopathies and tumorigenesis.[10–13, 2] Importantly, overduplication of centrioles is thought to be one cause of primary microcephaly, as 7 out of 13 known genes causing microcephaly encode for centriole proteins.[2]

Centrioles are barrel-shaped structures, consisting of a proximal and distal end, the distal end. The centriole duplication cycle is tightly coupled to the cell cycle, with each centriole duplicating once and only once per cell cycle.[4,6,14] The two centrioles comprising the centrosome are composed of an older or "mother" centriole and a newly forming procentriole or "daughter" centriole which forms orthogonally off the proximal end of the mother centriole.[15,16] The mother centriole is characterized by distal appendages, which aid in anchoring the centriole

to the cell membrane of quiescent cells forming the basal bodies and eliciting ciliogenesis.[17] Cycling cells however, maintain their centriole population to aid in forming the bipolar spindle during mitosis and ensuring faithful segregation of chromosomes and proper cytokinesis. The daughter centriole was originally thought to be templated by the mother, although recent research suggests the mother centriole simply serves as a scaffold for recruiting and concentrating necessary centriole components.[18,19] The first of these components visible in the newly forming daughter centriole is Sas-6, a protein which oligomerizes to form the centriolar cartwheel.[20] This nine-fold symmetrical structure emanates orthogonally off the mother centriole and serves as the basis for the nine-fold triplet (or doublet in Drosophila) microtubule structure of the newly forming daughter centriole.[21,22] Several other proteins are recruited to the site of the growing daughter centriole throughout the cell cycle.

Seminal research in C. elegans provided the first insight into the hierarchical recruitment of proteins to the centriole required for normal centriole biogenesis, beginning first with Spd-2 and the recruitment of the kinase Zyg-1. Zyg-1 is known to phosphorylate and recruit the coiled-coil protein Sas-6, which brings Sas-5 and finally Sas-4. These five proteins are integral to maintaining the fidelity of centriole duplication.[1] Further research into Drosophila and humans led to the discovery of Plk4, the apparent homolog of Zyg-1. Although little sequence homology is shared, these two proteins share many of the same functions in centriole biogenesis.[23] This has been true for many of the homologs of centriole proteins from C. elegans to humans; they often differ in sequence, but retain similar functions. Proteomics has led to the discovery of

Gene
Plk4
Sas4
Sas6
Rcd4
Ana1
Ana2
Ana3
Asterless
CP110
Cep97
Cep135

Table 1. *Drosophila* genes required for centriole assembly.

several conserved proteins necessary for centriole duplication in Drosophila. (Table 1) Many pathways in centriole biogenesis are conserved between Drosophila and human, allowing for Drosophila centriole assembly to be a perfect model system to study centriole biogenesis.

1.2 The centriole duplication cycle

Centriole duplication is tightly coupled to the cell cycle. The canonical centriole duplication cycle consists of a licensing event sometime towards the end of mitosis/early G1, followed by procentriole formation in the beginning of S-phase and elongation as S-phase progresses.

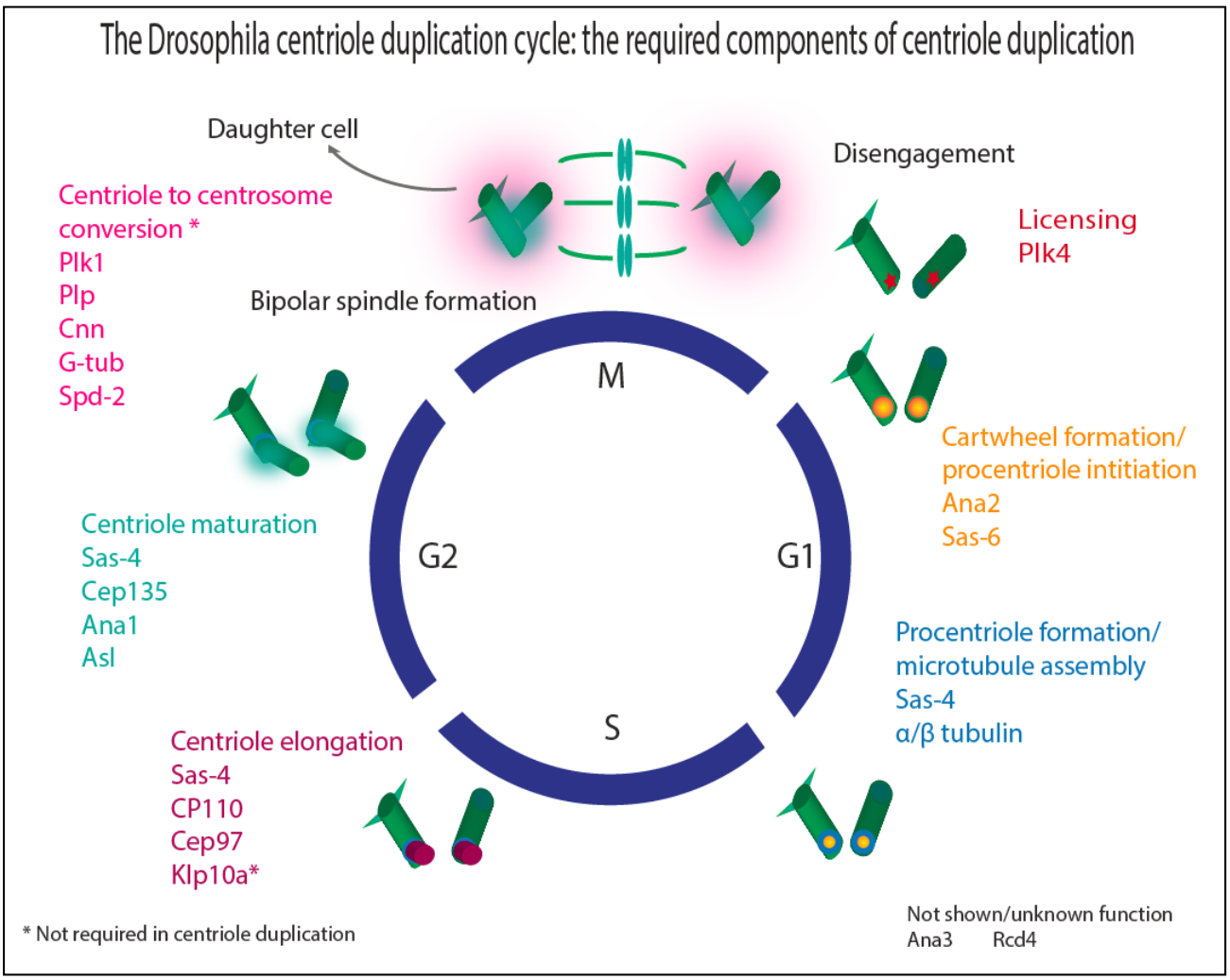

Figure 1: The centriole duplication cycle.

Centriole duplication begins in late mitosis/early G1 when centrioles disengage and are licensed to duplicate by the mitotic kinase Polo-like kinase 4 (Plk4). Plk4 phosphorylates Ana2/STIL and recruits it to the centriole. Phosphorylated Ana2/STIL recruits the cartwheel protein Sas-6. Ana2 and Sas-6 are recruited to the site of the growing daughter centriole in late mitosis in Drosophila, and at the G1/S transition in humans. Sas-4 next localizes to the centriole in early S-phase and begins to assemble the α/β tubulin dimers making up the centriolar wall. The capping proteins CP110 and Cep97 are recruited to the distal tips of the growing daughter centrioles in S-phase/G2, followed by, or concurrent with, the Cep135-Ana1/Cep295-Asl/Cep152 complex. Cep135 and Ana1 localize to the daughter centriole around the same time, near G2, followed by Asl at the G2/M transition. The PCM components Spd-2/Cep192, Cnn/Cep215, γ-tubulin, and Plp/Pericentrin are recruited to the mother centriole during mitosis to form a fully mature functional centrosome capable of nucleating microtubules.

centriole acquire pericentriolar material and progresses throughout G2 until mitosis when the daughter centriole matures during centriole to centrosome conversion. At this point, the centrosome will be able to nucleate microtubules and direct the plane of cell division through formation of the bipolar spindle.[6,15,16,24] Drosophila provides a simple model for centriole duplication, and so we will focus on this system in centriole duplication with some data being provided from the human counterparts.

1.3 Procentriole formation

In human cells, centrosome replication begins at the onset of S-phase, at the G1/S transition. Procentriole nucleation is initiated orthogonally off the mother centriole, beginning with the

phosphorylation of STIL/Ana2 by Plk4 to recruit Sas-6. Plk4 localizes to the centriole through an interaction with both Cep192/Spd-2 and Cep152/Asl in human cells, however only Asl is required to bring Plk4 to the centriole in flies.[25–32] Plk4 interacts with Asl in 2 domains; through an association with the tandem polobox of Plk4 (PB1/2) and both the N and C-termini of Asl (AslA and AslC, resp). Asl-A primarily promotes Plk4 dimerization and facilitates its degradation, whereas Asl-C stabilizes Plk4 to promote centriole amplification.[32] Interestingly, Drosophila Ana2 and Sas6 appear to be recruited to the site of the newly forming procentriole near the end of mitosis, when Plk4 levels and activity is highest at the centriole.[33] At this time, Plk4 localizes asymmetrically to a single spot on the mother centriole, likely licensing this location to begin the next round of duplication.[34] More research is necessary to determine if Ana2 and Sas-6 localize to this Plk4-dense spot on the mother centriole do to a direct interaction between Plk4 and Ana2 (as is shown in human cells with Plk4 and STIL in G1/S-phase)[35–39]or if Plk4 first primes a spot on the mother centriole through phosphorylation, which then helps recruit Ana2 and Sas-6, determining the first nucleating event in procentriole formation.

1.4 The cartwheel

The centriolar cartwheel was first described in 1960, by Gibbons and Grimstone in trychonympha basal bodies.[40] The cartwheel localizes to the proximal end of the daughter centriole in humans, and is formed of 9 radially distributed spokes emanating from a central hub region, which is now known to be formed from 9 Sas-6 dimers. (Figure 2A, B)[41] Sas-6 establishes the 9-fold symmetry of the centriole, organizing a tube-like centriole precursor. Sas-6 is composed of an N-terminal globular domain, a coiled-coil domain (CCD) and a C-terminal domain. The CCD is essential for the homodimerization of the protein, which then oligomerizes at the N-terminus to form the central hub of the cartwheel. 9 Sas-6 dimers come together to form

the central hub, with the C-terminal ends emanating radially outward.[20,22,41] The fundamental building block of the cartwheel comprises two Sas-6 rings rather than one, stabilized intramolecularly by the Ana2 tetramer.[42] (Figure 2B, C) Making cartwheel assembly dependent on the co-assembly of two rings could dramatically reinforce the tendency to form a ninefold symmetric ring. In human cells, Sas-6 is first recruited to the lumen of the mother centriole which aids in templating the assembly of the Sas-6 cartwheel, before being redistributed to the site of daughter centriole assembly.[43] In human cells, the central cartwheel is removed from the centriole during mitosis, at which point centriolar STIL and Sas-6 is degraded.[44–46] This process differs in Drosophila, as Sas-6 and Ana2, and presumably the cartwheel, can be seen on the mother centriole throughout the cell cycle.[33] The central cartwheel greatly influences the 9-fold triplet microtubule assembly which occurs in the next stage of procentriole formation.[47]

1.5 Microtubule assembly

The centriole is composed of a barrel-like structure made from the nine-fold triplet microtubules (most often seen in animal cells, importantly, nine-fold doublet microtubules seen in Drosophila) arranged in a cylinder, a process that greatly depends on Sas-6, Sas-4/CPAP and Cep135 among others[47–52]. (Figure 2B, C) Sas-4 is first recruited to the growing daughter centriole at the beginning of S-phase,[53–55] to be followed by Cep135, Ana1/Cep295 and Asl/Cep152 during G2. (Figure 1, Figure 2C)[56] Sas-4 is critical for the recruitment and stabilization of the centriolar microtubules; designated A, B, and C tubules, with the A tubule being "attached" to the central cartwheel through an interaction with Bld10p/Cep135.[48,57] Bld10p/Cep135 constitutes the cartwheel-spoke tip, or pinhead region, and stabilizes the 9-fold symmetry of the centriole as it directly interacts with both Sas-6 at its C-terminal region, and microtubules and the centriolar

protein Sas-4/CPAP at its N-terminus. [48,57] (Figure 2C) Depletion of Cep135 can lead to centriole structures with differing numbers of microtubule triplets and shorter centrioles. The triplet MT numbers were originally thought to be assembled from a Sas-6 scaffold, but new research has shown the possibility of an interdependent relationship between the Sas-6 cartwheel and MTs to form the 9-fold structure because likely cartwheel-independent mechanisms operate in concert with the cartwheel to determine the nine-fold symmetric structure of centrioles.[47,57] Once the cartwheel is removed in human cells in mitosis, the stability of the centriole decreases. Another protein, Cep295/Ana1 is required to stabilize these cartwheel-less structures,[58] however, this process is unclear in Drosophila.

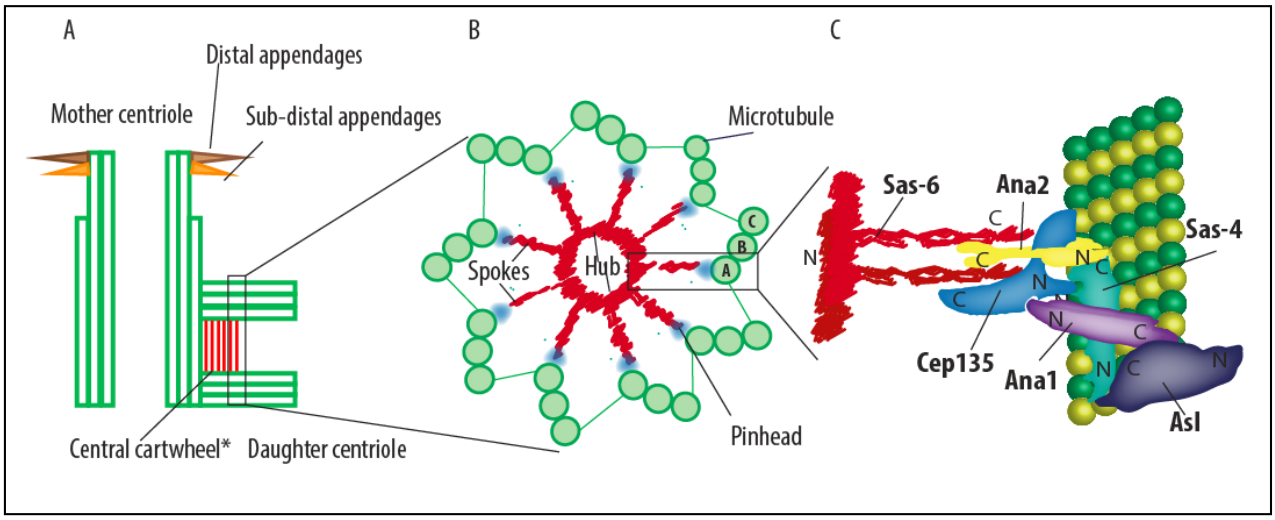

Figure 2. Centriole architecture.

A. The mother centriole is characterized by distal and sub-distal appendages, while the daughetr emanates at a right angle from the proximal end of the mother.The central cartwheel can be seen at the proximal end of the mother and daughter in Drosophila, and at the daughter in the humans. B. The cartwheel is characterized by 9 dimers of Sas-6 orgainzed radially to form a central hub and 9 radially oriented spokes. Sas-6 is attached to the A-tubule through an interaction with Cep135. C. Molecular architecture of the lumenal side of the centriolar wall reveals 2 Sas-6

homodimers stacked on top of each other stabilized by 4 Ana2 molecules (shown here as a homodimer). The C-terminus of Ana2 is phosphorylated and binds the CCD of Sas-6. Ana2-N-terminus interacts with the C terminus of Sas-4. Sas-4 C-terminus also interacts with the N-terminus of Cep135, while Sas-4 N-terminus interacts with both microtubules and Asl C-terminus. Ana1 connects Cep135 to Asl through a N-terminal interaction with Cep135 N-terminus and a C-terminal interaction with Asl C-terminus. Modified from [48]

1.6 Centriole elongation

After procentrioles are nucleated by the cartwheel and initial microtubule attachment, they begin elongating in S-phase through G2 and into the next cell cycle. A number of conserved molecules are involved in the regulation of centriole elongation. Sas-4/CPAP stabilizes the cartwheel structure and plays an important role in recruiting MTs to the cartwheel structure during centriole elongation. Overexpression of Sas-4/ CPAP has been shown to result in overly long centrioles which may fractionate as they become less stable.[51,52,59–61]

Several interactions are key to centriole elongation, many centering on interactions between Sas-4 and other essential centriole proteins. The interactions between Sas-4/CPAP and Ana2/STIL and Cep135 are integral to centriole elongation and stabilization.[48,62] Centrobin has been shown to interact with sas-4/CPAP and tubulin dimers at the daughter centriole and promote centriole elongation and stability.[50] In human cells, Cep120 and SPICE are also involved in regulating centriole elongation in concert with CPAP.[59] One regulator of centriole elongation in humans through its kinase activity is Plk2. Plk2 has been shown to phosphorylate CPAP at 2 key residues to promote centriole assembly and possible elongation.[60]

Centriole elongation is counteracted by the capping protein CP110 and its interacting proteins. CP110 localizes to the distal end of the centrioles and its depletion leads to overly long centrioles.[52,63] CP110 interacts with Cep97 and the kinesin-13 homolog Kif24/Klp10a. CP110, Cep97 and Klp10a localize to the centriole at some point during S/G2, although more work needs to be done in Drosophila to determine the order, and time of localization.[64,65] Kif24/ Klp10a is a microtubule-dependent motor protein that negatively regulates cilia formation by mediating recruitment of CP110 to mother centriole in cycling cells, leading to restrict nucleation of cilia at centrioles in human cells. Cep97 recruits CP110 to the centrosome and depletion of Cep97 also results in centriole elongation. Loss of Kif24/Klp10a leads to the disappearance of CP110 from mother centrioles but not from abnormally long centrioles. [64,65]

1.7 Centriole Maturation/Centriole to centrosome conversion

The acquisition of pericentriolar material (PCM) is a step in centriole assembly known as centrosome maturation, or more recently as centriole-to-centrosome conversion. The procentriole, or daughter centriole assembles from S to G2 and achieves the majority of its length during this time, however it is not yet competent to recruit PCM or duplicate in the next cell cycle.[4,56] Several proteins have been identified as key to generating a mature centriole competent to duplicate in the next stage of the cell cycle and recruit the PCM required for proper centrosome function. The sequential loading of Cep135, Ana1 and Asl occurs from late interphase to early mitosis to allow the daughter centriole to convert to a mother.[56] Drosophila embryos depleted of Ana1 failed to duplicate centrioles and localize Asl to daughter centrioles.[56,66,67] This led to a failure to accumulate Plp and gamma-tubulin, indicating a failure to recruit PCM. [66,67] The next step in centriole-to-centrosome conversion is characterized by the

acquisition of PCM proteins; namely the γ -Tubulin Ring Complex (required for nucleating MTs) γ-TuRC, Centrosomin (Cnn), Spindle defective protein-2 (Spd-2)/Cep192, Asterless (Asl)/Cep152 (not strictly a PCM protein), Sas-4/CPAP (not strictly a PCM protein) and Plp/Pericentrin. Recently, four independent studies examined PCM spatial organization using new techniques in microscopy to reveal the specific contribution and organization of centrosomal proteins required for centrosome maturation.[53,68–70] Together they showed that the PCM comprises two major domains with distinct molecular composition and architecture. PCM proteins are shown to be recruited exclusively to the mother centriole.[71] PCM proteins are organized in concentric toroids around mother centrioles in interphase and is organized in two major layers of proteins: (i) molecular fibers comprising the elongated coiled-coil proteins Plp/Pericentrin and Cep152/Asl have their C termini near the centriole wall and their N termini extending toward the periphery; and (ii) a PCM matrix comprising Cep215/Cnn, γ-tubulin, and Cep192/Spd- 2 molecules. (Figure 3) In G2/M, the PCM proximal layer is expanded through the formation of an outer matrix consisting of expansion of the PCM proximal layer of interphase cells during G2/M through the formation of an outer matrix of Cep215/Cnn, Pericentrin/Plp, and Cep192/Spd-2 molecules. γ TuRCs are embedded within the PCM and promote microtubule nucleation during mitosis. In Drosophila, PCM expansion does not contain the matrix associated portion of Plp, but expands the component of Plp associated with the centriole.[71] CPAP/Sas-4 localizes both to the centriole and the PCM in addition to the proximal region of the centriole

and plays a role in PCM recruitment independent of its role in centriole and plays a role in PCM recruitment independent of its role in centriole duplication.

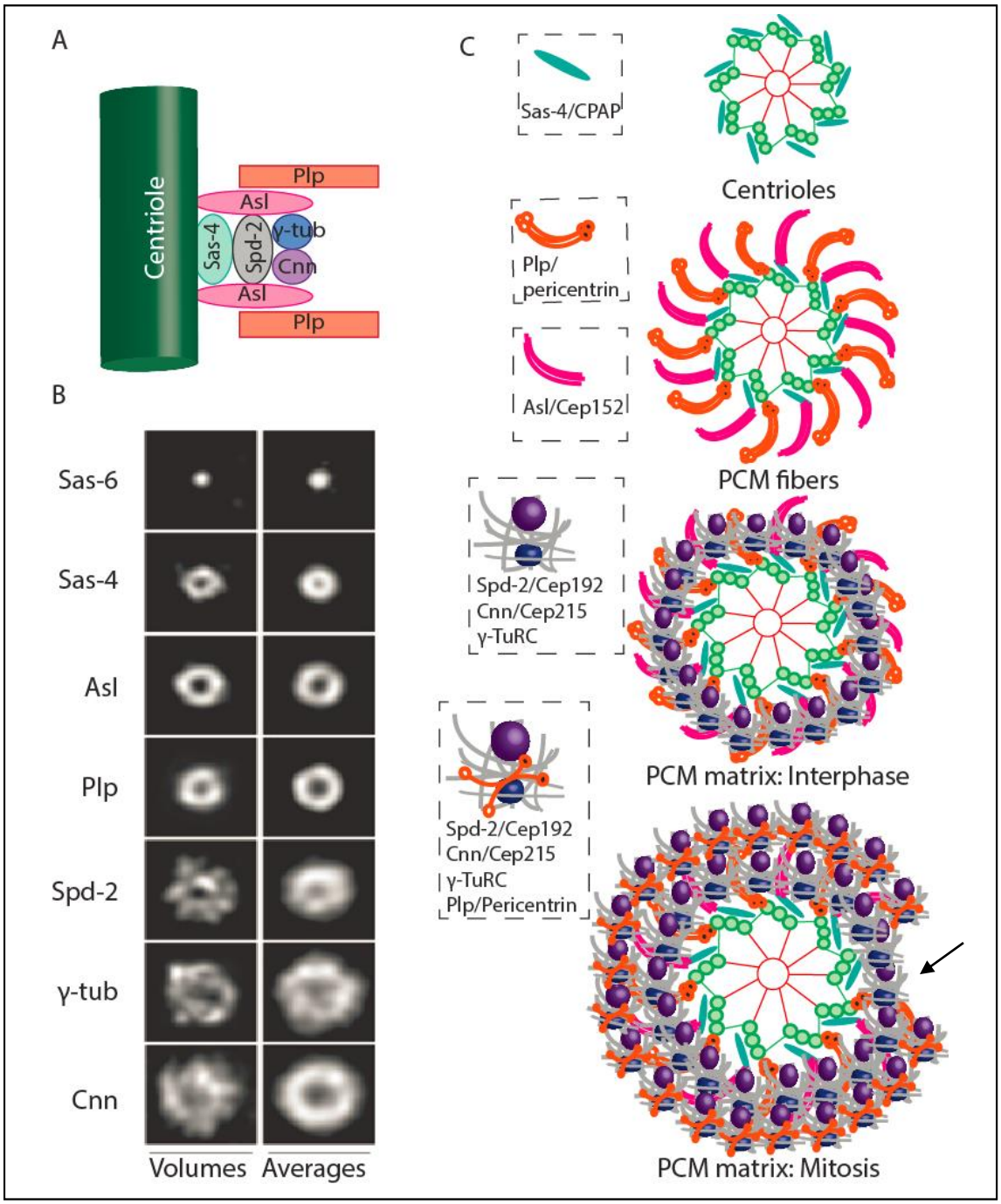

Figure 3. Recruitment of PCM components.

A, B. PCM components are organized in concentric toroids around the mother centriole during interphase. C. CPAP/Sas-4 closely associates with the wall of the mother centriole; followed by components of PCM, such as Cep192/Spd-2, whereas proteins involved in nucleating microtubules, γ-tubulin ring complex (γTuRC) and Cep215 are found in the outer layers. Pericentrin/Plp and Cep152/Asl have an extended conformation and are organized radially, with one end close to the centriole wall and the other end extending outwards. Additional PCM is acquired upon entry into mitosis forming an extended outer matrix of PCM proteins. The extended mitotic matrix contains Pericentrin/Plp, CEP192/Spd-2, Cep215/Cnn and γTuRC. PCM proteins are diminished at the site of procentriole assembly. (Arrow) The main features of PCM organization are conserved between humans and flies. Modified from [70,71]

CPAP/Sas-4 interacts with several PCM proteins, namely, Cnn, Asl/Cep152, and duplication. CPAP/Sas-4 interacts with several PCM proteins, namely, Cnn, Asl/Cep152, and Plp/Pericentrin forming a complex termed the S-CAP complex.[68,72,73] This scaffolding complex is thought to tether the PCM proteins to the centriole. A recent study has also shown that Sas-4 and several of the S-CAP complex proteins localize to the centriole at distinct times in the cell cycle, thus stating that the S-CAP complex may not be formed prior to localizing to the centriole.[53]

The centrosome shows an increased ability to nucleate and anchor microtubules towards the end of G2 phase and during mitosis.[15,17] Plk1/Polo and Aurora A kinases are required for this process. Plk1/Polo plays crucial roles in the initiation of centrosome maturation. Plk1/Polo phosphorylates the PCM proteins, Pericentrin/Plp, Cep192/Spd-2, NEDD1/Grip71, and

Cep215/Cnn. (Polo activity on Grip71 in Drosophila is less clear)[74,75] Plk1/Polo phosphorylates Pcnt/Plp to recruit Cep192/Spd-2, NEDD1/Grip71, γ-tubulin, Aurora A, and Plk1/Polo itself.[76] Pcnt/Plp and Cep192/Spd-2 depend on each other to localize to the centrosome, and both are required to recruit NEDD1/Grip71 and γ-tubulin.[77–79] NEDD1/Grip71 is a γ-tubulin interacting protein required for the recruitment of γ-tubulin to centrosomes and the subsequent nucleation of microtubules.[77,80] Cnn/Cep215 associates with the γ-TuRC and stimulates microtubule nucleation.[81,82] Following Plk1/Polo activation, a continuous stream of Plk1/Polo activity is required to maintain the PCM architecture at the centrosome.[17]

The licensing event

1.8 The Plk4 pathway

Prior to centriole duplication, the mitotic kinase, Polo-like kinase 4 (Plk4) licenses the mature centriole to begin replication during mitosis, much like DNA replication is a licensed event. Once licensed, the centriole is capable of assembling a procentriole in M-/S-/G2-phase environments. A centriole licensing factor must satisfy three criteria: (1) the factor must 'license' the centriole prior to the duplication event at the G1/S-phase transition, (2) the factor should be inactivated or eliminated during all other cell cycle phases to limit duplication to only one event per cell cycle, and (3) ectopic activity of the licensing factor should induce centriole overduplication during permissible cell cycle phases (S and G2).[15] We identified the conserved serine/threonine kinase Plk4 as a licensing factor that localizes to mitotic centrioles and modifies or 'primes' them to duplicate later during S-phase.[23,83,84] Although it is not known how Plk4 kinase activity promotes centriole assembly, Plk4 is necessary and, more significantly, is sufficient to induce centriole amplification (i.e., overduplication) when overexpressed.[85] After

mitosis, Plk4 is targeted for proteolytic degradation by the SCF^{Slimb} E3 ubiquitin-ligase.[34,83,86–90] However, even though Plk4 is degraded, centrioles remain competent to duplicate during S-phase. Furthermore, a non-degradable/SCF-resistant Plk4 mutant accumulates on S-phase centrioles and promotes overduplication.[89,90] Thus, timely degradation of Plk4 during interphase blocks centriole amplification. Our use of the descriptive label, "licensing factor", for Plk4 is intended to highlight its singular importance for initiating centriole duplication.

A recent study has concluded that the scaffolding protein Asl, licenses daughter centrioles to duplicate for the first time.[55] Novak et al, show in Drosophila embryos that Asl is initially not recruited to the daughter centrioles during S-phase but is in fact recruited at the end of mitosis and is irreversibly incorporated into the daughter centriole. This step is crucial for daughters to mature into mother centrioles and allow them to duplicate for the first time. This "dual licensing" model states that irreversible Asl incorporation licenses the daughter to duplicate for the first time, while centriole disengagement (discussed below) licenses mature mother centrioles to reduplicate. Importantly, Asl is required to bring Plk4 to the centriole and so may not in fact be "licensing" the daughter centriole, but allowing the daughter to recruit Plk4. Likewise, Asl does not satisfy the 2nd criteria for a licensing factor, as it is irreversibly incorporated into the centriole, it is not degraded in a cell-cycle specific manner and cannot act specifically as a switch.[91]

1.9 Centriole disengagement

Aside from Plk4 licensing, centriole disengagement is also a requirement for centriole duplication.[6,14] The mother and daughter centriole are tightly linked by an orthogonal connection

from S-phase through mitosis. During late mitosis, the orthogonal connection and the PCM are dissolved, and centrioles disengage. Two distinct stages of centriole disengagement have been described at different stages of the cell cycle. The first stage occurs in early mitosis and requires PLK1 activity. The second stage of disengagement occurs in late mitosis, when centriole pairs lose their orthogonal connection, and involves Separase-dependent proteolytic cleavage of PCNT.[92–94] According to Lee et al., Separase-dependent cleavage of PCNTB is necessary and sufficient for centriole disengagement during mitosis. Several studies have indicated the importance of centriole disengagement as a precursor to centriole duplication. Initial studies showed that: 1. The mother centriole is induced to reduplicate following the laser ablation of the daughter centriole during S-phase in human cells.[93] 2. Centriole duplication is inhibited when cells do not disengage in mitosis.[95] 3. Centrioles are able to prematurely disengage in cells arrested in S or G2 phase. [96] Recently, two elegantly performed studies have shown that first, a mutant form of Pericentrin resistant to cleavage by Separase produces centrioles that do not disengage or duplicate.[92] Secondly, the intercentriolar linker protein, Cep68, has been shown to be phosphorylated by Plk1, allowing recognition of the E3 ubiquitin ligase $SCF^{\beta TrCP}$, and to be subsequently degraded. Cep68 forms a complex with other PCM/linker proteins Pericentrin and Cep215. Degradation of Cep68 leads to the removal of Cep215 from the periphery of the PCM, followed by Pericentrin cleavage mediating removal of Cep215 from the core of the centriole. Cep 215 removal from the centrosome promotes centriole disengagement and separation allowing for subsequent centriole duplication.[97] These pathways have proven to be necessary in human cells, however, more work in Drosophila is necessary to see if centriole disengagement is a requirement for duplication.

We do not see disengagement as a true licensing mechanism as the third criteria for licensing is not satisfied. Furthermore, there are several indications that centriole duplication can occur when centrioles are engaged. The phenomena of multiple daughters around a single mother indicates that more than one centriole can grow from an engaged mother centriole.[98] Plk4 overexpression has been known to induce formation of multiple daughter centrioles around a single mother, yielding a rosette-like phenotype.[85] Interestingly, in a recent study, Plk4 overexpression was shown to not only form multiple daughter centrioles from a single mother, but high overexpression yielded de novo centriole formation, a process that was once thought to be prohibited in the presence of a centriole to be template.[19] Thus, centriole duplication can occur in the presence of engaged centrioles. This provides the first study to show such a pathway is possible.

1.10 A multi-step model for Plk4 activation and regulation

Polo-like kinase 4 (Plk4) was first identified in mice sharing homology with the Drosophila Polo (Plk1 in humans), S. cerevisiae CDC5 and murine SAK. Homologs to Plk4 exist in most opisthokonts (organisms with a single posterior flagellum) except in the nematode C. elegans. Importantly, in c. elegans, the kinase Zyg-1 regulates centriole assembly and is thought to be a functional ortholog of Plk4. Plk4 belongs to the family of Polo kinases, consisting of 5 kinases in humans (Plk1, Plk2, Plk3, Plk4 and Plk5) but only 2 in Drosophila (Polo and Plk4). [86] The Polo kinase family are unique in that they encode Polo Boxes (PB), ~100 amino acid domains that serve as hubs of protein interaction.[99,100] The molecular structure of Plk4 differed from the other Polo kinases, as it contained a domain termed the Cryptic Polo Box and C-terminal Polo Box domain, instead of the 2 separate Polo boxes in other Polo kinases.[99] The atomic structure of the Cryptic

Polo Box, a conserved domain in Plk4, was solved by Slevin et al, revealing a composition of tandem Polo Boxes (PB1 and PB2) that form a stable homodimer.[101] (Figure 4A) Thus, Plk4 members contain a total of three PBs separated by two linkers (L1 and L2) (Notably, PB1-PB2 (not PB3) is necessary and sufficient for homodimerization in Drosophila, while all three PBs homodimerize in humans. [102] PB3's function was unknown unknown until recently, where we found that PB3 deletion (Δ) effectively inhibited kinase activity; the elevated protein levels of Plk4-ΔPB3 are near identical to kinase-dead Plk4 which is unable to self-destruct. (Figure 4B,C) In addition, centriole duplication fails in Plk4-ΔPB3-expressing cells.[102] Based on Plk1's mechanism of regulation, we reasoned that a possible function for PB3 is to relieve a previously unidentified autoinhibitory mechanism in Plk4. Activation of mitotic Plk1 requires phosphorylation of its T-loop but, during interphase, this is blocked by an obstructive linker located adjacent to its kinase domain[102]. We found that Plk4 autophosphorylates its T-loop for maximal activation and, interestingly, also modifies its nearby L1. We tested the scheme that (1) L1 could be the source of autoinhibition (as it is for Plk1), that (2) PB3 normally relieves this inhibition, and (3) after Plk4 is de-inhibited, it autophosphorylates L1 to prevent further autoinhibition. Strikingly phosphomimetic mutations (PM) in L1 which rescued kinase activity when introduced into the ΔPB3 mutant and restored its ability to self- destruct. L1-PM-ΔPB3 also induced centriole amplification when overexpressed suggesting that one of PB3's functions is to relieve autoinhibition. *In vitro* kinase assays with purified components revealed that PB3 alone is not sufficient to relieve autoinhibition and, thus, we proposed that an additional unidentified factor assists in kinase activation. The Maier lab recently discovered that STIL (the human homolog of fly Ana2) is the missing factor.[39] Independently, we made the identical discovery in *Drosophila*. Lastly, we identified L2 as the most extensively phosphorylated region and discovered that L2

phosphorylation promotes dimer separation. A multi-step model for Plk4 activation and regulation utilizing autoinhibition to promote Plk4 accumulation and homodimerization. Homodimerization then triggers PB3-mediated de-inhibition (assisted by Ana2) followed by extensive *trans*-autophosphorylation, Slimb recruitment, and dimer separation. (Figure 4D)

Plk4 kinase activity both regulates its own destruction and activation, but it is also involved in several other key events in centriole duplication and assembly. Not all of the Plk4 substrates have been discovered, but much research has been performed to determine the activities of this important kinase.

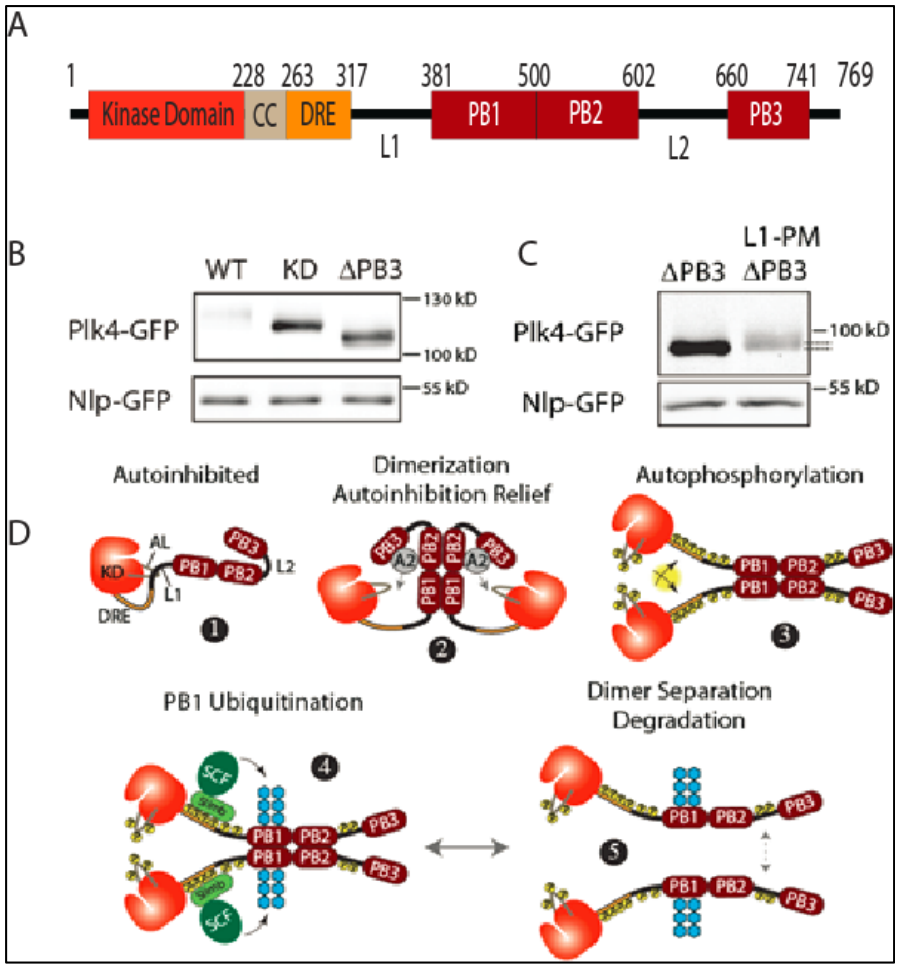

Figure 4. PB3 functions to relieve autoinhibition.

A) Structure of Drosophila Plk4 B, C) Anti-GFP immunoblots of S2 cell lysates expressing the indicated Plk4-GFP constructs and Nlp-GFP (loading control). Note the mobility shift of L1-PM-ΔPB3 compared to ΔPB3 (dashed lines), indicating that addition of L1-PM restored kinase activity. D) 5-step model of Plk4 activation. PB3 relieves autoinhibition through Ana2 to move L1 away from the activation loop. Blue hexagons, poly-ubiquitin chains. Dimer separation may cause disassembly of higher-order Plk4 complexes.

In a recent study by Firat Kralar et al, several Plk4 interactors were identified based on biotin identification proximity labeling in HEK293 cells.[82] In this elegant study, Plk4 was tagged with the e. coli biotin ligase BirA, transfected into HEK293T cell and incubated with an excess of biotin. The centrosome fraction was isolated by sucrose gradient, proteins were solubilized and the centrosome rich fraction was isolated by streptavidin beads. The isolated fraction was then analyzed by mass spectrometry to identify centrosomal proteins that interacted with Plk4.

Protein	NSAF
Plk4	1.52
SDCCAG3	1.34
CEP152	1.33
CEP192	1.28
CEP85	1.22
PCNT	1.13
KIAA1671	1.08
NEDD1	1.08
MAGED1	1.03
TTK	0.87
LZTS2	0.79
PLK1	0.78
ALMS	0.71
USP54	0.77
STIL	0.62

Table 2. Analysis by mass spectrometry of proximity interactors of PLK4. These interactors are ranked in the order of their normalized spectral abundance factor (NSAF) values.

Of these proteins, several have been independently identified as interactors and substrates of Plk4. Namely, Plk4, CEP152, and STIL have all been shown to be substrates and bidning partners of Plk4, while CEP192 has been shown to interact with Plk4.[25–30,33,35–39] Recently, another centriole protein, CPAP/Sas-4, has been discovered as a substrate of Plk4.[60]

Initially, the C.elegans ortholog of Plk4, Zyg-1, was reported to directly interact with Sas-6 and recruit it to the centriole. [103] This pathway is not conserved in Drosophila or humans, but Plk4 is involved in Sas-6 recruitment to the centriole. Several important studies were conducted recently showing the first postivie regalution of centriole assembly by a Plk4 substrate. In a seminal paper, Plk4 phosphorylates Ana2/STIL in the C-terminal conserved STAN domain to recruit Sas-6 to the centriole.[33] (Figure 5A) When a non-phosphoryaltable form of Ana2 is expressed, Sas-6 is no longer able to localize to the growing daughter centriole, and centriloe duplication fails. The crystal structure of this interaction was solved for STIL/Plk4 showing a conserved coiled-coil in STIL interacts with a psuedo-coiled-coil in PB3 of PLK4.[39] Interestingly, STIL interacts with Plk4 in another N-terminal region, labeled linker1 in this study, a region consisiting of the Downstream Regulatory Element (DRE) and Linker 1 (L1). In a separate study in Drosophila, we further resolve the interaction to inlcude a previously unidentified coiled-coil at te C-terminus of the kinase domain to be important for interaction with Ana2. The predicted coiled coil does not appear in the solved crystal strucutre of human Plk4 kinase domain, but is at the end of the crystallized protein and may not be stabilized. While phosporylation of Ana2/STIL STAN domain postively regulates centriole duplication, we found that phosphorylation of the N-terminus negatively regulates centriole duplication, creating a dual mechansim of Plk4 phosphhorylation. Plk4 may also directly regulate Sas-6 levels,a s a study has shown that Plk4 phosphorylates the E3 ubiquitin

ligase SCF^{FBXW5}. SCF^{FBXW5} ubiquitylates Sas-6 and targets it for destruction, but phosphoryaltion by Plk4 prevents this.[104] Sas-6 was also shown to be a target of the APC^{Cdh1}, perhaps leading to multiple regulatory mechansims for the levels of this protein.[105]

Plk4 is known to interact with Asl/Cep152 and this interaction is requried for the recruitment of Plk4 to the centriole in Drosophila and aids in Plk4 to the centriole in humans.[26,31,32,91 25–28] Asl/Cep152 interacts with both Plk4 and Sas-4/CPAP and forms a scaffold to recruit these important proteins to the centriole.[29] Notably, like Sas-4/CPAP, overexpression of Asl/Cep152 in the absence of Plk4 can induce MTOC formation which lack centrioles, but contain Sas-4/CPAP.[31] Cep152 was the first centriolar protein identified as a substrate of Plk4, however the results of the phosphorylation remains elusive.[25,106] However, Plk4 was shown to phosphorylate Cep152 *in vitro* with unknown consequences, with at least 1 residue on the N-terminus of CEP152 being phosphorylated. A recent study has shown that Plk4 is responsible for the reduction of Asl at the centriole during early spermatogenesis, an essential process in post-fertilization development. [106] Centrosome reduction - a process where centrosomes lose many of their components-is a conserved process in Drosophila and mammalian sperm. Additional studies provided indirect evidence for an essential role of centrosome reduction in embryo development. Plk4 was shown to phosphorylate Asl in the testes, and this phosphorylation regulates its ubiquitination and possible subsequent degradation. This regulation is likely specific to spermatogenesis, because Asl/Cep152 levels are constant in centrioles of dividing cells. (Figure 5B) In dividing cells, Plk4 interacts with both Asl N-terminus, promoting Plk4 homodimerization and autophosphorylation during interphase, and the Asl C-terminus, promoting Plk4 stability during mitosis.[32] In this case, Asl differentially effects Plk4 activation

and stability temporally to regulate centriole duplication, providing insight into the ability of Asl overexpression to drive centriole amplification. A third study has indicated Asl in the process of centriole length achievement in concert with Cep97, though a possible role for Plk4 in this process has not been studied.[107] The interaction of Plk4 with Asl is modified depending on cell type and stage of the cell-cycle.

Plk4 is also known to phosphorylate CPAP *in vitro*.[60] Cizmegolou et al, showed that Plk4 and Plk2 both phosphorylate CPAP on the same residue in the microtubule-binding domain (MBD). The study concluded that the centriole assembly effects were due to Plk2, as the phosphomimetic mutant did not rescue Plk4 depletion. Phosphorylated CPAP preferentially localizes to the centriole at G1/S-phase, and expresson of a non-phosphorylatable mutant does not induce centriole elongation. The study concludes that phosphorlyation by Plk2 functions to phosphorylate CPAP, perhaps to cause centriole elongation.(Figure 5C) While the phosphorylation of CPAP by Plk4 was deemed unimportant for centriole duplication, we have recently found that Plk4 is required for multiple steps in the centriole assembly process, not just CPAP function. It would be interesting to further study the consequences of CPAP phosphorylation by Plk4, and determine any functional consequences in Drosophila, which lacks Plk2.

In a recent study performed by Galleta et al., Cep135 has been identifed as the newest substrate of Plk4.[108] *In vitro* kinase assays led to the discovery of 9 sites in Cep135 phosphorylated by Plk4. Inserting the phsophomutants into a yeast-2-hybrid screen, they were able to identify a new interactor of Cep135 not previously known. Asl was shown to bind phosphomimetic

Cep135, but not the non-phosphorylatable or wild-type form. They went on to discover that

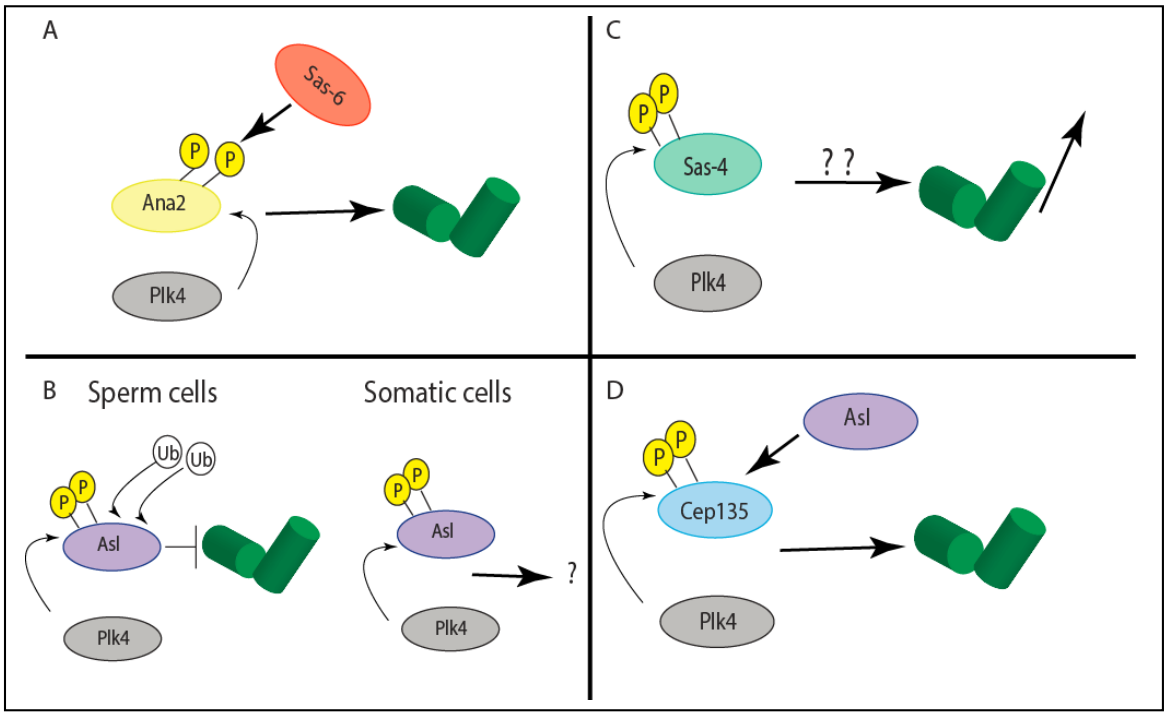

Figure 5. Centriolar substrates of Plk4

A. Pk4 phosphorylates Ana2 to recruit Sas-6 to the centriole and ensure centriole duplication. B. In sperm cells, Plk4 phosphorylates Asl, perhaps to recruit SCFSLIMB leading to subsequent Asl degradation and removal from the centriole. In somatic cells, Plk4 phosphorylates Asl with unknown consequences. C. Human Plk4 phosphorylates CPAP/Sas-4. The result of this phosphorylation is unknown. D. Plk4 phosphorylates Cep135 to recruit Asl to the centriole. In a positive feedback mechanism, Asl can bring more Plk4 allowing for further phosphorylation of centriole targets and subsequent centriole duplication.

phosphomimetic Cep135 was able to position Asl radially around the centriole, indicating Plk4 may play a role in positioning itself for further downstream phosphorylation events leading to centriole duplication. (Figure 5D) Importantly, reducing Cep135 did not affect Ana1 location.

More research needs to be performed to determine the consequence of Cep135 phosphorylation by Plk4.

The role of Plk4 in centriole duplication has been greatly studied over the past many years. New techniques in microscopy and proteomics have led to exciting new discoveries that need to be further researched. With the great amount of work being put into centriole duplication pathways, we will soon have new insights into how this organelle is being assembled.

1.11 References

1. Delattre M, Canard C, G??nczy P. Sequential Protein Recruitment in C. elegans Centriole Formation. *Curr Biol*. 2006;16(18):1844-1849. doi:10.1016/j.cub.2006.07.059.
2. Nigg EA, Cajanek L, Arquint C. The centrosome duplication cycle in health and disease. *FEBS Lett*. 2014;588(15):2366-2372. doi:10.1016/j.febslet.2014.06.030.
3. Gönczy P. Towards a molecular architecture of centriole assembly. *Nat Rev Mol Cell Biol*. 2012;13(7):425-435. doi:10.1038/nrm3373.
4. Robbins E, Jentzsch G, Micali A. The centriole cycle in synchronized HeLa cells. *J Cell Biol*. 1968;36(2):329-339. doi:10.1083/jcb.36.2.329.
5. Avidor-Reiss T, Gopalakrishnan J. Building a centriole. *Curr Opin Cell Biol*. 2013;25(1):1-6. doi:10.1016/j.ceb.2012.10.016.
6. Tsou, Meng-Fu Bryan; Stearns T. Mechanism limiting centrosome duplication to once per cell cycle. http://www.nature.com/nature/journal/v442/n7105/pdf/nature04985.pdf.
7. Lingle WL, Barrett SL, Negron VC, et al. Centrosome amplification drives chromosomal instability in breast tumor development. *Proc Natl Acad Sci U S A*. 2002;99(4):1978-1983.

doi:10.1073/pnas.032479999.

8. Negrini S, Gorgoulis VG, Halazonetis TD. Genomic instability--an evolving hallmark of cancer. *Nat Rev Mol Cell Biol*. 2010;11(3):220-228. doi:10.1038/nrm2858.

9. Ganem NJ, Godinho S a, Pellman D. NIH Public Access. 2010;460(7252):278-282. doi:10.1038/nature08136.A.

10. Lingle WL, Salisbury JL. Altered centrosome structure is associated with abnormal mitoses in human breast tumors. *Am J Pathol*. 1999;155(6):1941-1951. doi:10.1016/S0002-9440(10)65513-7.

11. Cunha-Ferreira I, Bento I, Bettencourt-Dias M. From zero to many: control of centriole number in development and disease. *Traffic*. 2009;10(5):482-498. doi:10.1111/j.1600-0854.2009.00905.x.

12. Bettencourt-Dias M, Hildebrandt F, Pellman D, Woods G, Godinho SA. Centrosomes and cilia in human disease. *Trends Genet*. 2011;27(8):307-315. doi:10.1016/j.tig.2011.05.004.

13. Zyss D, Gergely F. Centrosome function in cancer: guilty or innocent? *Trends Cell Biol*. 2009;19(7):334-346. doi:10.1016/j.tcb.2009.04.001.

14. Tsou MFB, Stearns T. Controlling centrosome number: Licenses and blocks. *Curr Opin Cell Biol*. 2006;18(1):74-78. doi:10.1016/j.ceb.2005.12.008.

15. Brownlee CW, Rogers GC. Show me your license, please: deregulation of centriole duplication mechanisms that promote amplification. *Cell Mol Life Sci*. 2013;70(6):1021-1034. doi:10.1007/s00018-012-1102-6.

16. Nigg E a, Stearns T. The centrosome cycle: Centriole biogenesis, duplication and inherent asymmetries. *Nat Cell Biol*. 2011;13(10):1154-1160. doi:10.1038/ncb2345.

17. Fujita H, Yoshino Y, Chiba N. Regulation of the centrosome cycle. *Mol Cell Oncol*.

2015;3556(August):00-00. doi:10.1080/23723556.2015.1075643.

18. Rodrigues-martins AA, Riparbelli M, Callaini G, Glover DM. Revisiting the Role of the Mother Centriole in Centriole Biogenesis. *Science*. 2007;316(5827):1046-1050.

19. Lopes CAM, Jana SC, Cunha-Ferreira I, et al. PLK4 trans-Autoactivation Controls Centriole Biogenesis in Space. *Dev Cell*. 2015;35(2):222-235. doi:10.1016/j.devcel.2015.09.020.

20. Gopalakrishnan J, Guichard P, Smith AH, et al. Self-assembling SAS-6 multimer is a core centriole building block. *J Biol Chem*. 2010;285(12):8759-8770. doi:10.1074/jbc.M109.092627.

21. Kitagawa D, Vakonakis I, Olieric N, et al. Structural basis of the 9-fold symmetry of centrioles. *Cell*. 2011;144(3):364-375. doi:10.1016/j.cell.2011.01.008.

22. Nakazawa Y, Hiraki M, Kamiya R, Hirono M. SAS-6 is a Cartwheel Protein that Establishes the 9-Fold Symmetry of the Centriole. *Curr Biol*. 2007;17(24):2169-2174. doi:10.1016/j.cub.2007.11.046.

23. Habedanck R, Stierhof Y-D, Wilkinson CJ, Nigg E a. The Polo kinase Plk4 functions in centriole duplication. *Nat Cell Biol*. 2005;7(11):1140-1146. doi:10.1038/ncb1320.

24. Wang W-J, Soni RK, Uryu K, Tsou M-FB. The conversion of centrioles to centrosomes: essential coupling of duplication with segregation. *J Cell Biol*. 2011;193(4):727-739. doi:10.1083/jcb.201101109.

25. Hatch EM, Kulukian A, Holland AJ, Cleveland DW, Stearns T. Cep152 interacts with Plk4 and is required for centriole duplication. *J Cell Biol*. 2010;191(4):721-729. doi:10.1083/jcb.201006049.

26. Blachon S, Gopalakrishnan J, Omori Y, et al. Drosophila asterless and vertebrate Cep152

are orthologs essential for centriole duplication. *Genetics*. 2008;180(4):2081-2094. doi:10.1534/genetics.108.095141.

27. Kim T-S, Park J-E, Shukla A, et al. Hierarchical recruitment of Plk4 and regulation of centriole biogenesis by two centrosomal scaffolds, Cep192 and Cep152. *Proc Natl Acad Sci U S A*. 2013;110(50):E4849-E4857. doi:10.1073/pnas.1319656110.
28. Sonnen KF, Gabryjonczyk A-M, Anselm E, Stierhof Y-D, Nigg E a. Human Cep192 and Cep152 cooperate in Plk4 recruitment and centriole duplication. *J Cell Sci*. 2013;126(Pt 14):3223-3233. doi:10.1242/jcs.129502.
29. Cizmecioglu O, Arnold M, Bahtz R, et al. Cep152 acts as a scaffold for recruitment of Plk4 and CPAP to the centrosome. *J Cell Biol*. 2010;191(4):731-739. doi:10.1083/jcb.201007107.
30. Hatch EM, Kulukian A, Holland AJ, Cleveland DW, Stearns T. Cep152 interacts with Plk4 and is required for centriole duplication. *J Cell Biol*. 2010;191(4):721-729. doi:10.1083/jcb.201006049.
31. Dzhindzhev NS, Yu QD, Weiskopf K, et al. Asterless is a scaffold for the onset of centriole assembly. *Nature*. 2010;467(7316):714-718. doi:10.1038/nature09445.
32. Klebba JE, Galletta BJ, Nye J, et al. Two Polo-like kinase 4 binding domains in Asterless perform distinct roles in regulating kinase stability. *J Cell Biol*. 2015;208(4):401-414. doi:10.1083/jcb.201410105.
33. Dzhindzhev NS, Tzolovsky G, Lipinszki Z, et al. Plk4 Phosphorylates Ana2 to Trigger Sas6 Recruitment and Procentriole Formation. *Curr Biol*. 2014:1-7. doi:10.1016/j.cub.2014.08.061.
34. Rogers GC, Rusan NM, Roberts DM, Peifer M, Rogers SL. The SCF Slimb ubiquitin

ligase regulates Plk4/Sak levels to block centriole reduplication. *J Cell Biol*. 2009;184(2):225-229. doi:10.1083/jcb.200808049.

35. Ohta M, Ashikawa T, Nozaki Y, et al. Plk4 directly interactes with STIL. *Nat Commun*. 2014;5:1-12. doi:10.1038/ncomms6267.

36. Zitouni S, Francia ME, Leal F, et al. CDK1 Prevents Unscheduled PLK4-STIL Complex Assembly in Centriole Biogenesis. *Curr Biol*. 2015:1127-1137. doi:10.1016/j.cub.2016.03.055.

37. Moyer TC, Clutario KM, Lambrus BG, Daggubati V, Holland AJ. Binding of STIL to Plk4 activates kinase activity to promote centriole assembly. *J Cell Biol*. 2015;209(6):863-878. doi:10.1083/jcb.201502088.

38. Kratz A-S, Bärenz F, Richter KT, Hoffmann I. Plk4-dependent phosphorylation of STIL is required for centriole duplication. *Biol Open*. 2015;4(3):370-377. doi:10.1242/bio.201411023.

39. Arquint C, Gabryjonczyk AM, Imseng S, et al. STIL binding to Polo-box 3 of PLK4 regulates centriole duplication. *Elife*. 2015;4(JULY2015):1-22. doi:10.7554/eLife.07888.

40. Gibbons IR, Grimstone A V. On flagellar structure in certain flagellates. *J Biophys Biochem Cytol*. 1960;7(4):697-716. doi:10.1083/jcb.7.4.697.

41. Hirono M. Cartwheel assembly. *Philos Trans R Soc Lond B Biol Sci*. 2014;369(1650):20130458 - . doi:10.1098/rstb.2013.0458.

42. Cottee MA, Muschalik N, Johnson S, Leveson J, Raff JW, Lea SM. The homo-oligomerisation of both Sas-6 and Ana2 is required for efficient centriole assembly in flies. *Elife*. 2015;4(MAY):1-65. doi:10.7554/eLife.07236.

43. Fong CS, Kim M, Yang TT, Liao JC, Tsou MFB. SAS-6 Assembly Templated by the

Lumen of Cartwheel-less Centrioles Precedes Centriole Duplication. *Dev Cell*. 2014;30(2):238-245. doi:10.1016/j.devcel.2014.05.008.

44. Arquint C, Sonnen KF, Stierhof Y-D, Nigg E a. Cell-cycle-regulated expression of STIL controls centriole number in human cells. *J Cell Sci*. 2012;125(Pt 5):1342-1352. doi:10.1242/jcs.099887.

45. Arquint C, Nigg EA. STIL microcephaly mutations interfere with APC/C-mediated degradation and cause centriole amplification. *Curr Biol*. 2014;24(4):351-360. doi:10.1016/j.cub.2013.12.016.

46. Stevens NR, Dobbelaere J, Brunk K, Franz A, Raff JW. Drosophila Ana2 is a conserved centriole duplication factor. *J Cell Biol*. 2010;188(3):313-323. doi:10.1083/jcb.200910016.

47. Hilbert M, Noga A, Frey D, et al. SAS-6 engineering reveals interdependence between cartwheel and microtubules in determining centriole architecture. *Nat Cell Biol*. 2016;18(4):393-403. doi:10.1038/ncb3329.

48. Lin Y-NY-CY-NY-C, Chang C-W, Hsu W-B, et al. Human microcephaly protein CEP135 binds to hSAS-6 and CPAP, and is required for centriole assembly. *EMBO J*. 2013;32(8):1141-1154. doi:10.1038/emboj.2013.56.

49. Chang C, Hsu W, Tsai J, Tang CC, Tang TK. CEP295 interacts with microtubules and is required for centriole elongation. *J Cell Sci*. 2016;(May):2501-2513. doi:10.1242/jcs.186338.

50. Gudi R, Zou C, Li J, Gao Q. Centrobin-tubulin interaction is required for centriole elongation and stability. *J Cell Biol*. 2011;193(4):711-725. doi:10.1083/jcb.201006135.

51. Tang CJ, Fu RH, Wu KS, Hsu WB, Tang TK. CPAP is a cell-cycle regulated protein that

controls centriole length. *Nat Cell Biol*. 2009;11(7):825-831. doi:10.1038/ncb1889.

52. Schmidt TI, Kleylein-Sohn J, Westendorf J, et al. Control of Centriole Length by CPAP and CP110. *Curr Biol*. 2009;19(12):1005-1011. doi:10.1016/j.cub.2009.05.016.

53. Sonnen KF, Schermelleh L, Leonhardt H, Nigg E a. 3D-structured illumination microscopy provides novel insight into architecture of human centrosomes. *Biol Open*. 2012;1(10):965-976. doi:10.1242/bio.20122337.

54. Conduit PT, Wainman A, Novak ZA, Weil TT, Raff JW. Re-examining the role of Drosophila Sas-4 in centrosome assembly using two-colour-3D-SIM FRAP. *Elife*. 2015;4(NOVEMBER2015):1-12. doi:10.7554/eLife.08483.

55. Novak ZA, Conduit PT, Wainman A, Raff JW. Asterless licenses daughter centrioles to duplicate for the first time in Drosophila embryos. *Curr Biol*. 2014;24(11):1276-1282. doi:10.1016/j.cub.2014.04.023.

56. Fu J, Lipinszki Z, Rangone H, et al. Conserved Molecular Interactions in Centriole-to-Centrosome Conversion. 2016;18(1):87-99. doi:10.1038/ncb3274.Conserved.

57. Hiraki M, Nakazawa Y, Kamiya R, Hirono M. Bld10p Constitutes the Cartwheel-Spoke Tip and Stabilizes the 9-Fold Symmetry of the Centriole. *Curr Biol*. 2007;17(20):1778-1783. doi:10.1016/j.cub.2007.09.021.

58. Izquierdo D, Wang WJ, Uryu K, Tsou MFB. Stabilization of cartwheel-less centrioles for duplication requires CEP295-mediated centriole-to-centrosome conversion. *Cell Rep*. 2014;8(4):957-965. doi:10.1016/j.celrep.2014.07.022.

59. Comartin D, Gupta GD, Fussner E, et al. CEP120 and SPICE1 cooperate with CPAP in centriole elongation. *Curr Biol*. 2013;23(14):1360-1366. doi:10.1016/j.cub.2013.06.002.

60. Chang J, Cizmecioglu O, Hoffmann I, Rhee K. PLK2 phosphorylation is critical for CPAP

function in procentriole formation during the centrosome cycle. *EMBO J*. 2010;29(14):2395-2406. doi:10.1038/emboj.2010.118.

61. Sharma A, Aher A, Dynes NJ, et al. Centriolar CPAP/SAS-4 Imparts Slow Processive Microtubule Growth. *Dev Cell*. 2016;37(4):362-376. doi:10.1016/j.devcel.2016.04.024.

62. Tang C-JC, Lin S-Y, Hsu W-B, et al. The human microcephaly protein STIL interacts with CPAP and is required for procentriole formation. *EMBO J*. 2011;30(23):4790-4804. doi:10.1038/emboj.2011.378.

63. Franz A, Roque H, Saurya S, Dobbelaere J, Raff JW. CP110 exhibits novel regulatory activities during centriole assembly in Drosophila. *J Cell Biol*. 2013;203(5):785-799. doi:10.1083/jcb.201305109.

64. Spektor A, Tsang WY, Khoo D, Dynlacht BD. Cep97 and CP110 Suppress a Cilia Assembly Program. *Cell*. 2007;130(4):678-690. doi:10.1016/j.cell.2007.06.027.

65. Delgehyr N, Rangone H, Fu J, et al. Klp10A, a microtubule-depolymerizing kinesin-13, cooperates with CP110 to control drosophila centriole length. *Curr Biol*. 2012;22(6):502-509. doi:10.1016/j.cub.2012.01.046.

66. Saurya S, Roque H, Novak ZA, Wainman A, Mustafa G. Drosophila Ana1 is required for centrosome assembly and centriole elongation. 2016;(May):2514-2525. doi:10.1242/jcs.186460.

67. Fu J, Glover D. How the newborn centriole becomes a mother. *Cell Cycle*. 2016;4101(July):1-2. doi:10.1080/15384101.2016.1164566.

68. Fu J, Glover DM. Structured illumination of the interface between centriole and peri-centriolar material. *Open Biol*. 2012;2(8):120104. doi:10.1098/rsob.120104.

69. Lawo S, Hasegan M, Gupta GD, Pelletier L. Subdiffraction imaging of centrosomes

reveals higher-order organizational features of pericentriolar material. *Nat Cell Biol*. 2012;12(1):308-317. doi:10.1038/ncb2591.

70. Mennella V, Keszthelyi B, McDonald KL, et al. Subdiffraction-resolution fluorescence microscopy reveals a domain of the centrosome critical for pericentriolar material organization. *Nat Cell Biol*. 2012;14(11):1159-1168. doi:10.1038/ncb2597.

71. Mennella V, Agard DA, Huang B, Pelletier L. Amorphous no more: Subdiffraction view of the pericentriolar material architecture. *Trends Cell Biol*. 2014;24(3):188-197. doi:10.1016/j.tcb.2013.10.001.

72. Gopalakrishnan J, Mennella V, Blachon S, et al. Sas-4 provides a scaffold for cytoplasmic complexes and tethers them in a centrosome. *Nat Commun*. 2011;2(May):359. doi:10.1038/ncomms1367.

73. Zheng X, Gooi LM, Wason A, et al. Conserved TCP domain of Sas-4/CPAP is essential for pericentriolar material tethering during centrosome biogenesis. *Proc Natl Acad Sci U S A*. 2014;111(3):E354-E363. doi:10.1073/pnas.1317535111.

74. Santamaria A, Wang B, Elowe S, et al. The Plk1-dependent phosphoproteome of the early mitotic spindle. *Mol Cell Proteomics*. 2011;10(1):M110.004457. doi:10.1074/mcp.M110.004457.

75. Conduit PT, Feng Z, Richens JH, et al. The centrosome-specific phosphorylation of Cnn by Polo/Plk1 drives Cnn scaffold assembly and centrosome maturation. *Dev Cell*. 2014;28(6):659-669. doi:10.1016/j.devcel.2014.02.013.

76. Lee K, Rhee K. PLK1 phosphorylation of pericentrin initiates centrosome maturation at the onset of mitosis. *J Cell Biol*. 2011;195(7):1093-1101. doi:10.1083/jcb.201106093.

77. Gomez-Ferreria MA, Bashkurov M, Helbig AO, et al. Novel NEDD1 phosphorylation

sites regulate γ-tubulin binding and mitotic spindle assembly. *J Cell Sci*. 2012;125(Pt 16):3745-3751. doi:10.1242/jcs.105130.

78. Giansanti MG, Bucciarelli E, Bonaccorsi S, Gatti M. Drosophila SPD-2 Is an Essential Centriole Component Required for PCM Recruitment and Astral-Microtubule Nucleation. *Curr Biol*. 2008;18(4):303-309. doi:10.1016/j.cub.2008.01.058.

79. Dix CI, Raff JW. Drosophila Spd-2 Recruits PCM to the Sperm Centriole, but Is Dispensable for Centriole Duplication. *Curr Biol*. 2007;17(20):1759-1764. doi:10.1016/j.cub.2007.08.065.

80. Scrofani J, Sardon T, Meunier S, Vernos I. Microtubule nucleation in mitosis by a RanGTP-dependent protein complex. *Curr Biol*. 2015;25(2):131-140. doi:10.1016/j.cub.2014.11.025.

81. Choi YK, Liu P, Sze SK, Dai C, Qi RZ. CDK5RAP2 stimulates microtubule nucleation by the ??-tubulin ring complex. *J Cell Biol*. 2010;191(6):1089-1095. doi:10.1083/jcb.201007030.

82. Firat-Karalar EN, Rauniyar N, Yates JR, Stearns T. Proximity interactions among centrosome components identify regulators of centriole duplication. *Curr Biol*. 2014;24(6):664-670. doi:10.1016/j.cub.2014.01.067.

83. Rogers GC, Rusan NM, Roberts DM, Peifer M, Rogers SL. The SCF Slimb ubiquitin ligase regulates Plk4/Sak levels to block centriole reduplication. *J Cell Biol*. 2009;184(2):225-239. doi:10.1083/jcb.200808049.

84. Bettencourt-Dias M, Rodrigues-Martins A, Carpenter L, et al. SAK/PLK4 is required for centriole duplication and flagella development. *Curr Biol*. 2005;15(24):2199-2207. doi:10.1016/j.cub.2005.11.042.

85. Kleylein-Sohn J, Westendorf J, Le Clech M, Habedanck R, Stierhof Y-D, Nigg E a. Plk4-induced centriole biogenesis in human cells. *Dev Cell*. 2007;13(2):190-202. doi:10.1016/j.devcel.2007.07.002.

86. Sillibourne JE, Bornens M. Polo-like kinase 4: the odd one out of the family. *Cell Div*. 2010;5:25. doi:10.1186/1747-1028-5-25.

87. Klebba JE, Buster DW, Nguyen AL, et al. Polo-like kinase 4 autodestructs by generating its slimb-binding phosphodegron. *Curr Biol*. 2013;23(22):2255-2261. doi:10.1016/j.cub.2013.09.019.

88. Holland AJ, Fachinetti D, Zhu Q, et al. The autoregulated instability of Polo-like kinase 4 limits centrosome duplication to once per cell cycle. *Genes Dev*. 2012;26(24):2684-2689. doi:10.1101/gad.207027.112.

89. Holland AJ, Lan W, Niessen S, Hoover H, Cleveland DW. Polo-like kinase 4 kinase activity limits centrosome overduplication by autoregulating its own stability. *J Cell Biol*. 2010;188(2):191-198. doi:10.1083/jcb.200911102.

90. Guderian G, Westendorf J, Uldschmid A, Nigg EA. Plk4 trans-autophosphorylation regulates centriole number by controlling betaTrCP-mediated degradation. *J Cell Sci*. 2010;123(Pt 13):2163-2169. doi:10.1242/jcs.068502.

91. Varmark H, Llamazares S, Rebollo E, et al. Asterless Is a Centriolar Protein Required for Centrosome Function and Embryo Development in Drosophila. *Curr Biol*. 2007;17(20):1735-1745. doi:10.1016/j.cub.2007.09.031.

92. Lee K, Rhee K. Separase-dependent cleavage of pericentrin B is necessary and sufficient for centriole disengagement during mitosis. *Cell Cycle*. 2012;11(13):2476-2485. doi:10.4161/cc.20878.

93. Tsou MFB, Wang WJ, George KA, Uryu K, Stearns T, Jallepalli P V. Polo Kinase and Separase Regulate the Mitotic Licensing of Centriole Duplication in Human Cells. *Dev Cell*. 2009;17(3):344-354. doi:10.1016/j.devcel.2009.07.015.

94. Kim J, Lee K, Rhee K. PLK1 regulation of PCNT cleavage ensures fidelity of centriole separation during mitotic exit. *Nat Commun*. 2015;6:10076. doi:10.1038/ncomms10076.

95. J L, P H, V M, Khodjakov A. Control of Daughter Centriole assembly by the Pericantriolar Material. *Nat Cell Biol*. 2008;10(3):322-328. doi:10.1126/scisignal.2001449.Engineering.

96. Loncarek, J; Hergert, P; Khodjakov A. Centriole reduplication during prolonged interphase requires procentriole maturation governed by Plk1: *Curr Biol*. 2011;20(14):1277-1282. doi:10.1016/j.cub.2010.05.050.Centriole.

97. Pagan JK, Marzio A, Jones MJK, et al. Degradation of Cep68 and PCNT cleavage mediate Cep215 removal from the PCM to allow centriole separation, disengagement and licensing. *Nat Cell Biol*. 2015;17(1):31-43. doi:10.1038/ncb3076.Degradation.

98. Peel N, Stevens NR, Basto R, Raff JW. Overexpressing Centriole-Replication Proteins In Vivo Induces Centriole Overduplication and De Novo Formation. *Curr Biol*. 2007;17(10):834-843. doi:10.1016/j.cub.2007.04.036.

99. Zitouni S, Nabais C, Jana SC, Guerrero A, Bettencourt-Dias M. Polo-like kinases: structural variations lead to multiple functions. *Nat Rev Mol Cell Biol*. 2014;15(7):433-452. doi:10.1038/nrm3819.

100. Archambault V, Lépine G, Kachaner D. Understanding the Polo Kinase machine. *Oncogene*. 2015;(November 2014):1-9. doi:10.1038/onc.2014.451.

101. Slevin LK, Nye J, Pinkerton DC, Buster DW, Rogers GC, Slep KC. The structure of the

Plk4 cryptic polo box reveals two tandem polo boxes required for centriole duplication. *Structure*. 2012;20(11):1905-1917. doi:10.1016/j.str.2012.08.025.

102. Klebba JE, Buster DW, McLamarrah TA, Rusan NM, Rogers GC. Autoinhibition and relief mechanism for Polo-like kinase 4. *Proc Natl Acad Sci U S A*. 2015;112(7):E657-E666. doi:10.1073/pnas.1417967112.

103. Hutchinson D, Ho V, Dodd M, Dawson HN, Zumwalt AC, Colton CA. Direct Binding of SAS-6 to ZYG-1 Recruits SAS-6 to the Mother Centriole for Cartwheel Assembly. *Dev Cell*. 2013;148(4):825-832. doi:10.1038/jid.2014.371.

104. Puklowski A, Homsi Y, Keller D, et al. The SCF-FBXW5 E3-ubiquitin ligase is regulated by PLK4 and targets HsSAS-6 to control centrosome duplication. *Nat Cell Biol*. 2011;13(8):1004-1009. http://dx.doi.org/10.1038/ncb2282.

105. Strnad P, Leidel S, Vinogradova T, Euteneuer U, Khodjakov A, Gönczy P. Regulated HsSAS-6 Levels Ensure Formation of a Single Procentriole per Centriole during the Centrosome Duplication Cycle. *Dev Cell*. 2007;13(2):203-213. doi:10.1016/j.devcel.2007.07.004.

106. Khire A, Vizuet AA, Davila E, Avidor-Reiss T. Asterless Reduction during Spermiogenesis Is Regulated by Plk4 and Is Essential for Zygote Development in Drosophila. *Curr Biol*. 2015;25(22):2956-2963. doi:10.1016/j.cub.2015.09.045.

107. Galletta BJ, Jacobs KC, Fagerstrom CJ, Rusan NM. Asterless is required for centriole length control and sperm development. *J Cell Biol*. 2016;213(4):435-450. doi:10.1083/jcb.201501120.

108. Galletta BJ, Fagerstrom CJ, Schoborg TA, et al. *A Detailed Centrosome Interactome Provides Insight into Organelle Assembly and Human Disease*.

109. Kitagawa D, Kohlmaier G, Keller D, et al. Spindle positioning in human cells relies on proper centriole formation and on the microcephaly proteins CPAP and STIL. *J Cell Sci*. 2011;124(Pt 22):3884-3893. doi:10.1242/jcs.089888.

110. Hsu W Bin, Hung LY, Tang CJC, Su CL, Chang Y, Tang TK. Functional characterization of the microtubule-binding and -destabilizing domains of CPAP and d-SAS-4. *Exp Cell Res*. 2008;314(14):2591-2602. doi:10.1016/j.yexcr.2008.05.012.

111. Hatzopoulos GN, Erat MC, Cutts E, et al. Structural analysis of the G-box domain of the microcephaly protein CPAP suggests a role in centriole architecture. *Structure*. 2013;21(11):2069-2077. doi:10.1016/j.str.2013.08.019.

112. Cutts EE, Inglis A, Stansfeld PJ, Vakonakis I, Hatzopoulos GN. The centriolar protein CPAP G-box: an amyloid fibril in a single domain. *Biochem Soc Trans*. 2015;43(5):838-843. doi:10.1042/BST20150082.

113. Zi Yang, David e Stone SWL. Prion promoted phosphorylation of heterologous amyloid is coupled with ubiquitin-proteasome system inhibition and toxicity. *Mol Microbiol*. 2014;93(5):1043-1056. doi:10.1111/mmi.12716.Prion.

CHAPTER TWO: A DETAILED CENTROSOME INTERACTOME PROVIDES INSIGHT INTO ORGANELLE ASSEMBLY AND HUMAN DISEASE

*BJG performed and analyzed all the experiments unless otherwise stated. BJG and NMR conceived of experiments and wrote the manuscript. KCS and CJF designed and cloned all constructs. TAS generated the Plk4 null allele. JMR and DWB performed *in vitro* kinase assay. TAM and GCR performed Cep135 and Plk4 IPs*

2.1 Abstract

The centrosome, comprised of centrioles and pericentriolar material (PCM), is the major microtubule-organizing center (MTOC) of many cells, best known for its role in mitotic spindle organization. How centrosome proteins are accurately assembled to carry out its many functions remains poorly understood. The non-membrane bound nature of the centrosome dictates that protein-protein interactions drive its assembly. To investigate this massive macromolecular organelle, we generated a "domain level" centrosome interactome using direct protein-protein interaction data from a focused yeast-two hybrid screen (Y2H). We then used biochemistry, cell biology and the model organism Drosophila to provide insight into protein organization, the kinase regulatory machinery required for centrosome assembly, and the molecular underpinning of human disease related to centrosome dysfunction. Finally, we identified a novel role for Plk4, the master regulator of centriole duplication. We show that Plk4 phosphorylates Cep135 to properly position the essential centriole component Asterless. This interaction landscape affords a critical framework for research of normal and aberrant centrosomes.

2.2 Results and discussion

We performed a directed Y2H screen (Fig. 1a) on 21 conserved *Drosophila* centrosome proteins (11 Centriole, 5 PCM, 5 Kinases; Fig. S1a; Table S1). 16 proteins were subdivided into 45, 200-600 amino acid polypeptides (Table S2), avoiding known or predicted motifs and secondary structures. All 4624 interaction combinations were tested using a four-tier stringency reporter system (Fig. S1b, c), providing information about weak and strong interactions. The highest stringency test identified 189 interactions (Fig. 1b, Excel file), a 10-fold increase over genome-wide approaches[1-4]**.** We report interactions at all stringencies online.

To identify 'high confidence interactions' (HCIs), we applied a scoring system based on Y2H strength and the assumption that the least promiscuous proteins are likely to show *bona fide* interactions (Table S3). Of the 37 (top 20%) HCIs, 13 are known, including the interactions between the master centriole duplication kinase Plk4 and its stabilizing centriolar-anchor Asl[5,6]. 14 HCIs are formed by full-length (FL) proteins, as we would predict given the low frequency of FL interaction. Of the 15 proteins tested as FL and fragments, only 6 showed interactions as FL, while at least one fragment from all 15 interacted with one or more other component. Taken together, this suggests intermolecular interactions are masked by intramolecular interactions within FL proteins, a common regulatory mechanism employed for centrosome regulation. For example, Cnn^{FL} and Spd-2^{F1} do not interact, but Cnn^{F1}-Spd-2^{F1} is an HCI. Cnn phosphorylation or interaction with additional proteins *in vivo* could relieve Cnn^{FL} autoinhibition and promote Cnn^{F1}-Spd-2^{F1} interaction, which is precisely what has been shown for *C. elegans* Spd-5 (Cnn)-Spd-2 network assembly[7,8]. Although we highlight one method of prioritizing the interactome, others could be used to identify HCIs.

A set of four conserved core proteins, Sas-6, Ana2, Cep135 and Sas-4 are required to build, organize and maintain the centriole[9]. Our screen identified 5 interactions among these centriole proteins (Fig. 2a, Fig. S2a), adding to the limited known interactions and structural data. While current models of centriole architecture predict heavy reliance on stable protein-protein interactions, the interactions we identified do not support a simple model where all interactions are represented in a final static structure. Our data is more consistent with a dynamic model where some transient interactions are required during centriole assembly. To illustrate the dynamic behavior of these proteins, and their possible transient interactions, we focused on Sas-4, which forms 4 of 5 inter-centriolar interactions identified. *Drosophila* Sas-4 has been shown to form a ring around the centriole with a radius of 100-150nm and localize to early daughter centrioles[10,11], while mammalian CPAP localizes simultaneously to a ring and a dot[12]. Our SIM shows Sas-4 localization to very dynamic (Fig. 2b-d), found on daughter centrioles as a dot (outer edge=109±11nm) and on mother centrioles as a larger dot (outer edge=144±13nm) or a ring (outer edge=187±31nm). Sas-4 shows strong interaction with Ana2$^{C\text{-}term}$, which localizes as a dot on mothers and daughters with an outer edge of 79.4±8nm, and with Cep135$^{N\text{-}term}$, which localizes as rings on mothers and daughters with an outer edge of 120±9nm (Fig. 2b-d). Combined with the highly variable Sas-4 localization, we suggest that Sas-4 interacts with Ana2$^{C\text{-}term}$ (Fig. 2a, interactions 1,2,3; Fig. S2b, b' = co-immunoprecipitation [IP]) early in centriole construction, followed by interaction with Cep135$^{N\text{-}term}$ in later stages of construction (Fig. 2a, interaction 5, Fig. S2c = co-IP). The largest mother centriole Sas-4 rings may represent an additional role for Sas-4, such as the proposed role for Sas-4 as a PCM scaffold[13]. Thus, our interactome can be used to parse apart and uncover new roles for multifunctional proteins such as Sas-4.

Beyond the core centriole proteins, our interactome provides context for other molecules within the centriole. For example, Ana1, an essential centriole protein, forms 11 interactions with core centriole proteins (Fig. S2e). Three interactions are HCIs, two of which form between Ana1$^{N\text{-}term}$ and Cep135$^{N\text{-}term}$, which was recently implicated in an early centriole assembly pathway[14]. This strongly validates our data and approach, encouraging future studies on the remaining Ana1 interactions, including a rare interaction with Sas-6 we confirmed by co-IP (Fig. S2f).

One striking observation is the high frequency of self-association – 16 fragments (9 known, 7 novel) across 12 proteins (Fig. S3). This suggests that higher-order oligomerization is a ubiquitous mechanism used to construct and regulate centrosomes, as demonstrated for Ana2, Sas-6, Asl, Cnn, and Plk4[15-18]. As a new example, we explore the Cep135$^{N\text{-}term}$ and Cep135$^{C\text{-}term}$ self-association, verified by co-IP (Fig. S4). In *Drosophila* spermatocytes (Fig. 2e), Cep135$^{N\text{-}term}$ is resolved as a ring with an outer edge of 131±13nm, while Cep135$^{C\text{-}term}$ is diffraction limited with an outer edge of 79±7nm (Fig. 2f). This indicates that Cep135 adopts an extended confirmation reinforced by lateral inter-molecular interactions. It is highly likely that oligomerization is tightly regulated as it affords a powerful mechanism to control centrosome duplication, maturation and function. Investigating the oligomerization of Ana1, Lk6, Nek2, PLP, Sas-4, and Cep135 should be a priority.

Our interactome data supports two distinct, but not mutually exclusive, models of PCM regulation and function. Model 1: PCM proteins form a large number of multivalent interactions (Fig. 3a, Excel file; S5a) that can be leveraged to assemble a membraneless organelle. Our data strongly supports the hypothesis that centrosomes represent phase separated droplets [19] within

the cytoplasm that rely on extensive protein-protein interactions. In fact, we identified fragments within each of the PCM proteins that form many interactions, providing the multivalent interaction landscape require for phase separation. These fragments include Cnn^{F1} (19 interactions), Spd-2^{F3} (11 interactions), PLP^{F3} (12 interactions), Asl^{F2} (10 interactions), and Asl^{F3} (21 interactions). This model can be tested by modulating the number of PCM interactions and assessing efficient organelle assembly *in vitro* and *in vivo*. Model 2: PCM is anchored to the centriole wall via bridging proteins. Our interactome reveals extensive binding between Spd2 and Cnn (Fig. 3a, S5a), the major PCM scaffold for γ-Tubulin ring complexes. Moreover, Spd2 and Cnn form strong interactions with Asl and PLP (Fig. 3a, S5a), which localize close to the centriole wall[11,20]. Thus, we have defined the direct protein-protein interactions that link the PCM with centrioles, a requisite for centrosome maturation. Specifically, we suggest that Asl-Cnn (Fig. 3a, int. #4, 6), or PLP-Cnn (Fig. 3a, int. #7, 11) are critical for PCM anchorage. Thus, our interactome can challenge existing paradigms while building new models. Furthermore, great effort has been afforded to identify the minimum components required for PCM function. Our interaction data provides a framework to refocus efforts for biochemical and *in vitro* reconstitution experiments on the interaction nodes we identified.

The model for Asl and PLP serving as anchoring proteins stems, in part, from their conformation, both extending outward from the centriole wall[11,20]. Asl and PLP do not rely on one another for localization, but a reciprocal functional dependency remains unexplored. We identified two interactions between Asl and PLP (Fig. 3a, #s 9, 10) and confirmed by co-IP (Fig S5b, b'). These interactions predict similar radial positioning of the interacting regions. We confirmed this using fluorescent tags showing that the Ctermini of Asl and PLP, bridged by

interaction 10, reside at 95±10nm and 86±7nm respectively (Fig. 3b, c, S5c,[11]), while the middle region of Asl and PLP reside at 135±11nm and 145±13nm, bridged by interaction #9 (Fig 3b, c, S5c). Interestingly, the position of the N-termini of these truncations is almost identical to the published position of the N-termini of the full-length proteins[11], indicating that the first 357 and 1376 amino acids of Asl and PLP, respectively, adopt a globular fold. Many centrosomal proteins, including the bridging proteins Asl/Cep152 and PLP/Pcnt, are linked to autosomal recessive primary microcephaly (MCPH) in humans[21]. We hypothesized that MCPH disease mutations in Cep152 or Pcnt might disrupt their direct binding, or their binding to other MCPH proteins. Review of the literature identified MCPH-causing deletion mutation 9460delAAG (Lys3154del) in Pcnt[22]. We found that Pcnt-Lys3154 is highly conserved (Fig. 3d). We found that deletion of this residue (Arg2720; $plp^{\Delta R}$) only disrupts the PLP^{F5}-Asl^{F3} interaction (Fig. 3e, f, int. #3; Fig. S6), while maintaining all 5 other PLP^{F5} interactions, including PLP^{F5}-CaM (Fig. 3e, f; Fig. S6). Critically, $plp^{\Delta R}$ transgenic *Drosophila* are not viable as adults (methods). Thus, our interactome can be used to pinpoint interactions affected by disease mutations, and as we show with PLP and Asl, can shed light on the interplay between MCPH genes.

Centrosome duplication and maturation are heavily reliant on mitotic kinase activity. We hypothesized that the interactome can uncover kinase substrates and explored this by investigating Plk4 partners (Fig. 4a, S7a). Cross-referencing the HCI list revealed 3 proteins: the two known plk4 substrates Asl and Ana2[5,6,23], in addition to Cep135. Co-IP and *in vitro* binding studies using purified proteins confirmed that the Plk4 Polo-Boxes1-2 cassette is both necessary and sufficient to bind Cep135 (Fig. S7b, c). *In vitro* kinase assays with recombinant $Plk4^{1\text{-}317}$ followed by mass-spectrometry revealed 9 phosphorylated residues in $Cep135^{N\text{-}term}$ (Fig. 4b, S8b,

Table S4). To determine if Cep135 function is regulated by phosphorylation, we generated and reintroduced a FL phosphomimetic Cep135 mutant ($Cep135^{9DE}$) into the Y2H screen. A single new interaction was gained between $Cep135^{9DE}$ and $Asl^{C\text{-}term}$ (Fig. 4c). We next tested if $Cep135^{WT}$, $Cep135^{9A}$, or $Cep135^{9DE}$ transgenes could rescue the previously documented Asl radial displacement in *cep135* mutant spermatocyte centrioles[24]. The radial positions of $Cep135^{9A}$ (251 nm ± 18) and $Cep135^{9DE}$ (248 nm ± 33) were similar, although both were slightly narrower than $Cep135^{WT}$ (261 ± 26 nm) (Figure S8c, d). Consistent with Cep135 phosphorylation having a role in positioning Asl, $Cep135^{9A}$ does not rescue the radial position of Asl, while a $Cep135^{WT}$ and $Cep135^{9DE}$ do (Fig. 4d, e). Importantly, loss of Cep135 does not disrupt the position of Ana1 (Figure S8e, f), suggesting there is no general defect in positioning centriole proteins.

Consistent with the Plk4-dependent positioning of Asl by Cep135, the Asl diameter on centrioles is significantly increased in a *plk4* mutant (Fig. 4f, g), sometimes to well over 400nm. Importantly, Asl positioning in the *plk4* mutant is partially rescued by expression of $Cep135^{9DE}$, but not $Cep135^{WT}$ or $Cep135^{9A}$ (Figure 4f, g). This supports a model where Plk4, via Cep135 phosphorylation, properly positions its own centriole anchor Asl, possibly in preparation for Plk4's downstream centriole duplication role (Fig. 4h).

Using *in vivo* experimental evidence in *Drosophila*, we demonstrate how large interaction information can lead to in depth mechanistic insight into macromolecular assemblies. By combing localization, dynamics and functional data with direct protein interaction information and mutant analysis, we show that interactions can predict inter- and intra-molecular

architecture, identify kinase substrates, and help gain an understanding of human disease, such as MCPH. Our study reveals new avenues for centrosome research and serves as a framework to explore other complex cellular processes.

2.3 Material and Methods

2.3.1 Plasmid construction

The sequence encoding the protein fragments used were amplified from cDNA clones by PCR using Phusion (New England Biolabs, Ipswich, MA) and the primers in Table 2, then introduced into Gateway Entry vectors using the pENTr/D-TOPO kit (Life Technologies). Gateway reactions were used to recombine cDNAs into the following destination vectors: pUGW (ubiquitin promoter, N-terminal GFP fusion, P-element and mini-white gene sequences for transgenic fly construction; *Drosophila* Genomics Resource Center), pATRW (actin promoter, N-terminal TagRFP; this study), pAWTR (actin promoter, C-terminal TagRFP; this study), pAFHW (actin promoter, N-terminal FLAG and HA fusion; *Drosophila* Genomics Resource Center), pAGW (actin promoter, N-terminal GFP; *Drosophila* Gateway Vector Collection), pAWG (actin promoter, Cterminal GFP; *Drosophila* Gateway Vector Collection), pDEST-pGADT7 (Y2H bait plasmid, GAL4 DNA-binding domain)[1], pDEST-pGBKT7-Amp (Y2H prey plasmid, GAL4 Activation domain[2]. 8 of the 9 mutations in the *cep135* cDNA were generated by DNA syntheses of the region (GenScript, Piscataway, NJ). The mutant sequence was then incorporated into the cDNA by Gibson cloning[3]. The 9th residue was mutated using the QuickChange II kit (Agilent Technologies, Santa Clara, CA).

2.3.2 Centrosome Y2H screen

The screen presented herein is designed following the approach outlined in Galletta and Rusan[4]. Since there are multiple advantages to utilizing full length proteins, as well as subfragments of proteins in Y2H studies, we utilized both in our screen. We subdivided our proteins using a structure based approach. We avoided dividing known structural motifs. However, the majority of the proteins in the screen do not have determined structures. In these cases, we utilized alignments and structure and motif prediction programs including Jpred3, Phyre2, the Simple Modular Architecture Research Tool (SMART) and Coils [5-8] and avoided making subdivisions in regions of predicted structure or high conservation. In addition to the centriole proteins discussed above, our screen included empty vectors to control against autoactivation, and two coiled-coil regions from non-centrosomal proteins, to control against non-specific coiled coil interactions.

Y2H experiments were based on modifications of the Matchmaker Gold system (Clonetech, Mountain View, CA) and performed following a significantly modified protocol[4]. All of the constructs listed in Table 2 were recombined into both Y2H bait and prey plasmids by Gateway recombination. All bait plasmids were individually transformed into the Y2HGold, a MAT**a** strain, and all prey plasmids into Y187, a MAT$\boldsymbol{\alpha}$ strain.

All bait strains were then individually mated to all prey strains in a 96 well format. 20 µL of an overnight culture of a single bait and a single prey strain were mixed with 100 µl of 2X Yeast Extract Peptone Adenine Dextrose (2X YPAD; 10 g/L yeast extract, 20 g/L peptone, 80 mg/L Adenine, 20 g/L D-glucose). Plates were incubated for 20 – 24 hours at 30ºC with shaking.

Approximately 3 µL of each mating reaction was transferred using a 48-pin multiblot replicator (VP 407AH, V&P Scientific, San Diego, CA) to DDO (SD –Leu –Trp) plates and grown for 5 days to select for diploids carrying bait and prey plasmids. Colonies were then replica plated to DDO, QDO (SD – Leu –Trp), DDOXA (DDO +Aureobasidin A, Clonetech, Moutain View, CA +X-α-Gal, Clonetech, Moutain View, CA and Gold Biotechnology, St. Louis, MO), and QDOXA (QDO +Aureobasidin A + X-α-Gal) plates and grown for 5 days at 30ºC. Colonies were then scored on the basis of growth and development of blue color on a scale of 0 (no growth / color) to 3 (robust growth / blue color). Any pair of protein fragments that revealed an interaction on any test plate was retested by recrossing the original yeast strains carrying the Y2H plasmids. 16 proteins or fragments activated the Y2H reporters on their own or failed to function in the system in one direction. One protein, $Ana2^{FL}$ could not be tested in either direction. None of the centrosome proteins or fragments showed an interaction with the coiled-coil controls under the most stringent conditions.

2.3.3 Identification of High Confidence Interactions (HCIs)

To prioritize our studies, we used a simple scoring system to select interactions of high confidence. We assume that polypeptides with fewer interactions are less "sticky" and therefore less prone to being false positives. We calculate the overall likelihood of each protein to interact, which we refer to as the Interaction Frequency (IF) = # of interactions / total tested interactions. IFs are then used to measure the interaction likelihood of two polypeptides (Poly 1 and Poly 2) by calculating IF^{poly1} x IF^{poly2}. Finally, we incorporate the strength of the Y2H interaction by

calculating an Interaction Score (IS) = (IF^{poly1} x IF^{poly2}) / Y2H strength (1-3) and display this as a percentage (Excel file, IS worksheet). The IS was used to rank all the interactions, with the lowest score indicating the highest confidence. We selected the top 20% (37 interactions) and refer to these as the HCIs (Table S3).

2.3.4 Drosophila cell culture

Drosophila S2 cells were cultured in Sf900II medium (Life Technologies, Grand Island, NY) and split every 3 – 4 days. Transfections were performed in six-well plates containing a confluent monolayer of cells using Effectene (Qiagen, Venlo, Netherlands) using 1 µg of each plasmid. All manipulations were performed 48 hours posttransfection.

2.3.5 Sample preparation and microscopy

Following transfection S2 cells were plated on #1.5 Concanvalin A-coated coverslips and allowed to attach for 20 – 30 minutes. Cells on coverslips were quickly washed twice with phosphate buffered saline (PBS) then fixed with 3.7% formaldehyde for 10 minutes. After fixation, cells were washed three times in PBS then extracted for 1 minute in Karsenti's solution (80 mM Pipes, 5 mM EGTA, 1 mM $MgSO_4$ and 0.5% Triton X-100). Cells were then post-fixed in 1 mg/ml $NaBH_4$ for 10 minutes, then rehydrated in PBS + 0.1% Tween 20. Cells were stained with DAPI (Thermo Fisher Scientific Inc.) for 30 minutes at room temperature and washed in PBS. Coverslips were then mounted on slides using Vectashield (Vector Laboratories, Burlingame, CA).

For experiments in spermatocytes, testes from wandering 3rd instar larvae were dissected in *Drosophila* S2 media and fixed for 20 minutes in 9% formaldehyde in PBS. Testes were washed three times in PBS + 0.3% Triton X-100 (PBST). Blocking was performed for 1 hour at room temperature in 5% normal goat serum with agitation. Guinea pig anti-Asl antibodies (1:1500; gift of G. Rogers, University of Arizona) were incubated with testes in block overnight at 4ºC. Testes were washed 3 times for 10 minutes in PBST. Anti-guinea pig secondary antibodies, conjugated with Alexa 568 (Life Technologies, Grand Island, NY), were incubated with testis for 4 – 8 hours at room temperature, followed by three washes in PBST. Testes were mounted in Vectashield under a #1.5 coverslip. All imaging is Structured Illumination Microscopy (SIM) performed on an OMX4 (GE Healthcare, Issaquah, WA) using immersion oil with a refractive index of 1.516. Images were reconstructed and registered using SoftWoRx 6.1.3 (GE Healthcare).

2.3.6 Centriole measurements

The position of N-termini was inferred using the following N-terminally tagged GFP/TagRFP proteins in S2 Cells or flies: Sas-4^{FL} (Fig. 2b-d), Cep135^{FL} (Fig. 2e, f; S8c, d), PLP^{F3-F5} (Fig. 3b, c; S5c), and Asl^{F2-F3} (Fig. 3b, c; S5c). The position of C-termini was inferred using the following C-terminally tagged GFP/TagRFP proteins in S2 Cells or flies: Ana2^{FL} (Fig. 2b-d), Cep135^{FL} (Fig. 2e, f), Asl^{F3} (Fig. 3b, c; S5c), PLP^{F5} (Fig. 3b, c; S5c), Ana1^{FL} (Fig. S8e, f). Asterless position in Figure 4 was determined using an antibody raised against the entire Asl protein.

Image analysis was performed in ImageJ (National Institutes of Health, Bethesda, MD). Linescans were performed across the diameter of centrioles and the resulting data was fit to the sum of two Gaussians. Ana2 data was fit to a single Gaussian. We report two measurements. The

"peak" measurement, which uses on the two peaks of the Gaussians, and conveys the position of the center of the distribution of a protein, or terminus. The "outer edge" measurement, which relies on the full-width-half-maximum (FWHM), is used to convey the possible maximum extension of a protein. The outer edge is also used when comparisons are made with diffraction limited proteins, as a peak measurement would simply provide the center of the centriole. While we calculate the 'Diameter' of the peaks and outer edges, we report the 'Radius' in Figure 2d, 2f, 3c in keeping with literature standards. For the comparison in Fig. 2C, individual linescans across centrioles were normalized to their peak fluorescence and manually aligned. The average ± SD at each position was calculated and is presented. The resulting curves were fit as above and the fits are presented. All data analysis utilized Excel (Microsoft, Redmond, WA) and Prism (GraphPad, La Jolla, CA) software. All statistical comparisons were done by unpaired t tests, with Welch's corrections when appropriate.

2.3.7 Immunoprecipitation and immunoblotting.

For each co-IP, 50 µl of a slurry of Protein-A conjugated Dynabeads (Life Technologies, Grand Island, NY) was incubated with 0.5 µL rabbit anti-GFP antibodies (clone ab290; Abcam, Cambridge, UK) in phosphate buffered saline (PBS) with 0.01% Tween 20 for 30 minutes at 4ºC. *Drosophila* S2 cells, from a single well of a 6-well dish, expressing the indicated constructs were harvested by centrifugation, then lysed in 1 ml RIPA buffer (10 mM Tris-HCl, pH 7.5, 140 mM NaCl, 1 mM EDTA, 0.5 mM EGTA, 1% Triton X-100, 0.1% sodium deoxycholate, 0.1% sodium dodecyl sulfate, 1 mM DTT, 1 µg/ml pepstatin A, 1 µg/ml leupeptin, 1 mM PMSF) or CLB (50 mM Tris, pH 7.2, 125 mM NaCl, 0.1% Triton X-100, 1 mM DTT, 1 µg/ml pepstatin A, 1 µg/ml leupeptin, 1 mM PMSF). Lysates were precleared by centrifugation (5 minutes at 21,000 x g) at 4ºC.

A sample of the cleared lysates was taken and ran as "input" on immunoblots. The remaining lysate was then added to antibody bound beads and incubated with mixing for 30 minutes at 4ºC. Beads were washed 2-5 times for 5 minutes each in lysis buffer with mixing and beads were harvested by magnet in between washes. The beads were transferred to a fresh tube during the final wash. 65 µl of 2X Laemmli buffer sample buffer was added to the beads and the bound material was eluted by boiling for 5 minutes. IP and input samples were resolved by SDS-PAGE, transferred to PVDF membranes and detected by Western blots using mouse anti-GFP (1:5000, clone JL-8; Clonetech Laboratories, Mountain View, CA) and mouse anti-FLAG (clone M2; SigmaAldrich, St. Louis, MO) primary antibodies, followed by horseradish peroxidase conjugated anti-mouse secondary antibody (Thermo Fisher Scientific Inc.). Detection was performed using SuperSignal West Dura Extended Duration Substrate (Life Technologies) and visualized using a ChemiDoc MP Imaging System (BioRad, Hercules, CA). Some bands in Western Blots are saturated to allow for detection of lower intensity bands.

2.3.8 In vitro binding assay

CEP135^{F2} was PCR amplified from a full-length CEP135 cDNA, and subcloned into pMAL-c2x (NEB) to generate N-terminal MBP-tagged constructs. The Plk4^{F2} PB1PB2 domain was PCR amplified from a Plk4 cDNA and subcloned into pGEX-6p2 (GE Life Sciences). BL21 DE3 *E. coli* were grown at 37°C to an OD_{600} of 0.6, induced with 0.1 mM IPTG, and cells were shifted to 16°C for 18 hours. Cells were centrifuged for 10 minutes at 2100 x g, and then the pellets stored in Buffer A (PBS, 10 mM imidazole, 0.1% β-mercaptoethanol) at -80°C. Cells were lysed in Buffer A by either sonication or using a cell disruptor (Avestin), centrifuged at 23,000 x g for 20 min at 4°C, and the supernatant was mix with amylose-resin (NEB) or glutathione-resin (GE Life Sciences). Resins were washed in Buffer A and eluted with Buffer A + 10 mM glutathione

or 10mM maltose. Protein containing fractions were pooled, dialyzed overnight in Buffer B (25 mM HEPES pH 7.4, 150 mM NaCl, 1 mM DTT) for GST-pull down assays. Purified proteins were also concentrated using Amicon 10K Ultra spin concentrators (Millipore). GST-PB1-PB2 was immobilized on glutathione, mixed with MBP-CEP135^{F2}, rocked at 25°C for 35 min and pelleted at 500 x g for 1 min. Inputs and pellets were analyzed by SDS-PAGE.

2.3.9 In vitro phosphorylation assays

Drosophila Plk4 kinase domain + DRE (amino acids 1-317, "Plk4 1-317") Cterminally tagged with FLAG-His_6 was cloned into the pET28a vector, expressed in BL21 (DE3) bacteria, and purified on HisPur resin (Thermo Fisher Scientific Inc.) according to manufacturer's instructions. GST-tagged constructs of the N-terminal region of *Drosophila* Cep135 (amino acids 1-490 of isoform A, accession NP_648749) was bacterially expressed and purified using glutathione resin (Pierce) according to manufacturer's instructions. Purified GST, GST-Cep135 Plk4 1-317 and

50 µM total ATP (in some cases, spiked with [γ-^{32}P] ATP), and then incubated 1 h, 25°C, in

reaction buffer (40 mM Na HEPES, pH 7.3, 150 mM NaCl, 5 mM $MgCl_2$, 0.5 mM $MnCl_2$, 1 mM DTT, 10% glycerol). Control samples for mass spectrometry were generated by incubating Cep135 in the absence of Plk4 1-317. Samples were resolved on SDS-PAGE and then Coomassie stained. Stained gels were then either dried and examined by autoradiography, or selected bands were cut from the gels and processed for tandem mass spectrometry (MS/MS). Standard procedures were used to process (reduce, alkylate, trypsinize, and extract) gel samples prior to analysis by MS/MS. All MS/MS samples were analyzed using Mascot (Matrix Science, London, UK; version 1.4.0.288) to search the database, Mascot5_NCBInr_Drosophila melanogaster, with a fragment ion mass tolerance of 0.80 Da and a parent ion tolerance of 20

PPM. Carbamidomethylation of cysteine was specified as a fixed modification; oxidation of methionine and phosphorylation of serine, threonine and tyrosine were specified as variable modifications. Total coverage was 89% for both Plk4-treated and control Cep135 NT.

2.3.10 Fly stocks

Analysis of *cep135* mutants was done using hemizygotes of $cep135^{C04199}/Df(3L)Brd15^{9}$. All Cep135 transgenic lines were generated using the Cep135 cDNA, with the indicated mutations, cloned into pUGW, by BestGene, Inc. using standard P-element mediated transformation. The *plk4* mutant was fortuitously generated from a production intermediate for another project. A fragment containing upstream activating sequences (UAS) from yeast and fluorescent eye reporter was introduced into the promoter of the *plk4* locus, by CRISPR and homologous repair resulting in a disruption of the promoter of the gene and a >95% loss of *plk4* expression as evidenced by quantitative PCR (data not shown). The $plp^{\Delta R}$ mutant was generated by site directed mutagenesis of the *plp* cDNA in pENTR/D. This sequence was then moved into pUWG and transgenic flies were generated by BestGene, Inc. $plp^{\Delta R}$; *plp2172/Df(3L)BrdR15* flies do not fully eclose from pupal cases and those that do are not motile, failing the previously established test for viability using *plp* transgenes[2]. The Ana1::tdTomato and Cep135::GFP flies were a gift of Tomer Avidor-Reiss (University of Toledo

2.3.11 References related to methods

1. Rossignol, P., Collier, S., Bush, M., Shaw, P. & Doonan, J. H. Arabidopsis POT1A interacts with TERT-V(I8), an N-terminal splicing variant of telomerase. Journal of cell science 120, 3678-3687 (2007).

2. Galletta, B. J. et al. Drosophila pericentrin requires interaction with calmodulin for its function at centrosomes and neuronal basal bodies but not at sperm basal bodies. Mol Biol Cell 25, 2682-2694 (2014).

3. Gibson, D. G. Enzymatic assembly of overlapping DNA fragments. Methods Enzymol 498, 349-361 (2011).

4. Galletta, B. J. & Rusan, N. M. A yeast two-hybrid approach for probing proteinprotein interactions at the centrosome. Methods Cell Biol 129, 251-277 (2015).

5. Cole, C., Barber, J. D. & Barton, G. J. The Jpred 3 secondary structure prediction server. Nucleic Acids Res 36, W197-201 (2008).

6. Kelley, L. A. & Sternberg, M. J. Protein structure prediction on the Web: a case study using the Phyre server. Nat Protoc 4, 363-371 (2009).

7. Letunic, I., Doerks, T. & Bork, P. SMART: recent updates, new developments and status in 2015. Nucleic Acids Res 43, D257-D260 (2014).

8. Lupas, A., Van Dyke, M. & Stock, J. Predicting coiled coils from protein sequences. Science 252, 1162-1164 (1991).

9. Mottier-Pavie, V. & Megraw, T. L. Drosophila bld10 is a centriolar protein that regulates centriole, basal body, and motile cilium assembly. Molecular biology of the cell 20, 2605-2614 (2009).

2.4 References

1. Boxem, M. et al. A protein domain-based interactome network for C. elegans early embryogenesis. *Cell* **134**, 534-545 (2008).
2. Giot, L. et al. A protein interaction map of Drosophila melanogaster. *Science* **302**, 1727-1736 (2003).
3. Formstecher, E. et al. Protein interaction mapping: a Drosophila case study. *Genome Res* **15**, 376-384 (2005).
4. Stanyon, C. A. et al. A Drosophila protein-interaction map centered on cell-cycle regulators. *Genome Biol* **5**, R96 (2004).
5. Dzhindzhev, N. S. et al. Asterless is a scaffold for the onset of centriole assembly. *Nature* **467**, 714-718 (2010).
6. Klebba, J. E. et al. Two Polo-like kinase 4 binding domains in Asterless perform distinct roles in regulating kinase stability. *J Cell Biol* **208**, 401-414 (2015).
7. Woodruff, J. B. et al. Regulated assembly of a supramolecular centrosome scaffold in vitro. *Science* **348**, 808-812 (2015).
8. Wueseke, O. et al. The Caenorhabditis elegans pericentriolar material components SPD-2 and SPD-5 are monomeric in the cytoplasm before incorporation into the PCM matrix. *Mol Biol Cell* **25**, 2984-2992 (2014).
9. Fu, J., Hagan, I. M. & Glover, D. M. The centrosome and its duplication cycle. *Cold Spring Harb Perspect Biol* **7**, a015800 (2015).

10. Fu, J. & Glover, D. M. Structured illumination of the interface between centriole and peri-centriolar material. *Open biology* **2**, 120104 (2012).
11. Mennella, V. et al. Subdiffraction-resolution fluorescence microscopy reveals a domain of the centrosome critical for pericentriolar material organization. *Nat Cell Biol* **14**, 1159-1168 (2012).
12. Sonnen, K. F., Schermelleh, L., Leonhardt, H. & Nigg, E. A. 3D-structured illumination microscopy provides novel insight into architecture of human centrosomes. *Biol Open* **1**, 965-976 (2012).
13. Gopalakrishnan, J. et al. Sas-4 provides a scaffold for cytoplasmic complexes and tethers them in a centrosome. *Nat Commun* **2**, 359 (2011).
14. Fu, J. et al. Conserved molecular interactions in centriole-to-centrosome conversion. *Nat Cell Biol* (2015).
15. Cottee, M. A., Raff, J. W., Lea, S. M. & Roque, H. SAS-6 oligomerization: the key to the centriole? *Nat Chem Biol* **7**, 650-653 (2011).
16. Cottee, M. A. et al. The homo-oligomerisation of both Sas-6 and Ana2 is required for efficient centriole assembly in flies. *Elife* **4**, e07236 (2015).
17. Conduit, P. T. et al. The centrosome-specific phosphorylation of cnn by polo/plk1 drives cnn scaffold assembly and centrosome maturation. *Dev Cell* **28**, 659-669 (2014).
18. Slevin, L. K. et al. The structure of the plk4 cryptic polo box reveals two tandem polo boxes required for centriole duplication. *Structure* **20**, 1905-1917 (2012).
19. Zwicker, D., Decker, M., Jaensch, S., Hyman, A. A. & Julicher, F. Centrosomes are autocatalytic droplets of pericentriolar material organized by centrioles. *Proc Natl Acad Sci U S A* **111**, E2636-45 (2014).

20. Lawo, S., Hasegan, M., Gupta, G. D. & Pelletier, L. Subdiffraction imaging of centrosomes reveals higher-order organizational features of pericentriolar material. *Nat Cell Biol* **14**, 1148-1158 (2012).

21. Morris-Rosendahl, D. J. & Kaindl, A. M. What next-generation sequencing (NGS) technology has enabled us to learn about primary autosomal recessive microcephaly (MCPH). *Mol Cell Probes* **29**, 271-281 (2015).

22. Kantaputra, P. et al. The smallest teeth in the world are caused by mutations in the PCNT gene. *Am J Med Genet A* **155A**, 1398-1403 (2011).

23. Dzhindzhev, N. S. et al. Plk4 Phosphorylates Ana2 to Trigger Sas6 Recruitment and Procentriole Formation. *Curr Biol* **24**, 2526-2532 (2014).

24. Roque, H. et al. Drosophila Cep135/Bld10 maintains proper centriole structure but is dispensable for cartwheel formation. *J Cell Sci* **125**, 5881-5886 (2012).

25. Kratz, A. S., Barenz, F., Richter, K. T. & Hoffmann, I. Plk4-dependent phosphorylation of STIL is required for centriole duplication. *Biol Open* **4**, 370-377 (2015).

26. Ohta, M. et al. Direct interaction of Plk4 with STIL ensures formation of a single procentriole per parental centriole. *Nat Commun* **5**, 5267 (2014).

2.5 Figures

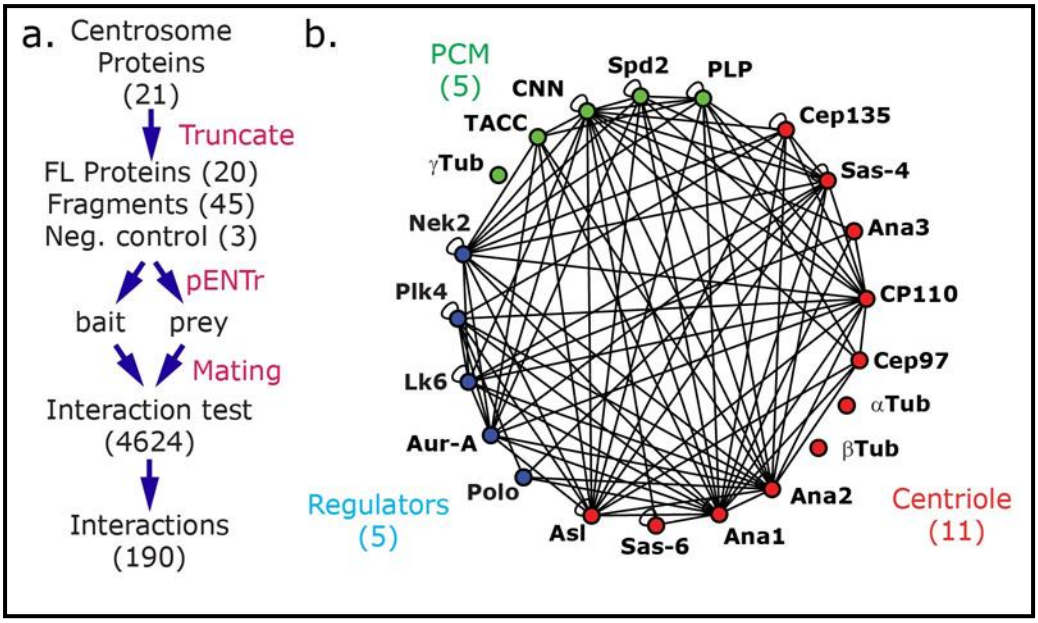

Figure 1. Y2H screen to determine the centrosome interactome

(**a**) Workflow of the centrosome array-based Y2H screen. (**b**) Summary of all interactions among the 21 centrosome proteins. Interactions details are summarized in supplemental material.

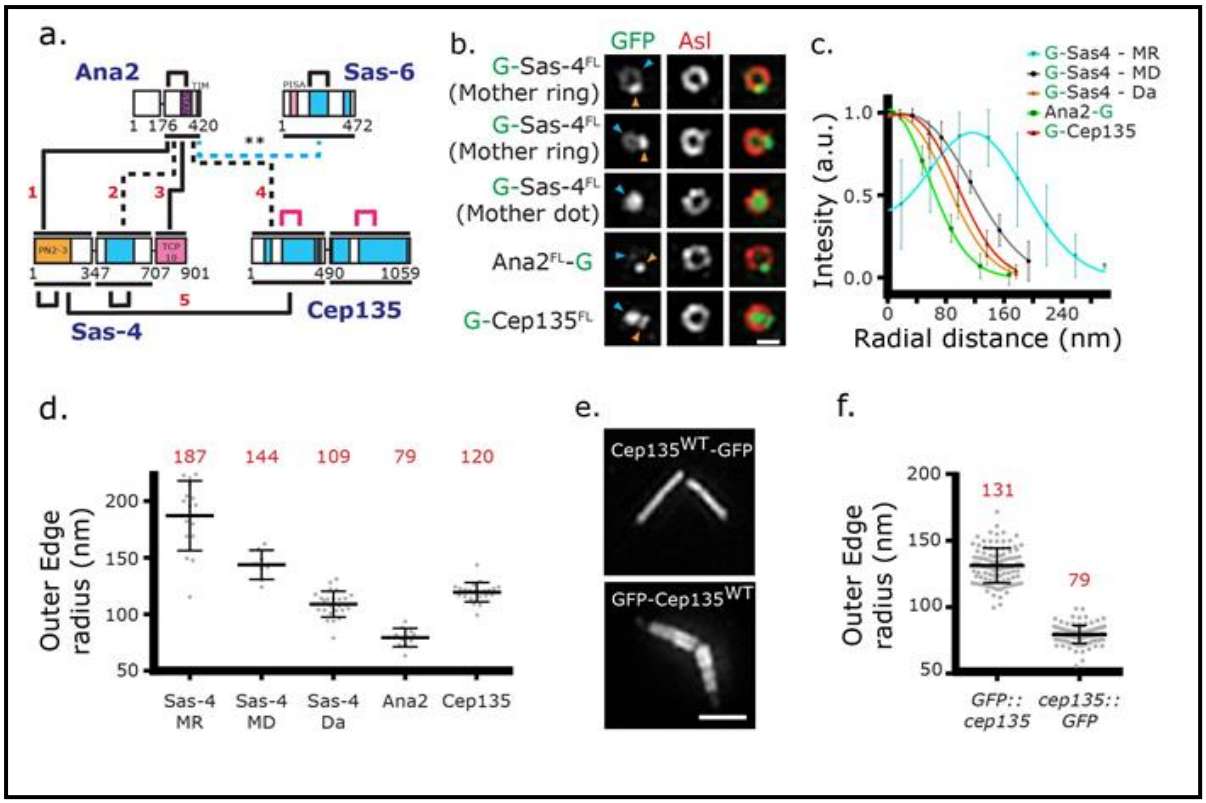

Figure 2. Centriole protein interactions reveal dynamic and stable components (a) Interactions (red numbers) among core centriole proteins. Numbers indicate amino acids, blue regions are predicted coiled-coils, dark black lines are interactions scoring 2 or 3, dashed lines scored 1, blue dotted line (**) indicates a phosphorylation dependent interaction (Fig. S8a; [23,25,26], black/pink loops indicate self-interactions). (b) Sas-4 presents as dots (D) or rings (R) in mothers (M) and only dots in daughters (Da). Ana2 is always a single dot, while Cep135$^{N\text{-term}}$ forms small rings. (c) Averaged intensities of line scans across centrioles aligned from the centriole center and moving out. Lines are fits to average data. Error is ± SD. N=8–25 centrioles. (d) Outer edge measurements showing mean (red number) of individual fits of data in c ±SD. (e) Positions of Cep135 N- and Ctermini in spermatocyte centrioles. (f) Outer edge measurements showing mean (red number) ±SD. Ns>100 centrioles. Scale bars b=400nm, e=1µm**.**

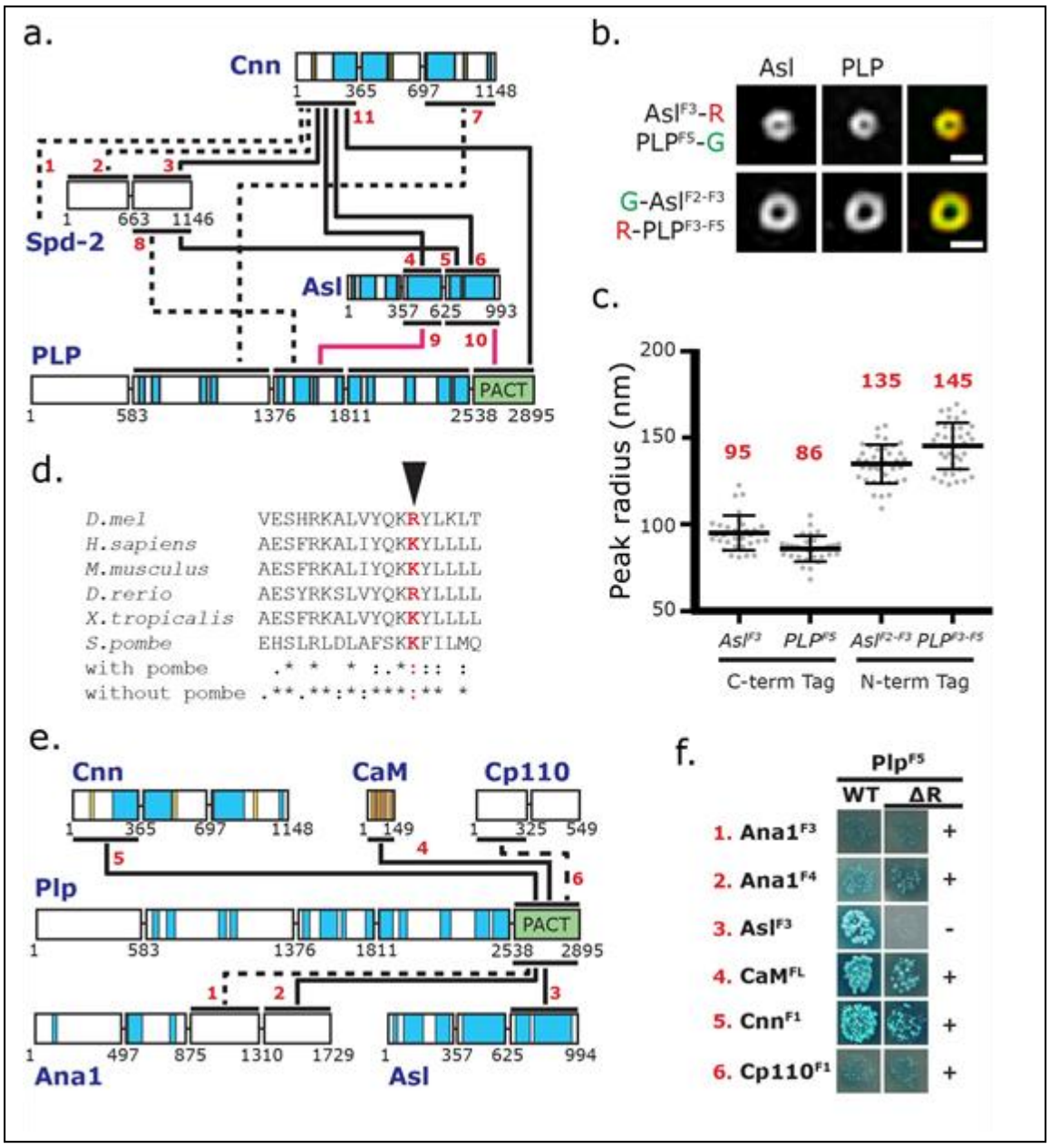

Figure 3. PCM protein interactions predict position and function

(a) Interactions among PCM proteins. (b) SIM of Asl and Plp in S2 cell centrioles showing the close proximity of the C-termini near the centriole wall, and the position of the central regions extended outward. (c) Peak radius measurements showing mean (red number) ±SD, Ns>30 centrioles. (d) Alignment within the PACT domain of Pcnt indicating the highly-conserved residue (red, arrowhead) mutated in MCPH patients 22. (e) Interactions identified with PLP2539-

2895 (includes PACT). (f) Y2H interactions of wild type (WT) and PLPΔR2720 (ΔR) versions of PLP2539-2895. ΔR results in the exclusive loss of the AslF3 interaction. Scale bars=400nm.

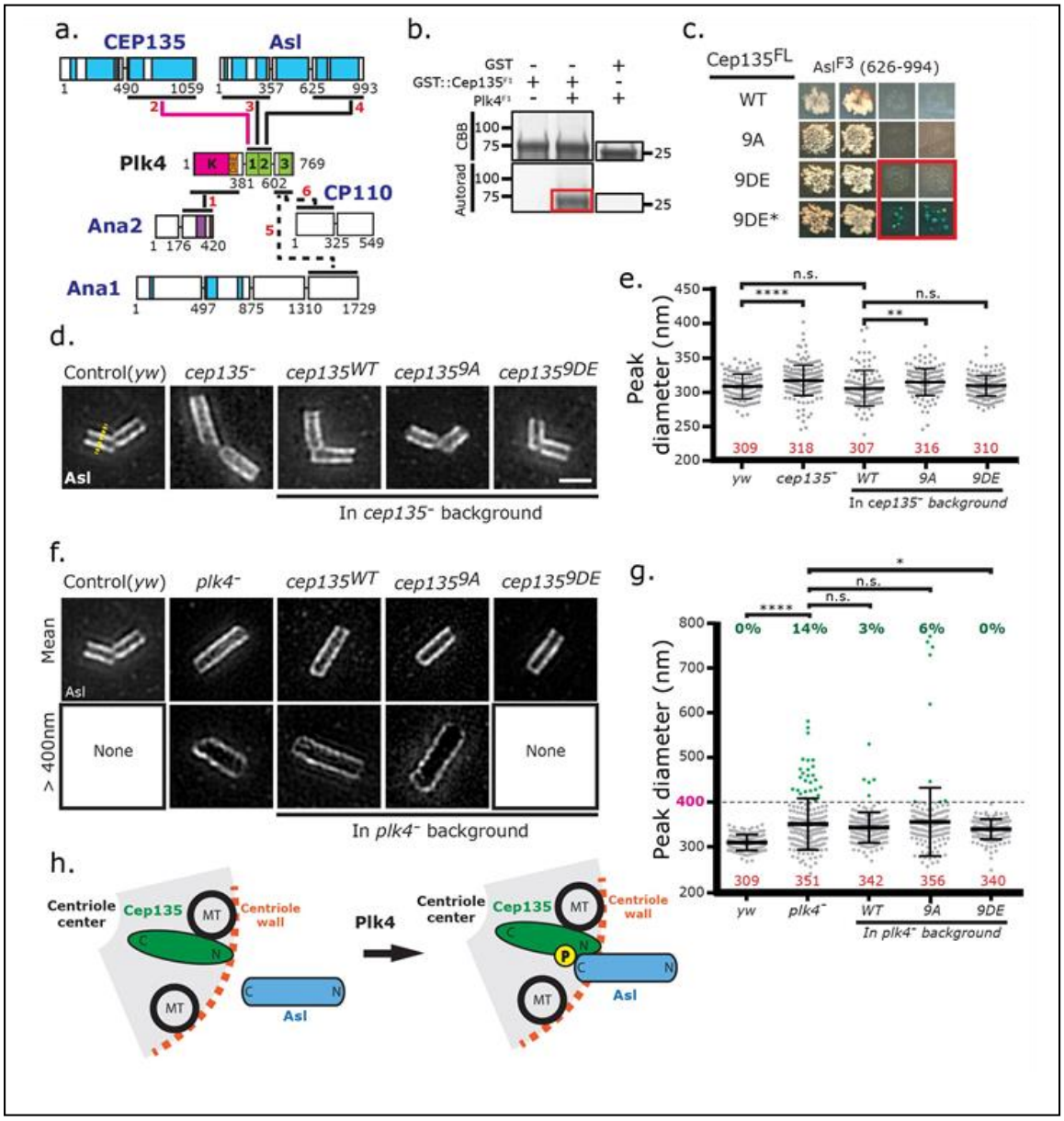

Figure 4. Plk4 phosphorylates Cep135 to position Asl

(a) All Plk4 interactions identified in screen (red numbers). (**b**) Plk4 *in vitro* kinase assay phosphorylates Cep135$^{1\text{-}490}$ (red box). Coomassie brilliant blue (CBB) gel (top) and autorad

(bottom); GST used as negative control (right). (**c**) Phosphomimetic $Cep135^{FL9DE}$ gains interaction with Asl^{F3} (red box), while $Cep135^{FL-WT}$ and $Cep135^{FL-9A}$ do not. Asterisk indicates 10-day growth. (**d**) SIM of Asl immunofluorescence in spermatocyte centrioles of indicated genotypes; representative linescan (yellow). (**e**) The expanded peak diameter of Asl in *cep135* mutant centrioles is rescued by $Cep135^{FL-WT}$ and $Cep135^{FL-9DE}$, but not $Cep135^{FL-9A}$. Bars indicate the mean (red numbers) ±SD; Ns>100 centrioles. (**f**) SIM of Asl immunofluorescence in spermatocyte centrioles. Representative centriole at the mean width (top) and >400nm (>5 SDs) of indicated genotypes; yw and $Cep135^{FL-9DE}$ (in *plk4* background) show no centrioles >400nm. (g) *plk4* mutant centrioles show great expansion of Asl peak diameter, which is partially rescued by $Cep135^{FL-9DE}$. Bars indicate the mean (red numbers) ±SD; Ns>100 centrioles. (**h**) Model based showing how Cep135 is oriented in the centriole, with its N-terminus extending near the centriole wall. Phosphorylation of Cep135 by Plk4 induces a Cep135-Asl interaction that properly positions Asl within the centriole. ****=P<0.0001, **=P ≤ 0.01, *=P≤0.05, n.s.=not significant. Bars=1µm

2.5 Supplementary Figures

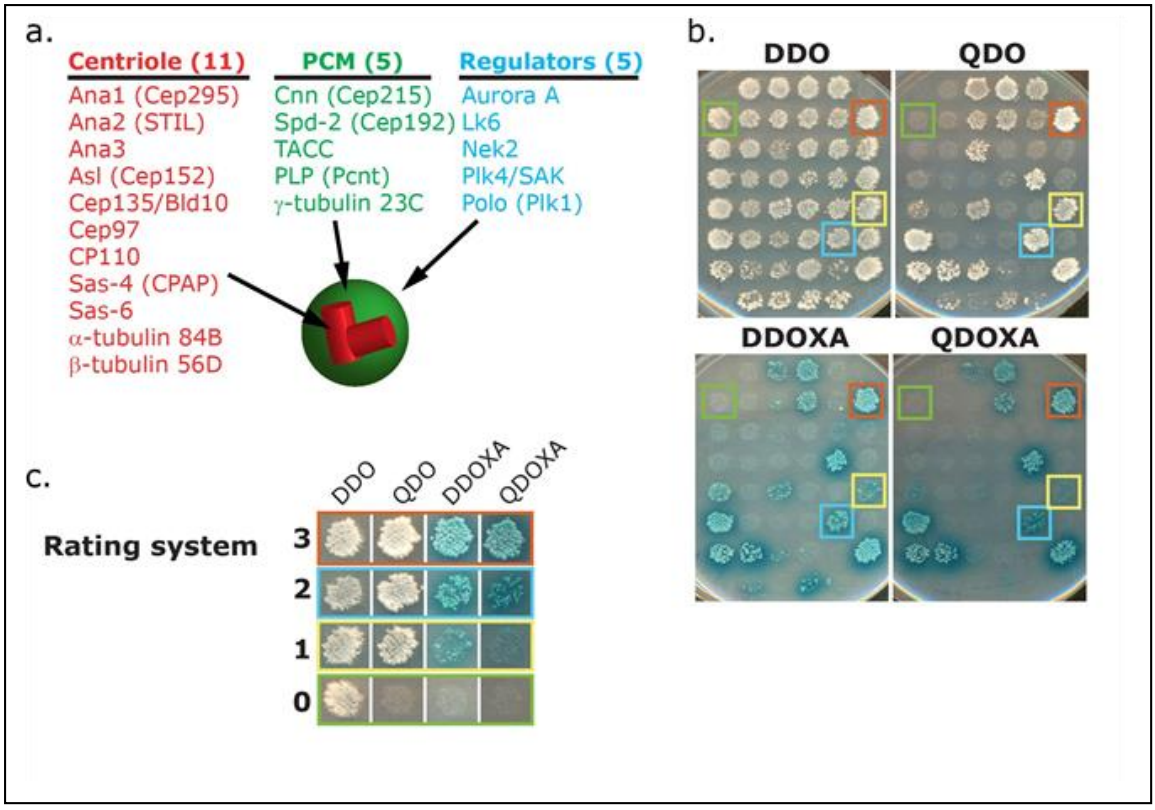

Figure S1. Details of Y2H screen design

(**a**) Proteins included in the Y2H screen including centriole proteins, PCM proteins and regulatory kinases. (**b**) Example of a single plate from the Y2H screen. Each colony tests the interaction between a single pair of proteins. DDO plates select for the presence of the Y2H plasmids. QDO plates select for the Y2H plasmids and test for the *ADE2* and *HIS3* reporters, the least stringent interaction condition tested. DDOXA plates select for the Y2H plasmids and test for the MEL1 and *AUR1-C* reporters. QDOXA plates select for the Y2H plasmids and tests for all four reporters, the most stringent conditions for interaction tested. Colored boxes are examples of colonies to highlight our rating system in c. (**c**) Example of the rating system used to score colonies. Column 1 – DDO plate, Column 2 – QDO plate, Column 3 - DDOXA plate,

Column 4 – QDOXA plate. The numbers indicate the relative amount of growth and blue color observed on the QDOXA plate (column 4).

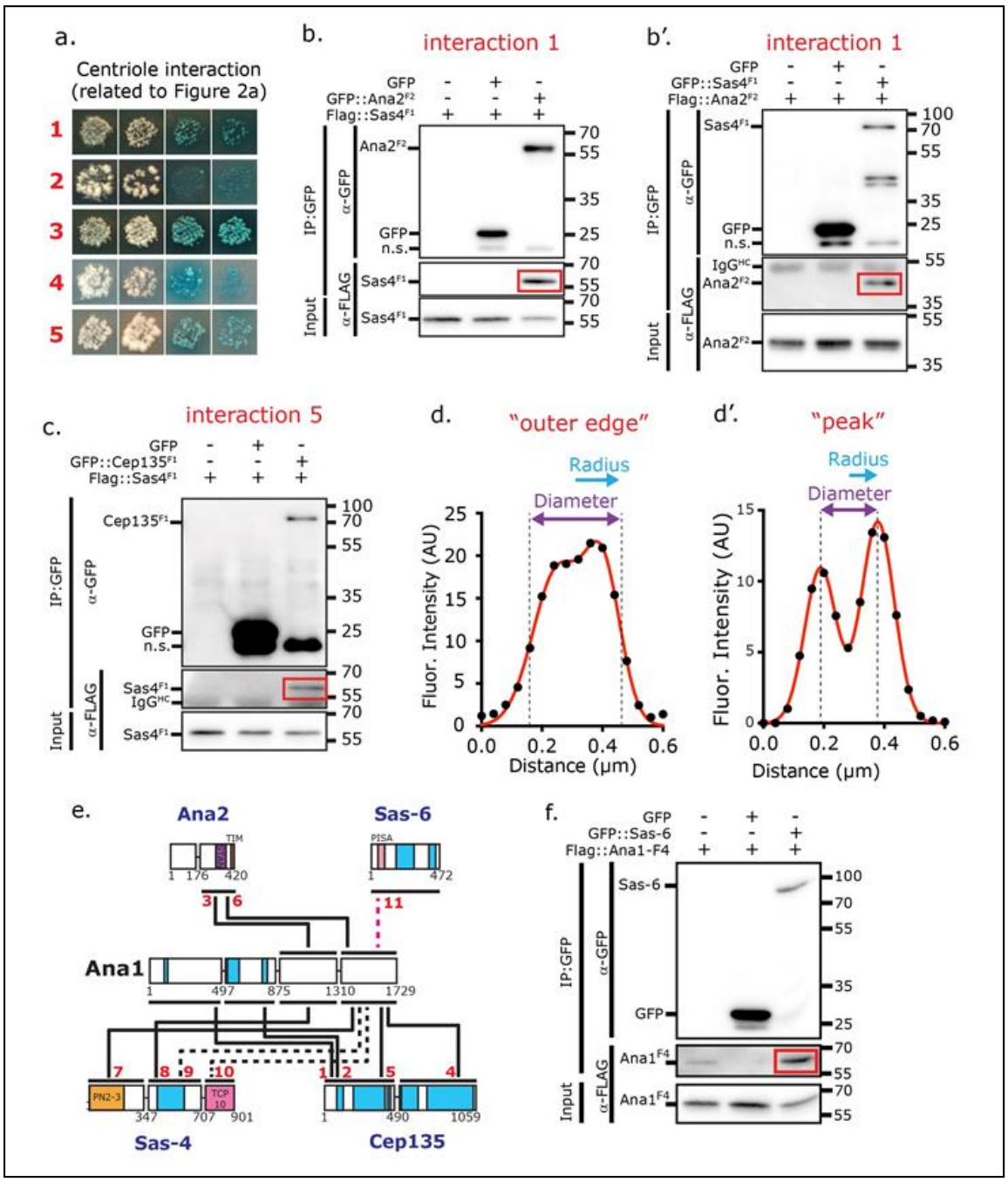

Figure S2. Information regarding Figure 2

(**a**) Results of Y2H interactions among the core centriole proteins. Red numbers refer to interactions indicated in Figure 2a. Y2H data is arranged as in S1c. (**b and b'**). Confirmation of Sas4^{F1} and Ana2^{F2} (interaction #1 from Figure 2a and S2a) by co-IP in both directions. Red box highlights protein in the IP. (**c**) Self-interaction of Cep135^{F1} shown by co-IP. (**d and d'**).

Examples of line scans across centrioles. Black circles indicate data. Red line is the fit to the sum of two Gaussians. Diameters (purple arrows) and Radii (blue arrows) are indicated for the Peak and Outer Edge measurements. (e) All 11 interactions identified between Ana1 and the core centriole proteins. (f) Ana1-Sas6 interaction (#11 in e) shown by co-IP. Sizes are in kDa in b, b', c and f.

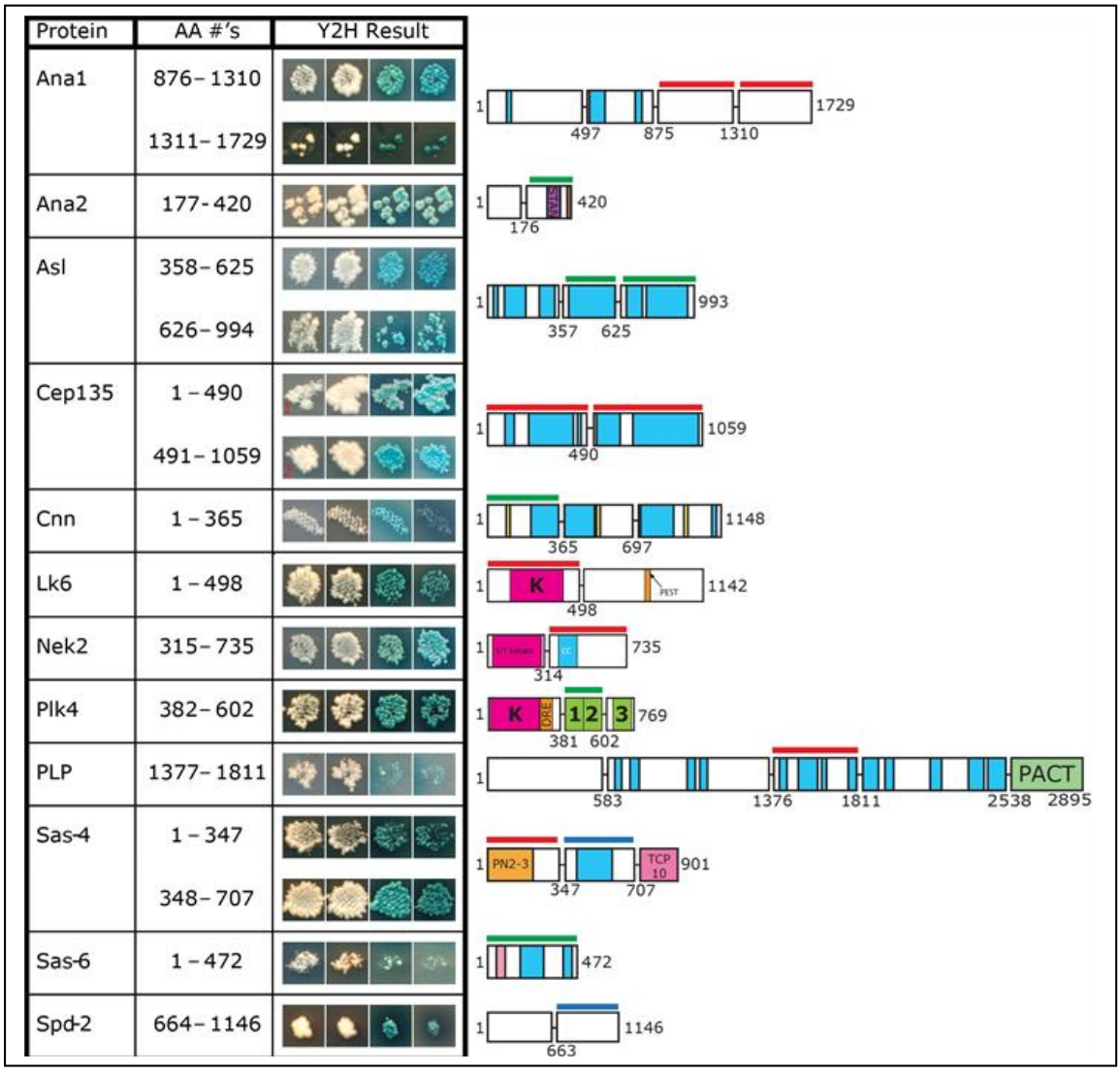

Figure S3. Protein oligomerization (self-association) domains

(a) Y2H data is arranged as in S1c. Red lines indicate fragments with novel interactions. Blue lines indicate fragments were the interaction is known in a different experimental system or where the region of interaction in *Drosophila* has been refined by our screen.

Green lines indicate previously described interactions. Numbers are amino acids.

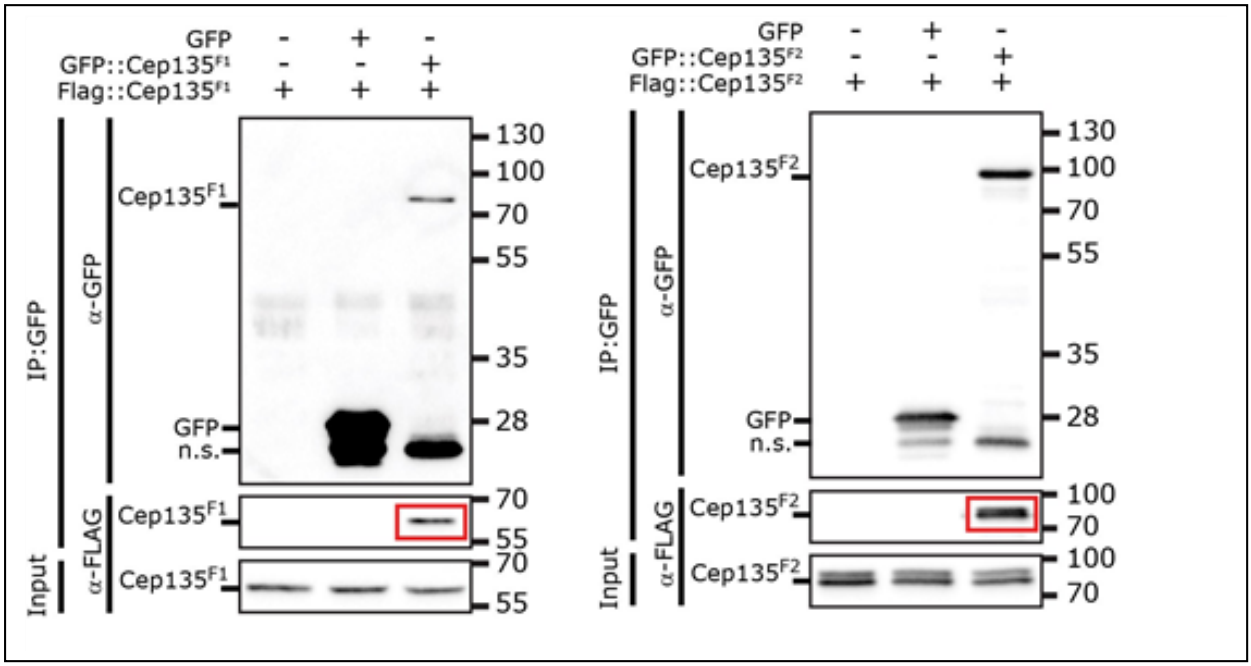

Figure S4. Cep135 self-association

Co-IPs showing Cep135N-term and Cep135C-term self-association. These data are in support of the Y2H data show in Figure 2a (pink loops). Red box highlights protein in the IP. Sizes are in kDa

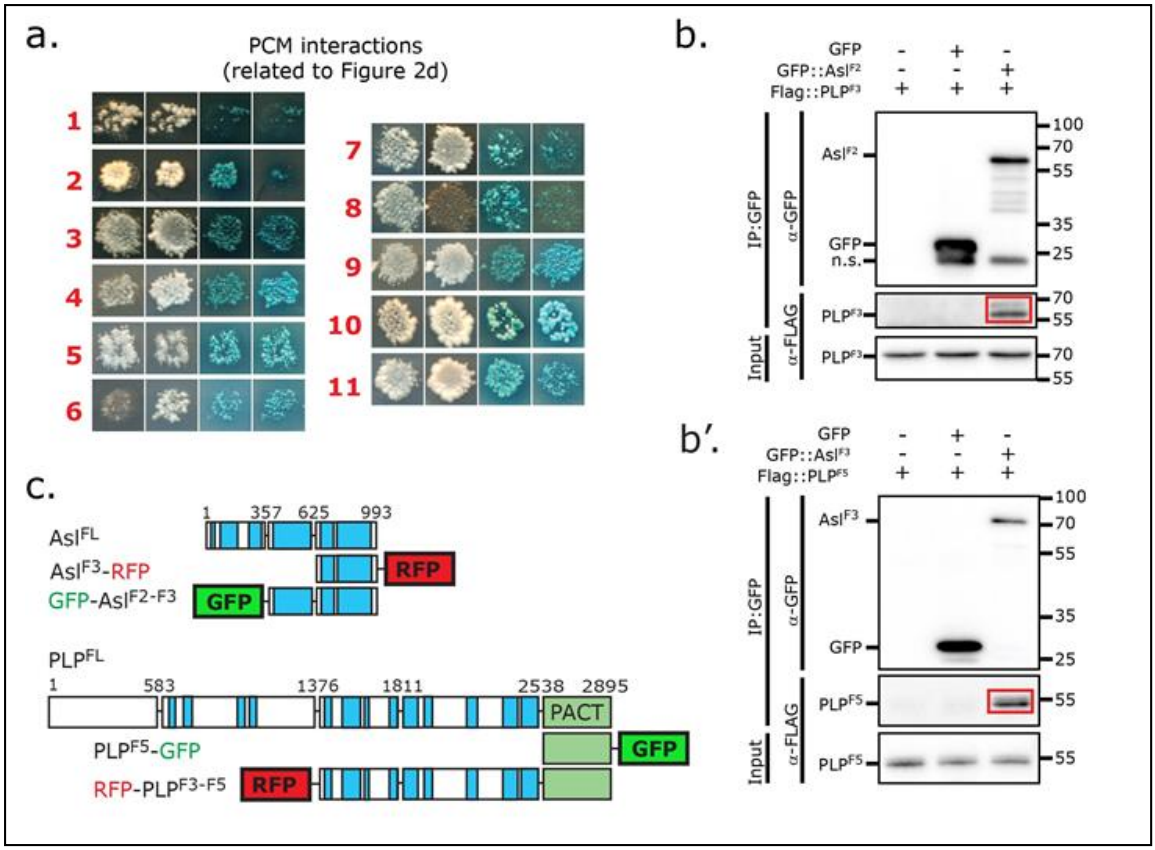

Figure S5. Information related to Figure 3

(**a**) Results of Y2H interactions among the PCM proteins. Red numbers refer to interactions indicated in Figure 3a. Y2H data is arranged as in S1c. (**b and b'**) Co-IP confirmation of Asl^{F2}-Plp^{F3} and Asl^{F3}-Plp^{F5} interactions (interaction #9 and 10 from Figure 3a). Red box highlights protein in the IP. Sizes are in kDa. (c) Schematics of Asl and PLP constructs used in Figure 3b.

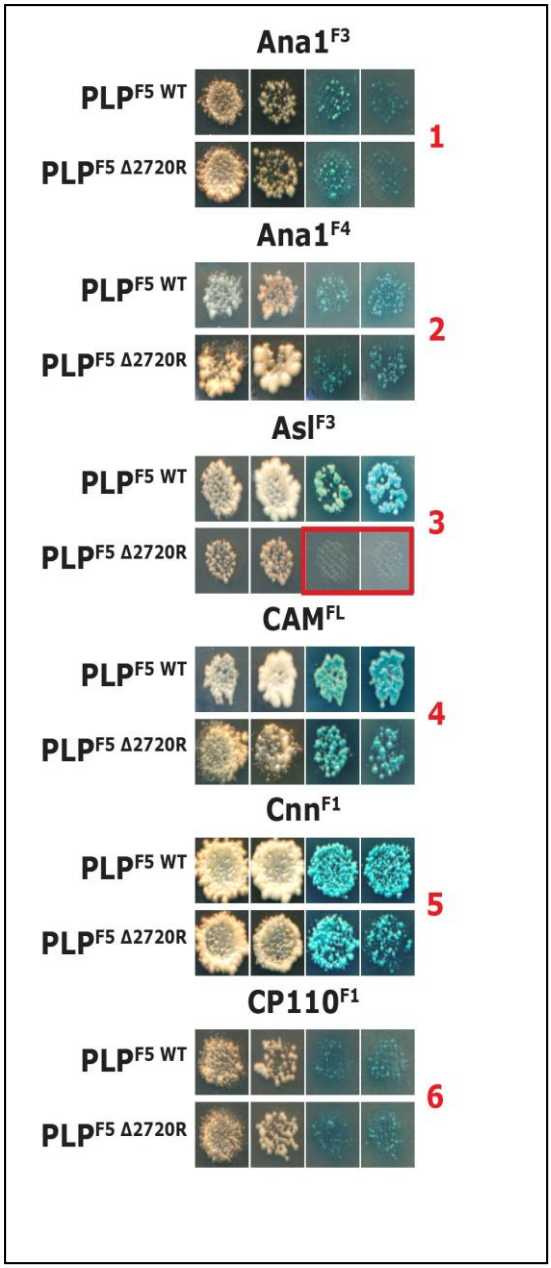

Figure S6. Information related to Figure 3d

Complete Y2H data for interactions of $Plp^{F5\text{-}WT}$ and $plp^{F5\text{-}\Delta 2720R}$ (MCPH mutant). PLP^{F5} = aa 2539 – 2895 and includes the PACT domain. Red numbers refer to interactions indicated in Figure 3e, f. Y2H data is arranged as in S1c. Red box highlights the significant loss of interaction between $plp^{F5\text{-}\Delta 2720R}$ and Asl^{F3}.

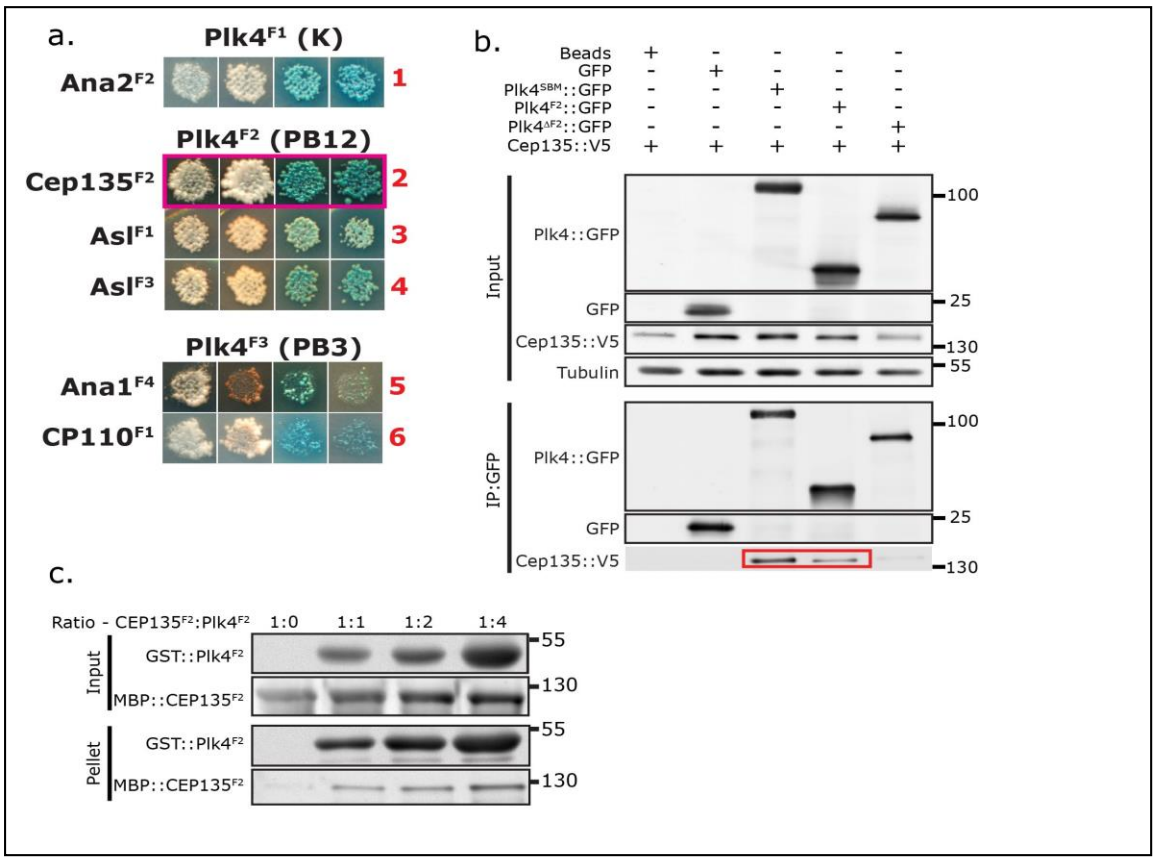

Figure S7. Information related to Figure 4

(**a**) Results of Y2H interactions with Plk4. Red numbers refer to interactions indicated in Figure 4a. Y2H data is arranged as in S1c. Pink box highlights the interaction of Plk4 with Cep135. (**b**) The middle of Plk4 (Plk4^{F2}, aa 382 -602), containing polo boxes 1 and 2, is necessary and sufficient for interaction with Cep135. GFP was IPed from S2 cells expressing the indicated constructs. Plk4^{SBM} contains a mutation in the slimb-binding domain that causes stabilization of Plk4[1]. Plk4$^{\Delta F2}$ is missing residues 382 – 602. Co-IP and blots with the indicated constructs was performed as in S2c, except that anti-V5 was used instead of anti-FLAG antibody. Red box highlights that Cep135 is Co-IPed by Plk4^{SBM} and Plk4^{F2}. Sizes are in kDa. (**c**) Recombinant Plk4^{F2} and Cep135^{F2} (aa 491 – 1059) interact *in vitro*. Recombinant Plk4^{F2} and Cep135^{F2} were

mixed at the indicated ratio and GST was pulled down. Increasing amounts of Plk4^{F2} pull down increasing amounts of Cep135.

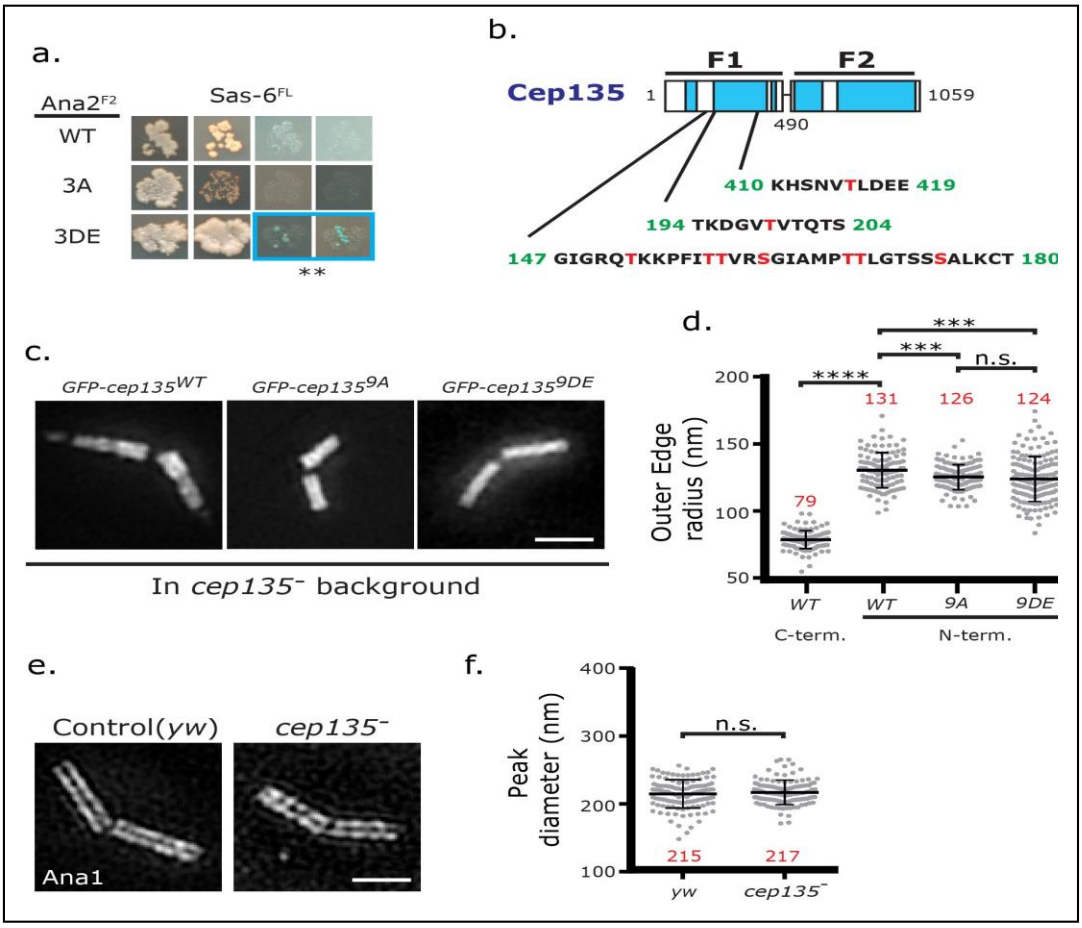

FigureS8. Information related to Figure 4

(**a**) Phosphomimetic (3DE) Ana2F2 interacts with Sas6FL (blue box), but wild type (WT) and unphosphorylatable (3A) Ana2F2 do not. Asterisks refer to the interaction in Figure 2a (blue dashed line). Y2H data is arranged as in S1c. (**b**) Schematic of Cep135 indicating the phosphorylated reduces identified by *in vitro* kinase assay with Plk4 (Figure 4b). (**c**) Images of spermatocyte centrioles from transgenic animals expressing the indicated constructs in the cep135 mutant background. GFP-tagged wild type (WT), unphosphorylatable (9A) and phosphomimetic (9DE) Cep135 all localize to centrioles in the spermatocytes of transgenic flies.

(**d**) Outer edge radii of Cep135 on spermatocyte centrioles. Bars indicate the mean (red numbers) ± standard deviation. Numbers of centrioles measured – WT C-term N=117 (same data as in Figure 2h), WT N-term N=109 (same data as in Figure 2h), 9A N=124, 9DE N=154. (**e**) Ana1::tdtomato direct fluorescence in control (yw) and cep135 mutant centrioles. Loss of Cep135 does not affect Ana1 positioning. (**f**) Peak diameter measurements of Ana1-labeled spermatocyte centrioles. Ana1 position is unaffected by the absence of Cep135. Bars indicate the mean (red numbers) ± standard deviation. Number of centrioles measured – yw N=124, cep135 N=112. **** = $P<0.0001$, *** = $P\leq 0.001$, "n.s." = not significant. Scale bars=1μm

1. Rogers, G. C., Rusan, N. M., Roberts, D. M., Peifer, M. & Rogers, S. L. The SCF Slimb ubiquitin ligase regulates Plk4/Sak levels to block centriole reduplication. *The Journal of cell biology* **184**, 225-239 (2009).

CHAPTER THREE: PLK4 PHOSPHORYLATION OF ANA2 INHIBITS THEIR ASSOCIATION AND SUPPRESSES CENTRIOLE DUPLICATION

All S2 cell work performed by TAM. In vitro kinase assays performed by DWB.

3.1 Abstract

Polo-like kinase 4 (Plk4) initiates an early step in centriole assembly by phosphorylating Ana2/STIL, a structural constituent of the procentriole. Here, we show that Plk4 binding to the central coiled-coil (CC) of Ana2 is a conserved event, involving both Polo-box 3 and a previously unidentified CC located adjacent to the kinase domain. Ana2 binding stimulates Plk4 kinase activity in vitro, and, in turn, is phosphorylated on three N-terminal residues. Previous studies showed that Plk4 phosphorylates the C-terminal STAN domain of Ana2/STIL, triggering binding and recruitment of the cartwheel protein Sas6 to the centriole assembly site. However, the physiological relevance of the N-terminal phosphorylations is unknown. Surprisingly, replacement of endogenous Ana2 with phosphomimetic Ana2-3E mutant disrupts the Plk4-Ana2 complex, consequently preventing Sas6 association and suppressing centriole duplication. Moreover, Ana2-3E localizes to centrioles suggesting that Ana2 recruitment to centrioles is independent of a direct interaction with Plk4. Thus, Plk4 both positively and negatively regulates centriole assembly by phosphorylating distinct regions in Ana2.

3.2 Introduction

Centriole duplication begins with the formation of a procentriole assembling orthogonally from the proximal end of each parent centriole (Fu et al., 2015). Procentriole assembly involves the hierarchical recruitment of a conserved set of proteins, SPD-2/DSpd-2/Cep192, Plk4/ZYG-1, SAS-5/Ana2/STIL, Sas6 and Sas4/CPAP, to a single assembly site on the mother centriole (Avidor-Reiss and Gopalakrishnan, 2013). Polo-like kinase 4 (Plk4) activity is essential for

centriole assembly and its overexpression induces not only amplification from pre-existing centrioles but also de novo assembly (Bettencourt-Dias et al., 2005; Habedanck et al., 2005; Peel et al., 2007; Rodrigues-Martins et al., 2007; Kleylein-Sohn et al., 2007; Holland et al., 2010; Lopes et al., 2015). Characterizing Plk4 regulation of specific substrates is key to understanding centriole biogenesis.

Drosophila Anastral Spindle 2 (Ana2; STIL in humans) is an essential core centriole protein that follows Plk4 to the daughter assembly site, and contains an N-terminal Sas4-binding site, a central coiled-coil (CC), and a C-terminal STAN domain (Fig. S1 A) (Goshima et al., 2007; Stevens et al., 2010a; Tang et al., 2011; Cottee et al., 2013; Hatzopoulos et al., 2013). Ana2 tetramerizes through the CC and binds Sas6, a rod-shaped protein, through the STAN domain (Stevens et al., 2010a; Shimanovskaya et al., 2013; Slevin et al., 2014; Cottee et al., 2015). Ana2 tetramers may bind and facilitate Sas6 assembly into rings on the mother centriole's surface, ultimately creating the stack of Sas6 rings that form the cartwheel of the nascent procentriole (Stevens et al., 2010b; Guichard et al., 2012; Cottee et al., 2015; Moyer et al., 2015; Rogala et al., 2015).

Plk4 extensively phosphorylates Ana2/STIL and, in particular, the STAN domain which promotes Sas6 binding (Dzhindzhev et al., 2014; Ohta et al., 2014; Arquint et al., 2015; Kratz et al., 2015; Moyer et al., 2015); a critical event providing a regulated mechanism for Sas6 recruitment to centrioles and procentriole formation. In addition, Plk4 phosphorylates several upstream residues in Ana2/STIL with unknown functional consequences. Plk4 also binds the CC domain in STIL (Ohta et al., 2014; Moyer et al., 2015; Kratz et al., 2015), involving PB3 and an

obscure second site located within its large linker (L1) region (Arquint et al., 2015). Current models suggest that Ana2 is recruited to centrioles through this interaction, as CC deletion mutants prevent Plk4 binding and centriole targeting (Ohta et al., 2014; Arquint et al., 2015; Cottee et al., 2015; Moyer et al., 2015). Our results suggest that Plk4 can suppress centriole assembly by phosphorylating residues outside the STAN domain and show that Ana2 localization to centrioles can occur without direct binding to Plk4.

3.3 Results

3.3.1 Ana2 interacts with two distinct regions of Plk4

To test if Plk4 and Ana2 binding occurs in Drosophila, we co-expressed transgenic V5-Ana2 and Plk4-GFP in S2 cells depleted of endogenous Ana2 (Fig. S1, B and C). Whereas full-length (FL) Ana2 co-immunoprecipitated (co-IP) with Plk4, Ana2 lacking the CC (ΔCC) did not (Fig. S1 D). Thus, the Plk4-Ana2 interaction is conserved in flies and requires the Ana2-CC.

Plk4 contains several functional domains (Klebba et al., 2015a): an N-terminal kinase domain followed by the Downstream Regulatory Element (DRE), and three Polo-boxes (PB1-3) interrupted by linkers L1 and L2 (Fig. 1 A). Mapping of the STIL binding domain in human Plk4 has generated conflicting results (Ohta et al., 2014; Arquint et al., 2015). To map Ana2 binding sites, we performed co-IP experiments using V5-Ana2 with either FL or truncated Plk4-GFP proteins (Fig. 1 A). Ana2 associates with Plk4-FL and PB3 but not PB1-PB2 (Fig. 1 B), in agreement with Arquint et al. (2015). Ana2 also weakly co-IPs with Plk4 1-381 and 1-317, which both lack PBs. Yeast two-hybrid analysis confirmed these results; Ana2 interacts with 1-381 and PB3, but not PB1-PB2 (Fig. S1 E). Therefore, Ana2 associates with two distinct regions

of Plk4: PB3 and an N-terminal region restricted to the kinase domain, CC, and DRE. The possibility that Plk4 kinase activity regulates Plk4/STIL interaction has been investigated but remains unresolved (Ohta et al., 2014; Moyer et al., 2015), so we examined this in Drosophila by co-expressing Ana2 with wild-type (WT) or kinase-dead (KD) Plk4 in S2 cells and then evaluating interactions by co-IP. Ana2 associated more with inactive KD-Plk4 than WT (Fig. 1 C), indicating that kinase activity suppresses this interaction in Drosophila.

Using protein structure prediction software, we identified a conserved, previously uncharacterized coiled-coil (Plk4-CC) within Plk4 1-317, immediately adjacent to the kinase domain (Figs. S1, F and G). To test the role of the Plk4-CC domain on Ana2 binding, we performed co-IPs from S2 cells expressing Plk4 constructs lacking PB3 and one or more N-terminal modules (Fig. 1 D). Ana2 association decreased ~2-fold by PB3 deletion and was significantly reduced a further ~2-fold by deletion of both the Plk4-CC and PB3 regions. Combined with the observation that Ana2 associates with a Plk4 truncation consisting of only CC-DRE (Fig. 1 E), this result pinpoints the Plk4-CC as the other Ana2-binding domain besides PB3, although we cannot rule out additional Ana2-binding domains.

3.3.2 Ana2 stimulates Plk4 kinase activity in vitro

STIL overexpression stimulates Plk4 kinase activity in cultured human cells (Ohta et al., 2014; Moyer et al., 2015). It has been proposed that STIL binding stimulates Plk4 activity by relieving L1-mediated autoinhibition (Arquint et al., 2015). In this model, STIL binds both PB3 and L1, and repositions L1 so that it no longer prevents Plk4 from autophosphorylating its activation loop. This model integrates well with our finding that the presence of L1 reduces Plk4 kinase

activity (Klebba et al., 2015a). If Ana2/STIL stimulates Plk4 activity by relieving L1-mediated autoinhibition, then Ana2 should not stimulate kinase activity of Plk4 lacking L1. To test this, purified minimal Plk4 protein (amino acids 1-317) containing kinase domain-CC-DRE but lacking L1 was assayed in vitro in the presence of increasing concentrations of GST-Ana2. Plk4 1-317 autophosphorylation was low in the absence of Ana2, but surprisingly, increased with addition of Ana2 in a dose-dependent manner (Figs. 2, A and B). A plot of the initial reaction velocities as a function of Ana2 concentration indicates that autophosphorylation rate is maximal when Ana2 is in 3-4x molar excess to Plk4 (Fig. 3 C). Notably, incubation of the autoinhibited Plk4 1-381 construct (which includes L1) with Ana2 failed to stimulate kinase activity (Figs. 2, D and E), suggesting that the PB3 domain is required for Ana2 to accelerate Plk4 autophosphorylation when L1 is present.

Plk4 activity is greatly increased by trans-autophosphorylation of its activation loop, which includes a conserved threonine, T172 (Swallow et al., 2005; Klebba et al., 2015a; Lopes et al., 2015). If Ana2 stimulates Plk4 kinase activity, then T172 phosphorylation should also increase. To test this, we generated Plk4 antibodies specific to phosphorylated T172 (Fig. S1 H) and found that phosphorylated T172 in Plk4 1-317 either increased or decreased depending on the presence or absence, respectively, of Ana2 (Fig. 2 F). Interestingly, anti-pT172 detected two bands of activated Plk4: an upper, ostensibly hyper-phosphorylated band (open arrowhead) and a lower, less phosphorylated band (filled arrowhead). Since prominent anti-pT172 staining first appears in the lower band, T172 may be one of the first autophosphorylated residues. Thus, while Ana2 may manipulate L1 to relieve autoinhibition, Ana2 also stimulates Plk4 kinase activity by a mechanism independent of L1. We propose that tetrameric Ana2 binds multiple

Plk4s in a proximity and orientation that facilitates trans-autophosphorylation.

3.3.3 Ana2 is a Plk4 and PP2A substrate

Previous studies show that Ana2/STIL is phosphorylated by Plk4 and that modification of the STAN domain promotes Sas6 binding (Dzhindzhev et al., 2014; Ohta et al., 2014; Arquint et al., 2015; Kratz et al., 2015; Moyer et al., 2015). We used tandem mass spectrometry (MS) to identify the phosphorylated residues of Ana2 incubated with Plk4 in vitro. Plk4 phosphorylated Ana2 on 5 residues (Fig. 3 A, Table S1 A), including 2 conserved residues within the STAN domain and 3 residues (T69, T159 and T242) flanking the Ana2-CC. Plk4 is not a highly promiscuous kinase; e.g., it does not phosphorylate Sas6 (Fig. S1 I).

Several Ana2 residues we mapped from in vitro samples were shown to be phosphorylated in cells co-expressing Plk4, including T69 (Dzhindzhev et al., 2014). We also examined in vivo phosphorylation by isolating GFP-Ana2 from asynchronous S2 cells and performing MS/MS (Table S1 B). From 83% coverage, we found that Ana2 is phosphorylated on 12 residues, including T159 (Fig. S2 A). Although Plk4 levels are very low in S2 cells (Rogers et al., 2009) and seem unlikely responsible for most Ana2 modifications.
Since SAS-5 (C. elegans Ana2 ortholog) is a Protein Phosphatase 2A (PP2A) substrate (Kitagawa et al., 2011; Song et al., 2011), we tested whether inhibition of PP2A with okadaic acid (OA) could reveal additional phospho-residues in Ana2. After treating cells with OA, we identified 6 more modified residues, including T242 (Fig. S2 A; Table S1 C). Additionally, we depleted individual subunits of the PP2A holoenzyme in S2 cells and then examined the mobility of endogenous Ana2 on SDS-PAGE (Fig. 3 B). Strikingly, depletion of Mts (PP2A catalytic

subunit), 29B (structural), Wrd or Wdb (regulatory), shifted Ana2 to a slower electrophoretic mobility, presumably due to its hyperphosphorylation. Wdb and Wrd are reported to display partial functional redundancy (Kotadia et al., 2008) but, curiously, the effect of double Wrd/Wdb RNAi was no different than single RNAi. In the reverse experiment, we tested whether overexpression of a regulatory subunit could shift Ana2 to the faster migrating/dephosphorylated species (Fig. 3 C). Only Wrd had this effect. Our findings do indicate that Ana2 is likely a PP2AWrd substrate and that phosphorylation of T242 may be a key event in Ana2 regulation. The connection between Wdb depletion and Ana2's phosphorylation state is unclear.

3.3.4 Phosphorylation of Ana2 by Plk4 suppresses centriole assembly

We next focused on the phosphorylatable residues T69/T159/T242 and examined their effects on centriole duplication. First, we generated non-phosphorylatable and phosphomimetic Ana2 by mutating all three residues to alanines (3A) or glutamic acids (3E) and transfected these into S2 cells depleted of endogenous Ana2. Centriole numbers were measured using the centriole marker PLP (Mennella et al., 2012; Fu and Glover, 2012) (Fig. 3 D). As expected, Ana2 depletion significantly decreased the percentage of cells with a normal number of centrioles. Centriole numbers were rescued in treated cells by expression of either WT Ana2 or Ana2-3A, but not by Ana2-3E or Ana2 lacking the CC domain (ΔCC) which is required for both centriole assembly and localization (Dzhindzhev et al., 2014; Ohta et al., 2014; Arquint et al., 2015; Cottee et al., 2015; Moyer et al., 2015). Notably, no Ana2 protein induced significant centriole amplification (>2 PLP spots). Thus, although Plk4 phosphorylates the STAN domain to promote centriole assembly, our results indicate that phosphorylation of the Ana2 N-terminus suppresses centriole duplication.

As an additional functional assay, we tested whether phospho-mutant Ana2 works synergistically with Plk4 in driving centriole amplification. By itself, high Plk4 expression induces supernumerary centrioles (Bettencourt-Dias et al., 2005; Habedanck et al., 2005), but when Plk4 is weakly expressed, the percentage of cells with >2 PLP spots is not changed significantly (Fig. 3 E). Co-expression of Plk4 with WT Ana2 (but not Ana2-3E or ΔCC) increased the percentage of cells with >2 PLP spots, though this was not significant. However, Ana2-3A co-expression moderately but significantly increased centriole amplification. Thus, the phosphorylation state of the Ana2 N-terminus plays an important role in regulating centriole number: phosphomimetic Ana2 suppresses centriole duplication, whereas non-phosphorylatable mutant induces centriole when co-expressed with the normally rate-limiting Plk4.

3.3.5 Ana2 phosphorylation by Plk4 blocks their association

How does phosphorylation of the Ana2 N-terminus inhibit centriole duplication? One possibility is that phosphorylation alters Ana2's interaction with known binding partners, including itself. Ana2 forms a tetramer through its CC, and point mutations that block oligomerization disrupt Ana2 function in vivo (Slevin et al., 2014; Cottee et al., 2015). Since the phosphorylation sites flank the Ana2-CC, we examined whether phosphomimetic Ana2-3E inhibits self-association. Ana2-ΔCC did not co-IP with Ana2-WT (Fig. 4 A), demonstrating that the CC is required for self-association, as it is for STIL (Arquint et al., 2015). However, Ana2-3E was able to co-IP with Ana2-3E, suggesting that N-terminally phosphorylated Ana2 can oligomerize, though it does not support centriole duplication. Sas4 binds Ana2 (Cottee et al., 2013; Hatzopoulos et al., 2013) and, thus, is an attractive candidate for regulation by Plk4. Sas4 associated with Ana2

regardless of its phosphorylation state (Fig. 4 B), consistent with previous in vitro studies (Dzhindzhev et al., 2014). However,Ana2-ΔCC association with Sas4 was markedly diminished, a surprising result since the Sas4-binding site in Ana2/STIL is well upstream of the Ana2-CC (Fig. S1 A). Thus, Ana2 oligomerization may be a prerequisite for Sas4 binding.

Last, we examined the interaction between Ana2 and Plk4 (Fig. 4 C). Both Ana2-WT and Ana2-3A co-IPed with Plk4. Strikingly, however, Plk4 failed almost entirely to IP with Ana2-3E, similar to Ana2-ΔCC. The 3A mutant clearly bound Plk4 more extensively than the 3E mutant, supporting the conclusion that N-terminal phosphorylation of Ana2 blocks Plk4 binding. Therefore, the relationship between Ana2 and Plk4 is complex: Ana2 binds Plk4 and increases Plk4 autophosphorylation, but Ana2 is itself phosphorylated by Plk4, inhibiting both Plk4 binding and centriole duplication.

3.3.6 Phosphomimetic Ana2-3E localizes to centrioles

The CC in Ana2/STIL is necessary for centriole localization, perhaps by directly binding Plk4 (Ohta et al, 2014; Arquint et al., 2015; Cottee et al., 2015; Moyer et al., 2015). Since Ana2-3E has an intact CC but fails to associate with Plk4, we predicted that Ana2-3E would not localize to centrioles. To test this, we transfected Ana2 (WT or mutant) into endogenous Ana2-depleted cells and examined its localization (Fig. S2 B). Ana2-ΔCC was not found on centrioles in most interphase cells, but Ana2-WT, 3A, and surprisingly, 3E, all localized to centrioles. Since 1) Ana2-3E binds Plk4 poorly but still localizes properly, and 2) endogenous Plk4 protein levels are extremely low, it is unlikely that Ana2 must directly bind Plk4 to target centrioles. Nevertheless, we observed that co-expression of Plk4 visually enhanced the levels of Ana2-WT, 3A, and 3E

(but not ΔCC) on centrioles, allowing us to quantify the frequency of centriole co-localization (Figs. 4 D and E). Therefore, we hypothesized that Plk4 regulates Ana2 targeting to centrioles by a means not requiring direct binding. To test whether Plk4 kinase activity is responsible for Ana2 localization, we co-expressed kinase-dead-(KD)-Plk4 with Ana2. Strikingly, the frequency of both WT-Ana2 and 3E localization to centrioles was significantly diminished (Figs. 4 D and E). Contrary to the prevailing model, our data suggest that Ana2 recruitment to centrioles requires the kinase activity of Plk4 rather than direct physical interaction. Indeed, a recent study showed that chemical inhibition of Plk4 causes rapid loss of centriolar STIL despite dramatically increasing centriolar Plk4 levels (Moyer et al., 2015). We propose that Plk4 phosphorylates another, currently unidentified, structural subunit(s) on the mother centriole surface, which serves as the initiating event of centriole duplication by generating a high-affinity binding site for Ana2 recruitment.

3.3.6 Phosphorylation of the Ana2 N-terminus blocks Sas6 binding

So far, our data indicate that Plk4 phosphorylation of the Ana2 N-terminus disrupts Plk4 binding and centriole duplication, but these modifications do not affect Ana2 localization or self-association. In contrast, Plk4 phosphorylation of the Ana2 C-terminal STAN domain promotes procentriole assembly by triggering Sas6 binding (Dzhindzhev et al., 2014; Ohta et al., 2014; Kratz et al., 2015; Moyer et al., 2015). Therefore, it is possible that phosphomimetic Ana2-3E suppresses centriole duplication because Plk4 binding is inhibited and unable to phosphorylate the STAN domain to recruit Sas6. We measured the association of expressed Ana2 and Sas6 in S2 cells by taking advantage of the observation that Ana2-Sas6 complexes are detectable if Plk4 is also expressed (Dzhindzhev et al., 2014). S2 cells were co-transfected with Sas6 and Ana2

(WT or mutant) along with Plk4 (active non-degradable [SBM] or kinase dead [KD] forms), and then Ana2-Sas6 association evaluated by co-IPs (Fig. 5 A). As expected, the association of Ana2-WT and Sas6 was significantly increased by active Plk4-SBM but not by inactive Plk4-KD. However, association of Ana2-3E with Sas6 was dramatically reduced, regardless of the expressed Plk4's activity. This result argues that N-terminal phosphorylation of Ana2 prevents an important step in centriole assembly -- the binding of Ana2 and Sas6 -- and serves as a regulatory block to centriole duplication.

3.4 Summary

In summary, our data support the unexpected conclusion that Plk4 activity suppresses centriole assembly by phosphorylating N-terminal residues in Ana2, thereby inhibiting further association with Ana2 and preventing Sas6 binding. We propose the following model of Plk4 activation and control of centriole duplication (Fig. 5 B): (1) The initial kinase activity of newly synthesized, monomeric Plk4 is low due to L1-mediated autoinhibition (Klebba et al., 2015a). (2) Plk4 dimerizes, and through its PB3 and CC domains, interacts with tetrameric Ana2 which relieves L1-induced autoinhibition and (3) stimulates Plk4 trans-autophosphorylation by closely positioning two kinase domains. In turn, the Ana2 N-terminus is phosphorylated, disrupting Plk4 association. This negative feedback mechanism effectively uses Plk4 activity to prevent centriole overduplication by preventing STAN modifications required for Sas6 binding. (4) We hypothesize that a mitotic phosphatase (possibly PP2AWrd) dephosphorylates the Ana2 N-terminus while sparing the STAN domain modifications, thereby allowing Plk4 association and Sas6 recruitment. (5) During interphase, the activity of the phosphatase is too low to prevent

Plk4-Ana2 dissociation, thereby establishing a regulatory obstruction to centriole overduplication.

3.5 Materials and Methods

3.5.1 Cell culture and double-stranded RNAi

Drosophila S2 cell culture, in vitro dsRNA synthesis, and RNAi treatments were performed as previously described (Rogers and Rogers, 2008). Cells were cultured in Sf900II SFM media (Life Technologies). RNAi was performed in 6 well plates. Cells (40-90% confluency) were treated with 10µg of dsRNA in 1ml of media and replenished with fresh media/dsRNA every day for 5-7 days. A ~550 bp control dsRNA was synthesized from DNA template amplified from a non-coding sequence of the pET28a vector (Clontech) using the primers 5'-ATCAGGCGCTCT TCCGC and 5'-GTTCGTGCACACAGCCC. (All primers used for dsRNA synthesis begin with the T7 promoter sequence 5'-TAATACGACTCACTATAGGG, followed by template-specific sequence). dsRNA targeting the Ana2 UTR was synthesized from EST LD22033 template by first deleting the Ana2 cDNA, and then joining 91 bp of 5'UTR with 78 bp of 3'UTR to create the following sequence: 5'-AGTTCCACCCCTAAGTCGATCGACTTCCAATTGGACAGATT CTCCCGCTCGAATTTAATTTAATCGGCAAATATAAACAAATACGCTCCAAAAGCATG TACAATGTTCGTTTTGTTATTTATGCATATGTCTATTTGCGATTTAAGTGGAAATATA TTTCAATACACGG-3'. This template was amplified using the primers 5'-CAGATTCTCCC GCTCG and 5'-TTCCGTGTATTGAAATATATTTCC. Immunoblots confirmed that Ana2 UTR RNAi depleted endogenous Ana2 by ~80-90% (Figure S1B).

3.5.2 Immunoblotting

S2 cell extracts were produced by lysing cells in cold PBS and 0.1% Triton X-100. Laemmli sample buffer was then added and samples boiled for 5 min. Samples of equal total protein were resolved by SDS-PAGE, blotted, probed with primary and secondary antibodies, and scanned on an Odyssey imager (Li-Cor Biosciences). Care was taken to avoid saturating the scans of blots. Antibodies used for Western blotting include rabbit anti-Ana2 (our laboratory), mouse anti-V5 monoclonal (Life Technologies), mouse anti-GFP monoclonal JL8 (Clontech), mouse anti-myc (Cell Signaling Technologies), mouse anti-α tubulin monoclonal DM1A (Sigma-Aldrich), and mouse anti-FLAG monoclonal (Sigma-Aldrich) used at 1:1,500 dilutions. IRDye 800CW secondary antibodies (Li-Cor Biosciences) were prepared according to the manufacturer's instructions and used at 1:3,000 dilutions.

To generate the anti-phospho-specific T172 Plk4 antibody, rabbit polyclonal antibodies were raised against the following phospho-peptide: Acetyl-PDERHM(pT)MCGTPN. A nonphospho-peptide (Acetyl-PDERHMTMCGTPN) was also synthesized (ThermoFisher). Antibodies were affinity-purified from antisera using Affi-Gel 10/15 resin (BioRad Laboratories) coupled to the phosphopeptide. The eluted material was then pre-absorbed over an Affi-Gel column coupled to the non-phosphospecific peptide. The eluate was collected and concentrated using 10K Ultrafree 2 ml concentrators (Millipore). Antibodies were used at a 1:1000 dilution.

3.5.3 Mass Spectrometry

Mass spectrometry was performed at the Taplin Mass Spectrometry Facility (Harvard Medical School) and the NHLBI Proteomics Core Facility (NIH). Samples of Ana2 were reduced (10µM

dithiothreitol, 55°C, 1hr), alkylated (55mM iodoacetamide, room temperature, 45min), and trypsin digested (~1µg trypsin, 37°C, 12hrs) in-gel, and then extracted. Peptide samples were loaded onto a Zorbax C18 trap column (Agilent Tech., Santa Clara, CA) to desalt the peptide mixture using an on-line Eksigent (Dublin, CA) nano-LC ultra HPLC system. The peptides were then separated on a 10 cm Picofrit Biobasic C18 analytical column (New Objective, Woburn, MA). Peptides were eluted over a 90 min linear gradient of 5-35% acetonitrile/water containing 0.1% formic acid at a flow rate of 250 nL/min, ionized by electrospray ionization (ESI) in positive mode, and analyzed on a LTQ Orbitrap Velos (Thermo Electron Corp., San Jose, CA) mass spectrometer. All LC MS analyses were carried out in "data-dependent" mode in which the top 6 most intense precursor ions detected in the MS1 precursor scan (m/z 300-2000) were selected for fragmentation via collision induced dissociation (CID). Precursor ions were measured in the orbitrap at a resolution of 60,000 (m/z 400) and all fragment ions were measured in the ion trap.

3.5.4 Immunofluorescence microscopy

S2 cells were fixed and processed as previously described (Rogers and Rogers, 2008) by spreading S2 cells on concanavalin A–coated, glass-bottom dishes and fixing with ice-cold methanol. Primary antibodies were diluted to concentrations ranging from 1 to 20 µg/ml. They included rabbit anti–PLP (Rogers et al., 2009), guinea pig anti-Asl (Klebba et al., 2013), and mouse anti-V5 (Life Technologies) antibodies. Goat secondary antibodies (conjugated with Cy2, Rhodamine red-X, or Cy5 [Jackson ImmunoResearch Laboratories, Inc.]) were used at 1:1,500. Hoechst 33342 (Life Technologies) was used at a final concentration of 3.2 µM. Cells were mounted in 0.1 M n-propyl galate, 90% (by volume) glycerol, and 10% PBS solution.

Specimens were imaged using a DeltaVision Core deconvolution system (Applied Precision) equipped with an Olympus IX71 microscope, a 100× objective (NA 1.4), and a cooled charge coupled

device camera (CoolSNAP HQ2; Photometrics). Images were acquired with softWoRx v1.2 software (Applied Science).

3.5.5 Constructs and transfection

Full-length cDNAs of Drosophila Ana2, Plk4, Sas4, and Sas6 were subcloned into a pMT vector containing in-frame coding sequences for EGFP, V5, or myc under control of the inducible metallothionein promoter. PCR-based site-directed mutagenesis with Phusion polymerase (ThermoFisher) was used to generate the various Ana2 and Plk4 deletion and point mutants. Transient transfections of S2 cells were performed as described (Nye et al., 2014). Briefly, ∼2–5 × 106 cells were pelleted by centrifugation, resuspended in 100 µl of transfection solution (5 mM KCl, 15 mM MgCl2, 120 mM sodium phosphate, 50 mM D-mannitol, pH 7.2) containing 1–3 µg of purified plasmid, transferred to a cuvette (2-mm gap size), and then electroporated using a Nucleofector 2b (Lonza), program G-030. Transfected cells were diluted immediately with 0.5 ml of SF-900 II medium and plated in a six-well cell-culture plate. Typically, cells were allowed 24 hrs to recover before further manipulation. Expression of all constructs was induced by addition of 100 µM–2 mM copper sulfate to the culture medium.

3.5.6 Yeast Two-Hybrid assay

Yeast two-hybrid (Y2H) experiments were carried out using the Matchmaker Gold Y2H system (Clontech) with significant modifications. pDEST-GADT7 and pDEST-GBKT7, modified

versions of Matchmaker vectors compatible with the Gateway cloning system (Life Technologies), were used (Rossignol et al., 2007). pDEST-GADT7 and pDEST-GBKT7 contain the 2 μ and pUC ori for growth in yeast and bacteria. Both contain the Gateway cassette and utilize the ADH1 promoter to drive expression in Saccharomyces cerevisiae. pDEST-GADT7 fuses the SV40 nuclear localization signal, the GAL4 activation domain and the HA epitope tag to the amino-terminus of the protein encoded by DNA inserted into the Gateway cassette. pDEST-GBKT7 fuses the SV40 nuclear localization signal, the GAL4 DNA binding domain and the c-Myc epitope tag to the amino-terminus of the protein encoded by DNA inserted into the Gateway cassette. pDest-pGBKT7 was modified by yeast-mediated recombination to confer resistance to ampicillin instead of kanamycin. pDEST-GADT7 and pDEST-GBKT7 plasmids containing fragments encoding the protein regions to be tested for interaction were transformed into Y187 and Y2HGold yeast strains respectively using standard techniques. Liquid cultures of yeast carrying these plasmids were grown at 30ºC, with shaking, to an OD600 ~0.5 in SD – leu or SD –trp media, as appropriate to maintain plasmid selection. Interactions were tested by mating, mixing 20 μl each of a Y187 strain and a Y2HGold strain in 100μl of 2X YPD media in a 96 well plate. Mating cultures were grown for 20-24 hrs at 30ºC with shaking. Cells were pinned onto SD –leu –trp (DDO) plates to select for diploids carrying both plasmids, using a Multi-Blot Replicator (VP 407AH, V&P Scientific) and grown for 5 days at 30ºC. These plates were then replica plated onto DDO, SD – ade –leu –trp –ura (QDO), SD – leu –trp + Aureobasidin A (Clontech) + X-α-Gal (Clontech and Gold Biotechnology) (DDOXA) and/or SD – ade –leu –trp –ura + Aureobasidin A + X-α-Gal (QDOXA). Replica plates were grown for 5 days at 30ºC. Interactions were scored based on growth and/or blue color, as appropriate.

3.5.7 In vitro kinase assays

Bacterially expressed constructs of Drosophila Plk4 (amino acids 1–317 or 1-381) C-terminally tagged with FLAG-His6 and full-length Drosophila Ana2 N-terminally tagged with Glutathione S-Transferase (also called "GST-Ana2") were purified on HisPur resin (ThermoFisher) or glutathione resin (NEB), respectively, according to manufacturer's instructions. Prior to assay, Plk4 was pre-treated with λ-phosphatase (because it appears to autophosphorylate to some extent when expressed in bacteria). Samples of protein reagents were resolved by SDS-PAGE and scans of the Coomassie-stained gels analyzed by densitometry (ImageJ, NIH) to determine protein purity. Total protein concentrations of the same reagents were measured by Bradford assay (BioRad). The total protein and purity measurements were used to calculate the concentration of each protein reagent. (Contaminants and proteolytic fragments are excluded by this calculation.) In vitro phosphorylation assays were performed with the indicated proteins at different molarities (see Results) by incubation with 100 μM ATP for the indicated times at 25°C in reaction buffer [40 mM Na HEPES (pH 7.3), 150 mM NaCl, 5 mM MgCl2, 0.5 mM MnCl2, 1 mM DTT, 10% (by volume) glycerol]. Samples were resolved by SDS-PAGE, and proteins visualized by Coomassie staining. Phosphorylation of protein substrates was evaluated by including γ-32P-ATP in assays and, subsequently, the presence of radiolabeled substrates detected by autoradiography or phosphorimaging (STORM, GE Healthcare) of dried gels. Phosphorylated residues within proteins were identified by tandem mass spectrometry (Table S1) of purified bacterially-expressed proteins phosphorylated in vitro (described above) in the presence of nonradioactive ATP.

3.5.8 GFP immunoprecipitation assays

GFP-binding protein (GBP) (Rothbauer et al., 2008) was fused to the Fc domain of human IgG (pIg-Tail) (R&D Systems), tagged with His6 in pET28a (EMD Biosciences), expressed in E. coli and purified on HisPur resin (ThermoFisher) according to manufacturer's instructions (Buster et al., 2013). Purified GBP was bound to magnetic Dyna Beads (ThermoFisher), and then crosslinked to the resin by incubating with 20mM dimethyl pimelimidate dihydrochloride in PBS, pH 8.3, 2 hours at 22°C, and then quenching the coupling reaction by incubating with 0.2M ethanolamine, pH 8.3, 1 hour at 22°C. Antibody-coated beads were washed three times with PBS-Tween20 (0.02%), then equilibrated in 1.0 ml of cell lysis buffer (CLB; 50 mM Tris, pH 7.2, 125 mM NaCl, 2 mM DTT, 0.1% Triton X-100, and 0.1 mM PMSF). Transfected cells expressing recombinant proteins were lysed in CLB, and the lysates clarified by centrifugation at 16,100 x g for 5 minutes at 4°C. 0.5-1% of the inputs were used for immunoblots. GBP-coated beads were rocked with lysate for 30 minutes at 4°C, washed four times with 1 ml CLB, and then boiled in Laemmli sample buffer.

3.5.9 Statistical analysis and curve fitting

Means of measurements were analyzed for significant differences by one-way ANOVA followed by Tukey's post-test (to evaluate differences between treatment pairs) using Prism 6 (GraphPad) software. Means are taken to be significantly different if $P < 0.05$. P values shown for pairwise comparisons of Tukey's post-test are adjusted for multiplicity. In figures, "*" indicates $0.05 > P \geq 0.01$, "**" indicates $0.01 > P \geq 0.001$, "***" indicates $0.001 > P$, and "ns" indicates $P \geq 0.05$ for the indicated pairwise comparison. Error bars in all figures indicate standard error of the

mean (SEM). Plots of in vitro phosphorylation assays were best-fit to second-order polynomials using nonlinear regression (Prism 6, GraphPad). Initial reaction rates were obtained from the slopes of the plots covering the 5-30 min time points; differences in the slopes were analyzed for significance using Prism 6.

3.6 References

Arquint, C., A.M. Gabryjonczyk, S. Imseng, R. Böhm, E. Sauer, S. Hiller, E.A. Nigg, and T. Maier. 2015. STIL binding to Polo-box 3 of PLK4 regulates centriole duplication. Elife. 4:doi:10.7554/eLife.07888.

Avidor-Reiss, T., and J. Gopalakrishnan. 2013. Building a centriole. Curr. Opin. Cell Biol. 25:72-77.

Bettencourt-Dias, M., A. Rodrigues-Martins, L. Carpenter, M. Riparbelli, L. Lehmann, M.K. Gatt, N. Carmo, F. Balloux, G. Callaini, and D.M. Glover. 2005. SAK/PLK4 is required for centriole duplication and flagella development. Curr. Biol. 15:2199-2207.

Brownlee, C.W., J.E. Klebba, D.W. Buster, and G.C. Rogers. 2011. The Protein Phosphatase 2A regulatory subunit Twins stabilizes Plk4 to induce centriole amplification. J. Cell Biol. 195:231-243.

Buster, D.W., S.G. Daniel, H.Q. Nguyen, S.L. Windler, L.C. Skwarek, M. Peterson, M. Roberts, J.H. Meserve, T. Hartl, J.E. Klebba, D. Bilder, G. Bosco, and G.C. Rogers. 2013. SCFSlimb ubiquitin ligase suppresses condensin II-mediated nuclear reorganization by degrading Cap-H2. J. Cell Biol. 201:49-63.

Cottee, M.A., N. Muschalik, Y.L. Wong, C.M. Johnson, S. Johnson, A. Andreeva, K. Oegema, S.M. Lea, J.W. Raff, and M. van Breugel, M. 2013. Crystal structures of the

CPAP/STIL complex reveal its role in centriole assembly and human microcephaly. eLife. 2:e01071. doi:10.7554/eLife.01071.

Cottee, M.A., N. Muschalik, S. Johnson, J. Leveson, J.W. Raff, and S.M. Lea. 2015. The homooligomerisation of both Sas-6 and Ana2 is required for efficient centriole assembly in flies. Elife. 4:e07236.

Dzhindzhev, N.S., G. Tzolovsky, Z. Lipinszki, S. Schneider, R. Lattao, J. Fu, J., Debski, M. Dadlez, D.M. and Glover. 2014. Plk4 phosphorylates Ana2 to trigger Sas6 recruitment and procentriole formation. Curr. Biol. 24:2526-2532.

Fu, J., and D.M. Glover. 2012. Structured illumination of the interface between centriole and peri-centriolar material. Open Biol. 2:120104. doi:10.1098/rsob.120104.

Fu, J., I.M. Hagan, and D.M. Glover. 2015. The centrosome and its duplication cycle. Cold Spring Harb. Perspect. Biol. 7:a015800.

Goshima, G., R. Wollman, S.S. Goodwin, N. Zhang, J.M. Scholey, R.D. Vale, and N. Stuurman. 2007. Genes required for mitotic spindle assembly in Drosophila S2 cells. Science. 316:417-421.

Guichard, P., A. Desfosses, A. Maheshwari, V. Hachet, C. Dietrich, A. Brune, T. Ishikawa, C. Sachse, and P. Gönczy, P. 2012. Cartwheel architecture of Trichonympha basal body. Science.337:553.

Habedanck, R., Y. Stierhof, C.J. Wilkinson, and E.A. Nigg. 2005. The Polo kinase Plk4 functions in centriole duplication. Nat. Cell Biol. 7:1140-1146.

Hannus, M., F. Feiguin, C.P. Heisenberg, and S. Eaton. 2002. Planar cell polarization requires Widerborst, a B’ regulatory subunit of protein phosphatase 2A. Development. 129:3493–3503.

Hatzopoulos, G.N., M.C. Erat, E. Cutts, K.B. Rogala, L.M. Slater, P.J. Stansfeld, and I. Vakonakis. 2013. Structural analysis of the G-box domain of the microcephaly protein CPAP suggests a role in centriole architecture. Structure. 21:2069-2077.

Holland, A.J., W. Lan, S. Niessen, H. Hoover, and D.W. Cleveland. 2010. Polo-like kinase 4 kinase activity limits centrosome overduplication by autoregulating its own stability. J. Cell Biol. 188:191-198.

Kitagawa, D., I. Vakonakis, N. Olieric, M. Hilbert, D. Keller, V. Olieric, M. Bortfeld, M.C. Erat, I. Flückiger, P. Gönczy, and M.O. Steinmetz. 2011. Structural basis of the 9-fold symmetry of centrioles. Cell. 144:364-375.

Klebba, J.E., D.W. Buster, A.L. Nguyen, S. Swatkoski, M. Gucek, N.M. Rusan, and G.C. Rogers. 2013. Polo-like kinase 4 autodestructs by generating its Slimb-binding phosphodegron. Curr. Biol. 23:2255-2261.

Klebba, J.E., D.W. Buster, T.A. McLamarrah, N.M. Rusan, and G.C. Rogers, G.C. 2015a. Autoinhibition and relief mechanism for Polo-like kinase 4. Proc. Natl. Acad. Sci. USA. 112:E657-666.

Klebba, J.E., B. Galletta, J. Nye, K. Plevock, D.W. Buster, N.A. Hollingsworth, K.C. Slep, N.M. Rusan, and G.C. Rogers. 2015b. Two Polo-like kinase 4 binding domains in Asterless play antagonistic roles in regulating kinase stability. J. Cell Biol. 208:401-414.

Kleylein-Sohn, J., J. Westendorf, M. Le Clech, R. Habedanck, Y.D. Stierhof, and E.A. Nigg. 2007. Plk4-induced centriole biogenesis in human cells. Dev. Cell. 13:190-202.

Kitagawa, D., I. Flückiger, J. Polanowska, D. Keller, J. Reboul, and P. Gönczy. 2011. PP2A phosphatase acts upon SAS-5 to ensure centriole formation in C. elegans embryos. Dev. Cell.20:550-562.

Kotadia, S., L.R. Kao, S.A. Comeford, R.T. Jones, R.E. Hammer, and T.L. Megraw. 2008. PP2A-dependent disruption of centrosome replication and cytoskeleton organization in Drosophila by SV40 small tumor antigen. Oncogene. 27:6334-6346.

Kratz, A.S., F. Bärenz, K.T. Richter, and I. Hoffmann. 2015. Plk4-dependent phosphorylation of STIL is required for centriole duplication. Biol. Open. 4:370-377.

Li, X., A. Scuderi, A. Letsou, and D.M. Virshup. 2002. B56-associated protein phosphatase 2A is required for survival and protects from apoptosis in Drosophila melanogaster. Mol. Cell. Biol. 22:3674–3684.

Lopes, C.A., S.C. Jana, I. Cunha-Ferreira, S. Zitouni, I. Bento, P. Duarte, S. Gilberto, F. Freixo,A. Guerrero, M. Francia, M. Lince-Faria, J. Carneiro, and M. Bettencourt-Dias. 2015. PLK4 trans-autoactivation controls centriole biogenesis in space. Dev. Cell. 35:222-235.

Mayer-Jaekel, R.E., S. Baumgartner, G. Bilbe, H. Ohkura, D.M. Glover, and B.A. Hemmings. 1992. Molecular cloning and developmental expression of the catalytic and 65-kDa regulatory subunits of protein phosphatase 2A in Drosophila. Mol. Biol. Cell. 3:287–298.

Mennella, V., B. Keszthelyi, K.L. McDonald, B. Chhun, F. Kan, G.C. Rogers, B. Huang, and D.A. Agard. 2012. Subdiffraction-resolution fluorescence microscopy reveals a domain of the centrosome critical for pericentriolar material organization. Nat. Cell Biol. 14:1159-1168.

Moyer, T.C., K.M. Clutario, B.G. Lambrus, V. Daggubati, and A.J. Holland, A.J. 2015. Binding of STIL to Plk4 activates kinase activity to promote centriole assembly. J. Cell Biol. 209:863-878.

Nakamura, T., H. Saito, and M. Takekawa, M. 2013. SAPK pathways and p53 cooperatively regulate PLK4 activity and centrosome integrity under stress. Nat. Commun. 4:1775. doi:10.1038/ncomms2752.

Nye, J., D.W. Buster, and G.C. Rogers. 2014. The use of cultured Drosophila cells for studying the microtubule cytoskeleton. Methods Mol. Biol. 1136:81-101.

Ohta, M., T. Ashikawa, Y. Nozaki, H. Kozuka-Hata, H., Goto, M. Inagaki, M., Oyama, and D.Kitagawa. 2014. Direct interaction of Plk4 with STIL ensures formation of a single procentriole per parent centriole. Nat. Commun. 5:5267. doi: 10.1038/ncomms6267.

Peel, N., N.R. Stevens, R. Basto, and J.W. Raff. 2007. Overexpressing centriole-replication proteins in vivo induces centriole overduplication and de novo formation. Curr. Biol. 17:834-843.

Rodrigues-Martins, A., M. Riparbelli, G. Callaini, D.M. Glover, and M. Bettencourt-Dias. 2007. Revisiting the role of the mother centriole in centriole biogenesis. Science. 316:1046-1050.

Shimanovskaya, E., R. Qiao, J. Lesigang, and G. Dong. 2013. The SAS-5 N-terminal domain is a tetramer, with implications for centriole assembly in C. elegans. Worm. 2:e25214.

Rogala, K.B., N.J. Dynes, G.N. Hatzopoulos, J. Yan, S.K. Pong, S.K., Robinson, C.M. Deane, P. Gönczy, and I. Vakonakis. 2015. The Caenorhabditis elegans protein SAS-5 forms large oligomeric assemblies critical for centriole formation. Elife. 29:e07410.

Rogers, G.C., N.M. Rusan, D.M. Roberts, M. Peifer, and S.L. Rogers. 2009. The SCF Slimb ubiquitin ligase regulates Plk4/Sak levels to block centriole reduplication. J. Cell Biol. 184:225-239.

Rogers, S.L., and G.C. Rogers. 2008. Culture of Drosophila S2 cells and their use for RNAi mediated loss-of-function studies and immunofluorescence microscopy. Nat. Protoc. 3:606-611.

Rossignol, P., S. Collier, M. Bush, P. Shaw, and J.H. Doonan. 2007. Arabidopsis POT1A

interacts with TERT-V(I8), an N-terminal splicing variant of telomerase. J. Cell Sci. 120:3678-3687.

Rothbauer, U., K. Zolghadr, S. Muyldermans, A. Schepers, M.C. Cardoso, and H. Leonhardt. 2008. A versatile nanotrap for biochemical and functional studies with fluorescent fusion proteins. Mol. Cell Proteomics. 7:282-289.

Slevin, L.K., E.M. Romes, M.G. Dandulakis, and K.C. Slep. 2014. The mechanisms of dynein light chain LC8-mediated oligomerization of the Ana2 centriole duplication factor. J. Biol.Chem. 289:20727-20739.

Snaith, H.A., C.G. Armstrong, Y. Guo, K. Kaiser, and P.T. Cohen. 1996. Deficiency of protein phosphatase 2A uncouples the nuclear and centrosome cycles and prevents attachment of microtubules to the kinetochore in Drosophila microtubule star (mts) embryos. J. Cell Sci. 109:3001–3012.

Song, M.H., Y. Liu, D.E. Anderson, W.J. Jahng, and K.F. O'Connell. 2011. Protein phosphatase 2A-SUR-6/B55 regulates centriole duplication in C. elegans by controlling the levels of centriole assembly factors. Dev. Cell. 20:563-571.

Stevens, N.R., J. Dobbelaere, K. Brunk, A. Franz, and J.W. Raff. 2010a. Drosophila Ana2 is a conserved centriole duplication factor. J. Cell Biol. 188:313-323.

Stevens, N.R., H. Roque, and J.W. Raff. 2010b. DSas-6 and Ana2 coassemble into tubules to promote centriole duplication and engagement. Dev. Cell. 19:913-919.

Swallow, C.J., M.A. Ko, N.U. Siddiqui, J.W. Hudson, and J.W. Dennis. 2005. Sak/Plk4 and mitotic fidelity. Oncogene. 24:306-312.

Tang, C.J., S.Y. Lin, W.B. Hsu, Y.N. Lin, C.T. Wu, Y.C. Lin, C.W. Chang, K.S. Wu, and T.K. Tang. 2011. The human microcephaly protein STIL interacts with CPAP and is required for

procentriole formation. EMBO J. 30:4790-4804.

Uemura, T., K. Shiomi, S. Togashi, and M. Takeichi. 1993. Mutation of twins encoding a regulator of protein phosphatase 2A leads to pattern duplication in Drosophila imaginal discs. Genes Dev. 7:429–440.

van Breugel, M., M. Hirono, A. Andreeva, H.A. Yanagisawa, S. Yamaguchi, Y. Nakazawa, N. Morgner, M. Petrovich, I.O. Ebong, C.V. Robinson, C.M. Johnson, D. Veprintsev, and B. Zuber. 2011. Structures of SAS-6 suggest its organization in centrioles. Science. 331:1196-1199.

Viquez, N.M., C.R. Li, Y.P. Wairkar, and A. DiAntonio. 2006. The B' protein phosphatase 2A regulatory subunit well-rounded regulates synaptic growth and cytoskeletal stability at the Drosophila neuromuscular junction. J. Neurosci. 26:9293

3.7 Figures

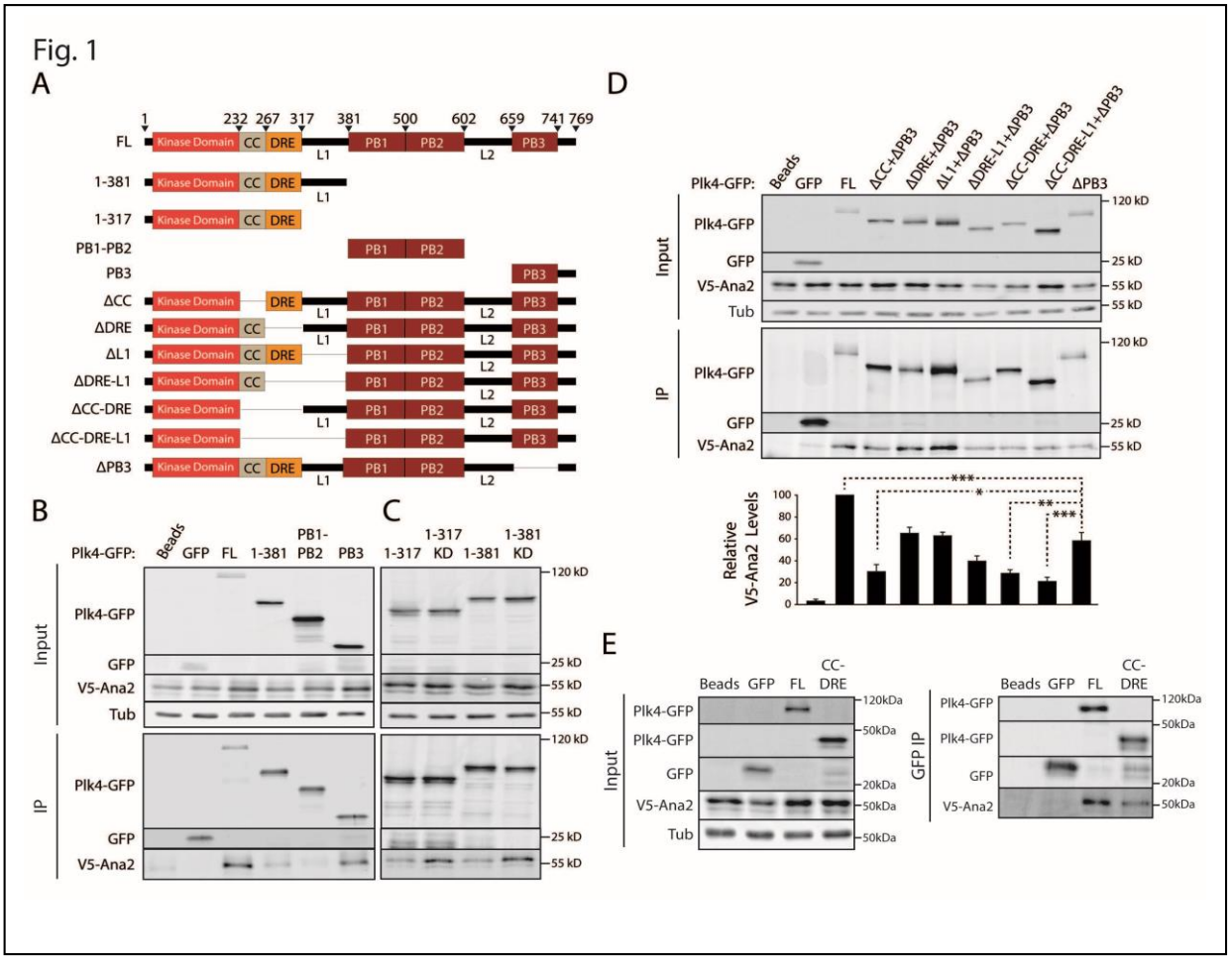

Figure 1. Ana2 binds both CC-DRE and PB3 domains in Plk4.

(A) Plk4 constructs used in immunoprecipitation (IP) experiments. CC, coiled-coil; DRE, Downstream Regulatory Element; PB, Polo Boxes; L1 and L2, linkers.

(B) Ana2 associates with Plk4 N-terminus (1-381) and C-terminus (PB3). S2 cells were co-transfected with Plk4-GFP full-length (FL) or deletion constructs and V5-Ana2. Anti-GFP IPs were performed from lysates of the transfected cells and probed for GFP, V5, and α-tubulin.

(C) L1 is not necessary for Ana2 association which also preferentially interacts with kinase-dead (KD) Plk4. IPs performed as in B.

(D) Ana2 associates with the CC and PB3 regions of Plk4. Graph depicts relative intensity of V5-Ana2 normalized to Plk4-GFP. Asterisks mark significant differences between treatments. Error bars, SEM; n = 3 independent experiments.

(E) The Plk4 CC-DRE domain is sufficient to associate with Ana2. IPs performed as in B.

Fig. 2

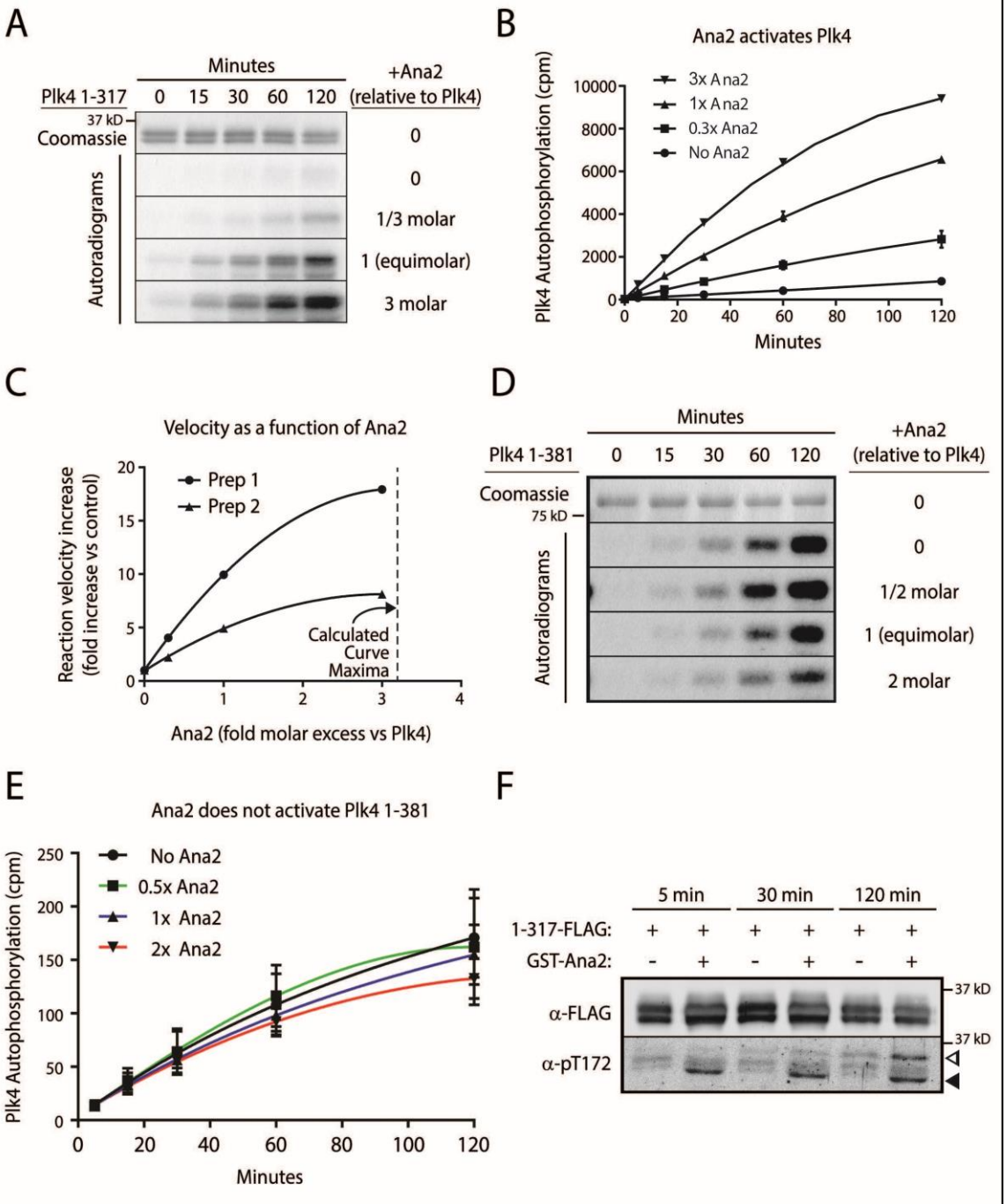
A
Minutes
Plk4 1-317
0
15
30
60
120
+Ana2 (relative to Plk4)
37 kD
Coomassie
Autoradiograms
0
0
1/3 molar
1 (equimolar)
3 molar
B
Ana2 activates Plk4
3x Ana2
1x Ana2
0.3x Ana2
No Ana2
Plk4 Autophosphorylation (cpm)
Minutes
C
Velocity as a function of Ana2
Prep 1
Prep 2
Reaction velocity increase (fold increase vs control)
Calculated Curve Maxima
Ana2 (fold molar excess vs Plk4)
D
Minutes
Plk4 1-381
+Ana2 (relative to Plk4)
Coomassie
75 kD
Autoradiograms
0
0
1/2 molar
1 (equimolar)
2 molar
E
Ana2 does not activate Plk4 1-381
No Ana2
0.5x Ana2
1x Ana2
2x Ana2
Plk4 Autophosphorylation (cpm)
Minutes
F
5 min
30 min
120 min
1-317-FLAG:
GST-Ana2:
α-FLAG
α-pT172
37 kD
37 kD

Figure 2. Ana2 stimulates Plk4 autophosphorylation in vitro.

(A) Purified Plk4 1-317-His was incubated with γ^{32}P-ATP and different concentrations of purified full-length GST-Ana2. Each reaction was sampled at intervals (15-120 min). The Top row, Coomassie-stained Plk4 1-317. 4 bottom rows, autoradiograms; the concentrations (molar amount relative to Plk4) of added Ana2 are indicated on the right.

(B) Ana2 significantly increases the rate of Plk4 autophosphorylation. Plk4 1-317 in samples resolved by SDS-PAGE were cut from gels, and ^{32}P-radiolabel measured by scintillation counting. The initial rates for all 4 plots are significantly different ($P<0.001$).

(C) The initial rates of autophosphorylation for two different Plk4 1-317 preparations were examined as in B, and the fold increase in rate as a function of Ana2 plotted. The maximum for each best-fit plot is reached when the Ana2 molar concentration exceeds Plk4 by 3-4x.

(D) Purified Plk4 1-381-His_6 was incubated with γ^{32}P-ATP and different concentrations of purified full-length GST-Ana2, and reactions performed as in A

(E) Ana2 does not affect the rate of Plk4 1-381 autophosphorylation. Plk4 1-381 autophosphorylation was measured as in B. The 4 best-fit plots are not significantly different.

(F) GST-Ana2 increases the autophosphorylation of activation loop residue T172 in Plk4 1-317. Purified Plk4 1-317-His was incubated with 3x molar GST-Ana2 and ATP, and the mixture sampled at the indicated timepoints. Westerns were probed with anti-FLAG (to detect

Plk4) and anti-phospho-T172 antibodies. Arrowheads mark 2 prominent pT172-positive species of Plk4 that appear in the presence of Ana2.

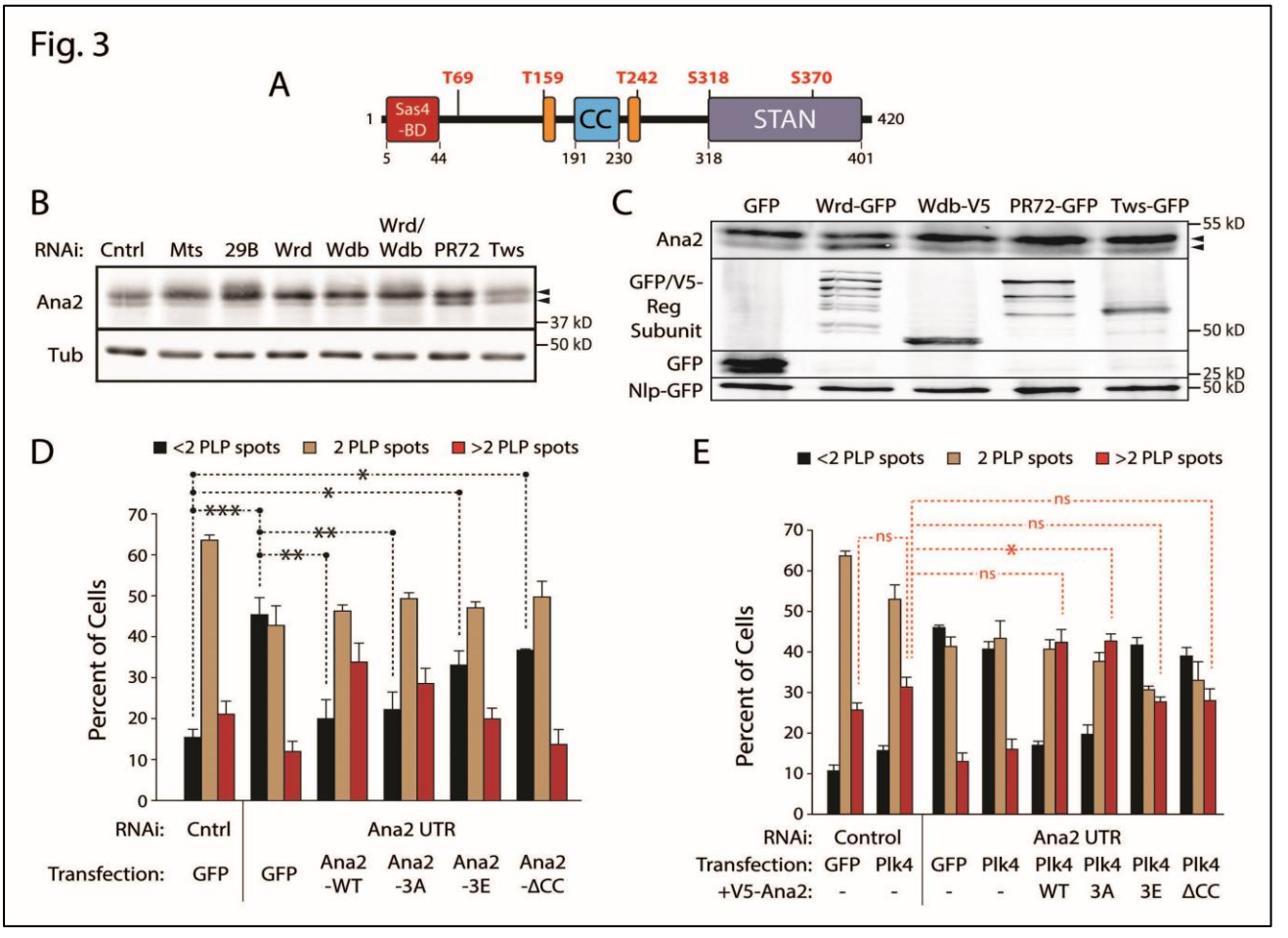

Figure 3. Ana2 is both a Plk4 and PP2A substrate. Phosphorylation of Ana2 residues

flanking the coiled-coil suppresses centriole duplication.

(A) Linear map of Ana2 depicting the Plk4 phosphorylation sites. Phospho-sites were identified by tandem MS/MS of purified GST-Ana2 phosphorylated in vitro by purified Plk4 1-317-His.

(B) S2 cells were depleted of PP2A subunits Mts (catalytic), 29B (structural) and Wrd, Wdb, Tws, or PR72 (regulatory) for 7 days. Immunoblots of cell lysates were probed for endogenous Ana2 and α-tubulin. Ana2 migrates as a doublet (arrowheads) but accumulates as slower migrating species after Mts, 29B, Wrd and Wdb depletion.

(C) Overexpression of Well rounded/Wrd-GFP overexpression shifts endogenous Ana2 (arrowheads) to a faster migrating species. Cells were transfected with inducible expression constructs. After 24-h recovery, expression was induced with 2 mM $CuSO_4$ for 24 h. Cotransfected Nlp-GFP was expressed under its endogenous promoter and served as a loading control in gels. Westerns of cell lysates were probed with α-GFP and α-V5.

(D) Phosphomimetic Ana2-3E disrupts centriole duplication. S2 cells were control-treated or depleted of endogenous Ana2 by RNAi for 7 days. On day 3, cells were transfected with the indicated inducible V5-Ana2 construct and the next day induced to express for 72 hours. Cells were immunostained for PLP and Asterless to mark centrioles, and the number of centrioles per

cell was counted. n = 100 cells in each of three experiments. Asterisks indicate significant differences. Error bars, SEM.

(E) Non-phosphorylatable Ana2-3A promotes Plk4-induced centriole amplification. S2 cells were prepared as described in D, except that Plk4-GFP was co-transfected with Ana2. The average percentages of cells containing the indicated number of centrioles are shown (n = 100 cells in each of four experiments). ns, not significant. Error bars, SEM.

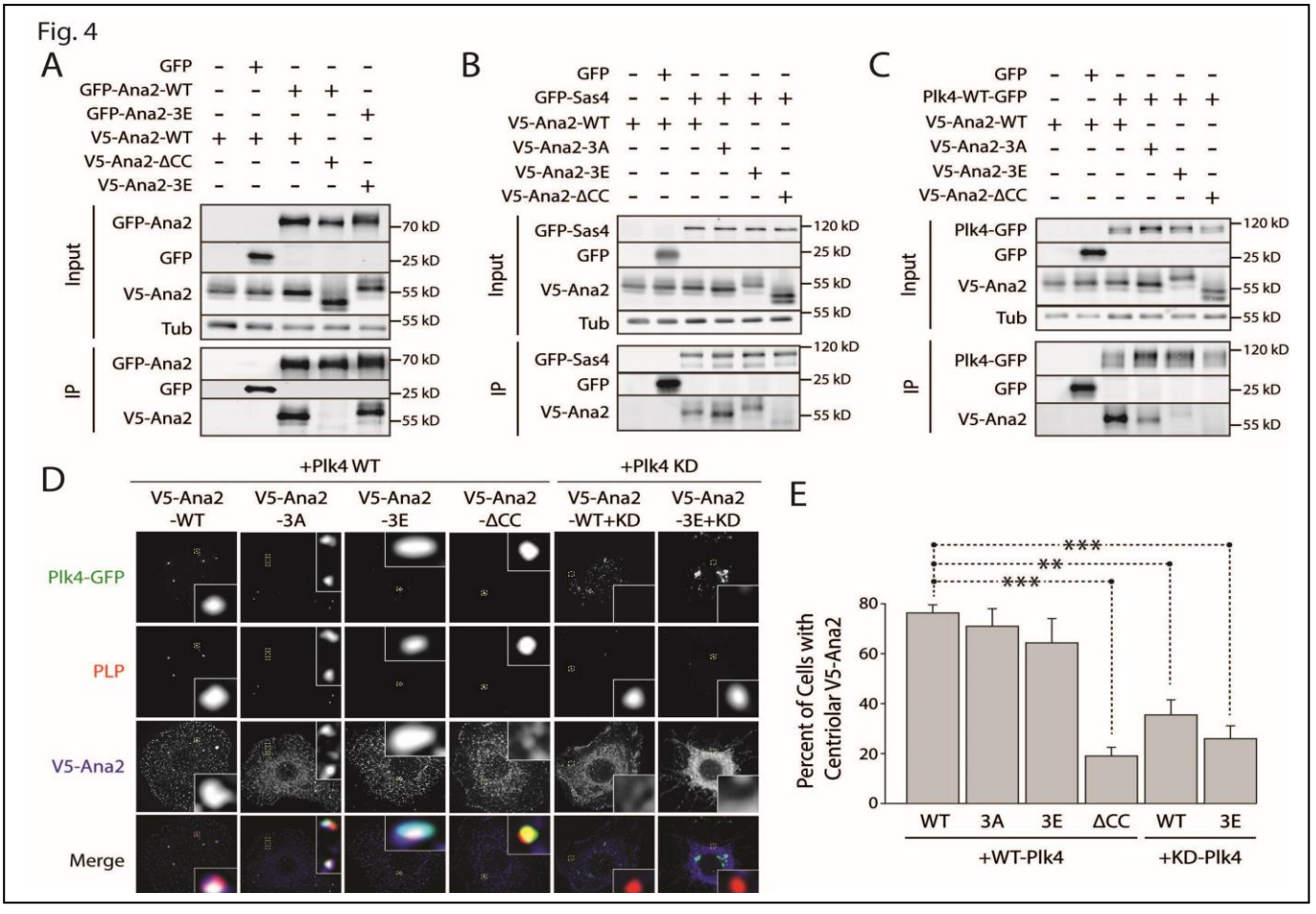

Figure 4. Plk4 phosphorylation of Ana2 disrupts their association but not Ana2 localization to centrioles.

(A-C) Phosphorylation of the Ana2 N-terminus does not prevent Ana2 binding to itself (A) or Sas4 (B), but does inhibit Plk4 binding (C). In contrast, the CC of Ana2 is required for Ana2

self-association (A) and binding to Sas4 and Plk4 (B, C). S2 cells were depleted of endogenous Ana2 by RNAi for 7 days. On day 5, cells were co-transfected with the indicated constructs and the next day induced to express for 24 hours. Anti-GFP IPs were then prepared from lysates, and immunoblots of the inputs and IPs probed for GFP, V5, and α-tubulin.

(D) Phosphomimetic Ana2-3E localizes to centrioles. S2 cells were depleted of endogenous Ana2 by RNAi for 5 days. On day 3, cells were co-transfected with WT or kinase-dead (KD) Plk4-GFP and a V5-Ana2 construct, allowed 24 hours to recover, and then induced to express for 24 hours. Representative images of cells show Plk4-GFP (green) and immunostained PLP (red) and V5-Ana2 (blue). Insets show boxed regions (yellow) at higher magnification. Note, KDPlk4 forms aggregates (Klebba et al., 2013). Scale, 5μm.

(E) S2 cells prepared as in D were imaged on day 5. Ana2 localization to centrioles was assessed from deconvolved Z-stacks. ($n \geq 50$ cells in each of three experiments). Asterisks mark significant differences. Error bars, SEM.

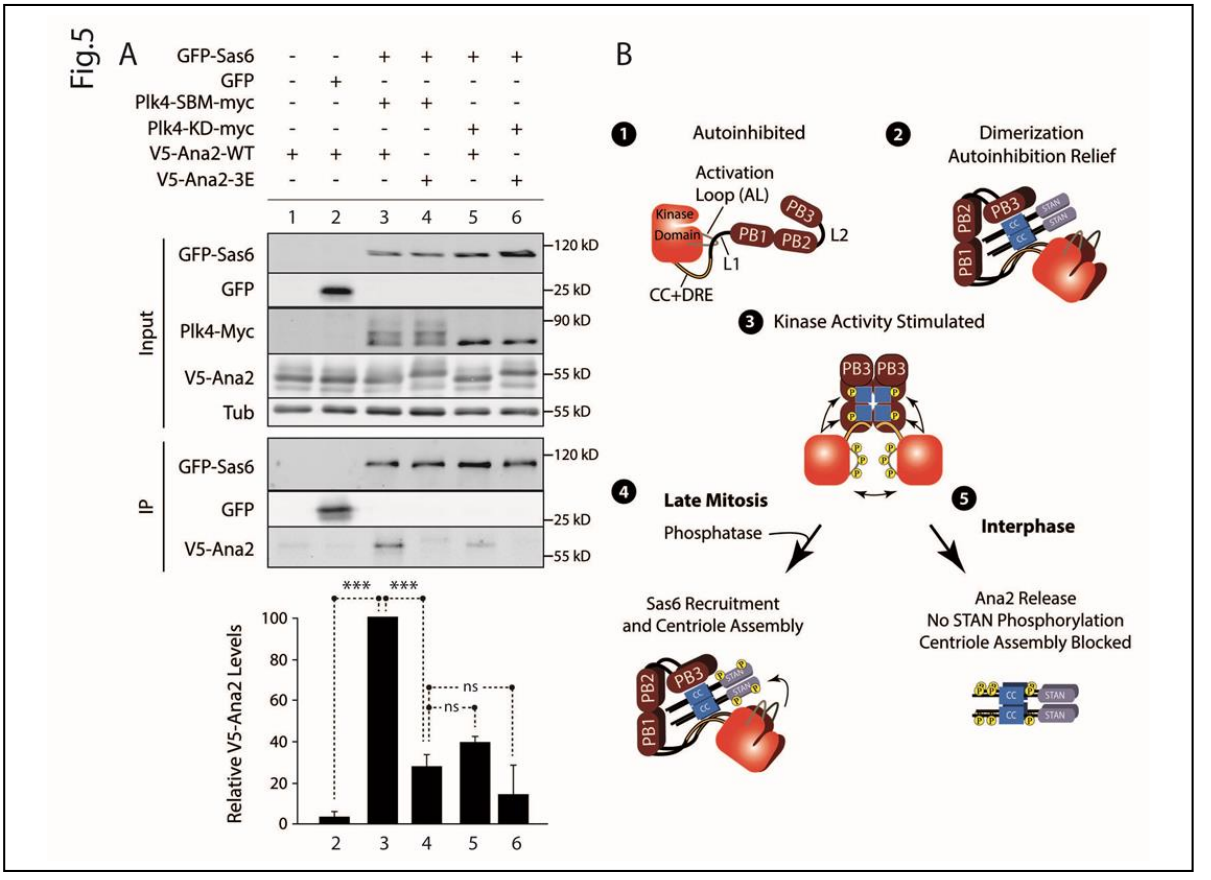

Figure 5. Ana2 phosphorylation by Plk4 inhibits its association with Sas6.

(A) Ana2-3E does not co-IP with Sas6 in the presence of stable, active Plk4. S2 cells were depleted of endogenous Ana2 by RNAi for 7 days. On day 5, cells were co-transfected with three inducible transgenes: 1) GFP-Sas6 (or control GFP), 2) V5-Ana2-WT (or 3E), and 3) nondegradable active Plk4-SBM-myc (or kinase-dead Plk4-KD-myc). Anti-GFP IPs of cell

lysates were probed for GFP, V5, myc and α-tubulin. For each treatment, levels of tagged V5-Ana2 in the IPs were determined by densitometry of the anti-V5 and GFP immunoblots, normalized to Ana2, and the results plotted relative to control (lane 3). Average relative intensities of V5-Ana2 of 3 independent experiments are plotted. Asterisks mark significant differences; ns, notsignificant. Error bars, SEM.

(B) Model: Plk4 both promotes and suppresses centriole assembly through phosphorylation of Ana2.

3.8 Supplemental materials

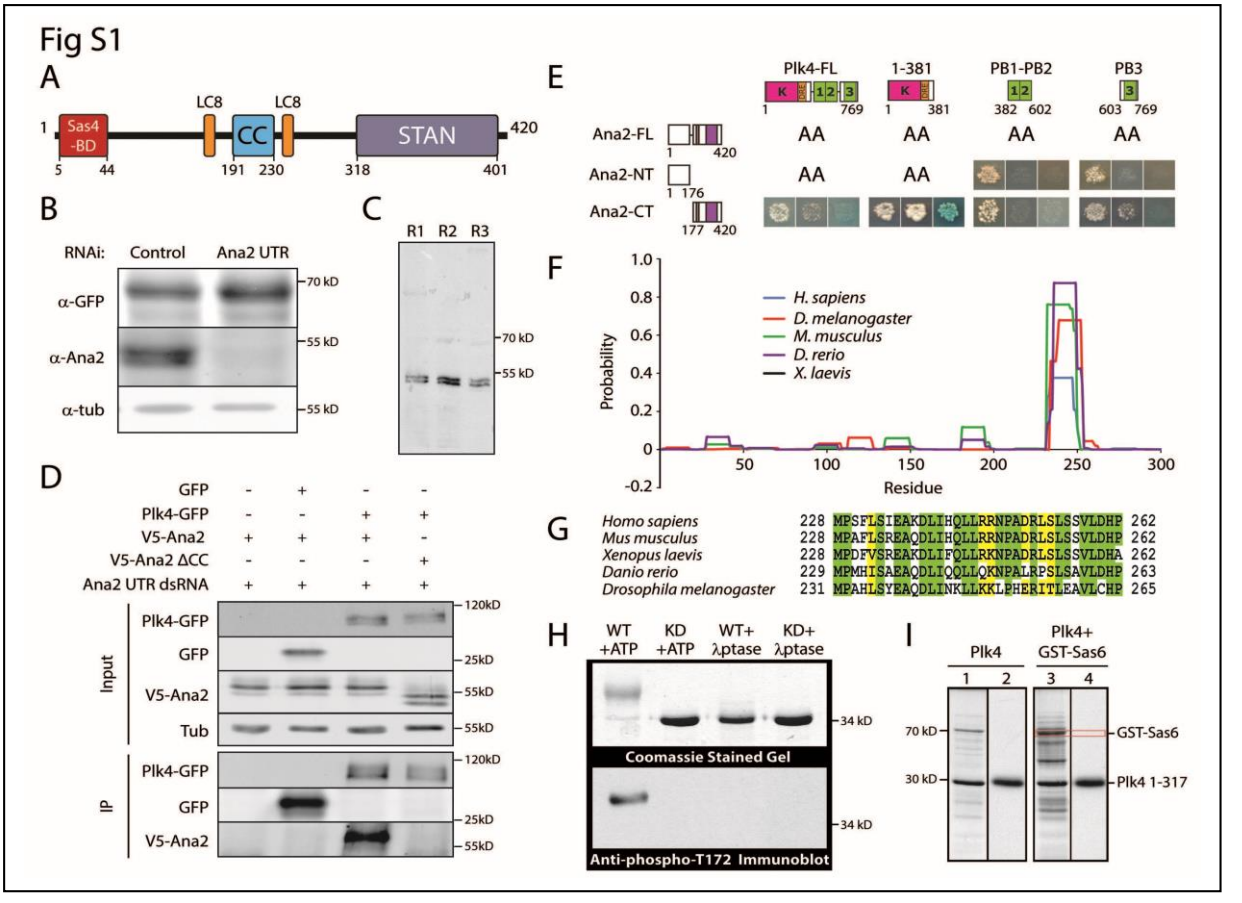

Figure S1. The coiled-coil domain of Ana2 binds the coiled-coil and Polo Box 3 (PB3) domains of Plk4.

(A) Linear map of the *Drosophila* Ana2 shows functional and structural domains including the Sas4 binding domain (red), cytoplasmic dynein light chain LC8-binding regions (amino

acids 159-168 and 237-246; orange) (Slevin et al., 2014), coiled-coil region (CC, blue), and the STil/ANa2 (STAN) motif (purple).

(B) Ana2 dsRNA was generated against sequence of the 5' and 3' UTRs. S2 cells were treated with control or Ana2 UTR RNAi for 7 days. On day 5, cells were transfected with GFP-Ana2, allowed to recover for 24 hours, and then induced to express transgenic GFP-Ana2 for an additional 24 hours. Anti-Ana2 immunoblots demonstrate effective endogenous Ana2 depletion (~90%). Anti-GFP immunoblots show that Ana2 UTR RNAi does not diminish exogenously expressed GFP-Ana2.

(C) The anti-Ana2 antibodies used in this study are specific. Three different rabbit polyclonal anti-Ana2 antibodies were raised against purified recombinant full-length GST-Ana2 and then affinity-purified with MBP-Ana2. The specificity of these antibodies (R1-3) on immunoblots of S2 cell lysates is shown. All antibodies react with the identical ~50 kDa protein which migrates on SDS-PAGE as a tight doublet.

(D) Ana2 but not Ana2 ΔCC co-immunoprecipitates (IPs) with Plk4. S2 cells were RNAi treated for 7 days to deplete endogenous Ana2. On day 5, cells were co-transfected with Plk4-GFP (or control GFP) and either V5-Ana2 wild-type or V5-Ana2 ΔCC; the following day, transgene expression was induced for 24 hrs. Anti-GFP IPs were then prepared from lysates, and immunoblots of the inputs and IPs probed for GFP, V5, and α-tubulin.

(E) Ana2 interacts specifically with Plk4-1-381 and PB3 by yeast two-hybrid (Y2H) analysis. Full-length (FL) and fragments of Ana2 and Plk4 were screened by Y2H. In each image, colonies from replica plating are shown and growth indicates the presence of both bait and prey. (Left panel) no selection, (middle panel) growth selection on QDO, (right panel) growth and color selection on DDOXA, blue color indicates an interaction. AA indicates that one or both protein fragments autoactivated the Y2H reporters on their own and could not be tested. Note that Ana2-CT, containing the coiled-coil region, interacts strongly with 1-381 (containing the CC-DRE region) and moderately with PB3, but not with PB1-PB2.

(F) Coiled–coil (CC) regions of Plk4 family members predicted by software from Pole Bioiformatique Lyonnaise (PBIL). The probability of CC structure was determined for the first 300 amino acids, using a 14 amino acid window and a 2.5 weight on positions ‘a’ and ‘d’. (G)

(G) Alignment of the 34 amino acid predicted CC encoded by Plk4 family members. Identical residues (green highlight) and resides with similar side chains (yellow highlight) are shown.

(H) Anti-phospho-Plk4 polyclonal antibody was generated to specifically recognize phosphoThr172 (T172), an autophosphorylated residue in the Plk4 activation loop and a readout for activated kinase. Bacterially-expressed, purified Plk4 1-317-His or kinase dead (KD) 1-317 His was incubated with ATP and subsequently, either treated with λ-phosphatase or left

untreated as a control. Anti-pT172 antibody specifically recognizes Plk4, but not Plk4 KD or Plk4 treated with λ-phosphatase. Coomassie-stained protein gel (top) and the corresponding immunoblot (bottom) are shown. Note that whereas KD and λ-phosphatase-treated Plk4 migrate on SDS-PAGE as a single fast-migrating non-phosphorylated species, autophosphorylated Plk4 (WT Plk4 incubated with ATP) migrates as a series of phosphorylated polypeptides, appearing as a diffuse band or even a short ladder, corresponding to several distinct phosphorylation steps (Klebba et al., 2015a).

(I) Plk4 does not phosphorylate Sas6 in vitro. Purified Plk4 1-317-His was incubated with γ^{32}PATP and with purified, full-length GST-Sas6 (lanes 3 and 4). Lanes 1 and 3, Coomassie-stained gel; lanes 2 and 4, corresponding autoradiograms. Plk4 autophosphorylates but does not phosphorylate GST-Sas6 (red box).

Fig. S2

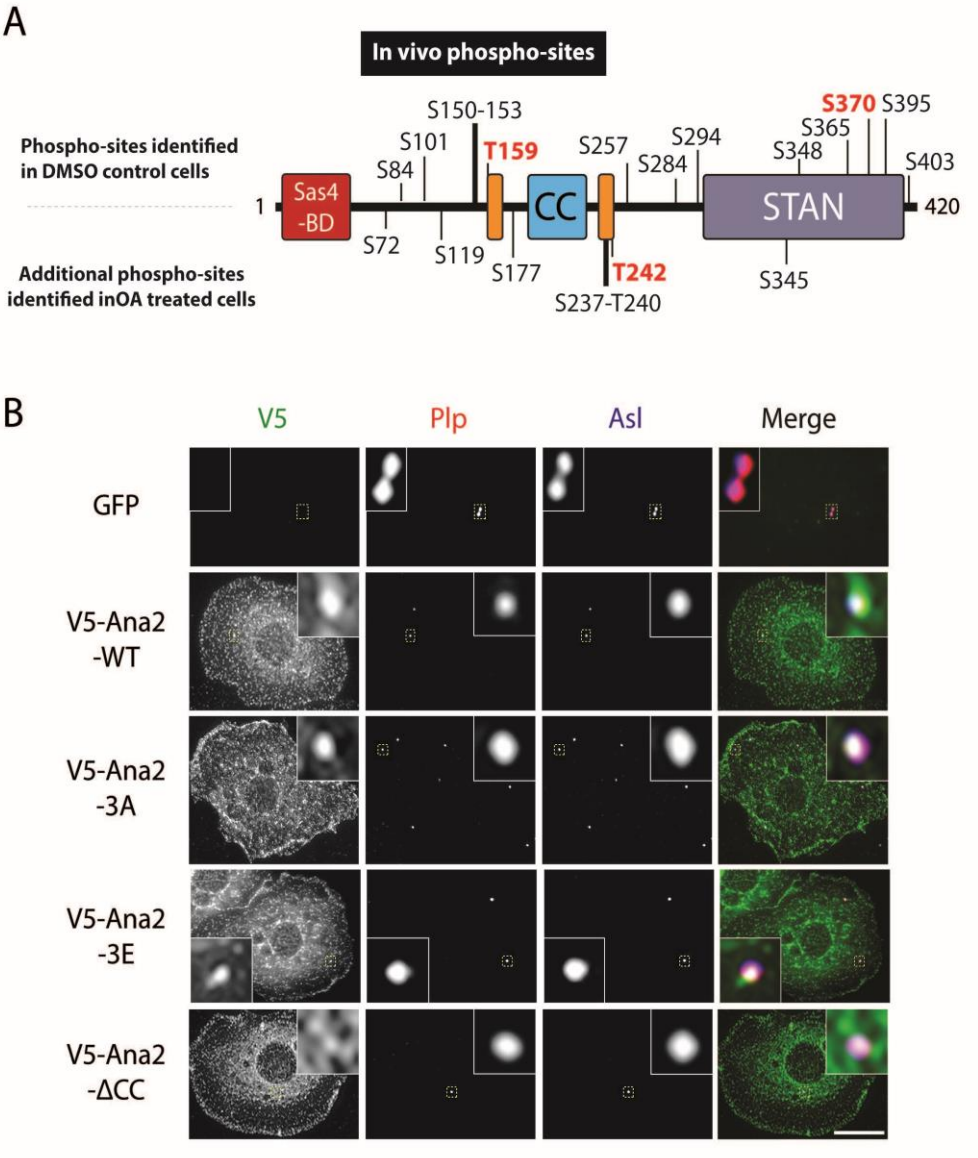
A
In vivo phospho-sites
Phospho-sites identified in DMSO control cells
Additional phospho-sites identified inOA treated cells
1
Sas4 -BD
CC
STAN
420
S72
S84
S101
S119
S150-153
T159
S177
S237-T240
T242
S257
S284
S294
S345
S348
S365
S370
S395
S403
B
V5
Plp
Asl
Merge
GFP
V5-Ana2 -WT
V5-Ana2 -3A
V5-Ana2 -3E
V5-Ana2 -ΔCC

Figure S2. Ana2 is extensively phosphorylated in cells, and phosphomimetic 3E mutations in the Ana2 N-terminus do not affect its localization to centrioles.

(A) Linear map of Ana2 depicting the in vivo phosphorylated sites identified from DMSOtreated control cells (top) and okadaic acid (OA)-treated cells (below). Some sites could not be precisely located: one residue within S150-S153 is phosphorylated (probably S150), and one residue within S237-T240 is phosphorylated.

(B) Phosphomimetic Ana2-3E localizes to centrioles in interphase S2 cells. Cells were depleted of endogenous Ana2 by RNAi for 5 days. On day 3, cells were co-transfected with GFP and the indicated V5-Ana2 construct, allowed 24 hours to recover, and then induced to express for 24 hours. Representative deconvolved maximum-intensity projections show immunostained V5Ana2 (green) and two centriole markers: PLP (red) and Asl (blue). Insets show boxed regions (yellow) at higher magnification. Note that Ana2 ΔCC does not target centrioles, but Ana2-3E does. Scale, 5μm.

(A) In vitro phosphorylation						
Site	**Peptide Sequence**	**XCorr**	**dCn**	**dCn2**	**Ions**	**z**
T69	R.AAP**T*** FASWK.K	1.22	0.58	0.67	13/16	2
T159	R.RLSSSSNADVL**T*** ICAGTQTDPFNPSPPR.K	4.47	0.12	0.55	28/108	3
T242	K.ASSTTG**T*** QCDILTTNQAGR.R	5.11	0.07	0.36	22/36	2
S318	R.IPQLAKPNTEK**S*** MVMNELALK.Y	3.46	0.29	0.64	28/80	3
S370	K.SPNPEPLRPIDNIGHAQSPNDI**S*** NASYK.Y	3.24	0.09	0.57	37/108	3

(B) Control DMSO-treated cells (in vivo)					
Site	**Peptide Sequence**	**Mascot Ion Score**	**Mascot Identity Score**	**Mascot Delta Score**	**z**
S84	R.VNF**S*** PILATELGPR.T	94.6	44.8	69.3	2
S101	R.TAPSSN**S*** PCSSKEYQVMPR.D	53.7	47.4	10.1	2
S150	R.RL**S*** SSSNADVLTICAGTQTDPFNPSPPR.K	64.8	50.1	0.8	4
T159	R.RLSSSSNADVL**T*** ICAGTQTDPFNPSPPR.K	47.3	50.2	0.0	3
S257	R.RL**S*** PIMQDYIAEEEEPLPPPQAR.V	64.3	49.5	17.0	4
S284	R.VIPQFP**S*** PRPHPPIAQSTGYR.A	46.6	46.4	1.7	2
S294	R.VIPQFPSPRPHPPIAQ**S*** TGYR.A	40.0	46.3	4.0	2
S348	R.LGASPK**S*** PNPEPLRPIDNIGHAQSPNDISNASYK.Y	63.2	50.3	2.2	3
S365	K.SPNPEPLRPIDNIGHAQ**S*** PNDISNASYK.Y	62.8	50.1	19.0	3
S370	K.SPNPEPLRPIDNIGHAQSPNDI**S*** NASYK.Y	57.8	50.0	0.6	3
S395	R.LLPEEQLEPVCPQ**S*** PMAATAPSPHIQLDLENIR.N	109.0	49.1	3.1	3
S403	R.LLPEEQLEPVCPQSPMAATAP**S*** PHIQLDLENIR.N	110.9	50.8	2.9	3

(C) OA-treated cells (in vivo)					
Site	**Peptide Sequence**	**Mascot Ion Score**	**Mascot Identity Score**	**Mascot Delta Score**	**z**
S72	R.AAPTFA**S*** WK.K	31.0	41.2	11.7	2
S84	R.VNF**S*** PILATELGPR.T	101.3	45.2	72.9	2
S101	R.TAPSSN**S*** PCSSKEYQVMPR.D	57.2	47.4	10.4	2
S119	R.DRNYA**S*** DAQQTTNHMNCNAGGYNAEPK.Q	44. 7	48.7	1.4	3
S150	R.RL**S*** SSSNADVLTICAGTQTDPFNPSPPR.K	64.4	50.3	0.0	3
T159	R.RLSSSSNADVL**T*** ICAGTQTDPFNPSPPR.K	56.3	50.3	9.1	3
S177	R.K**S*** LPQVVYSDIDVSNLANK.S	123.9	47.1	0.0	2
T242	R.AKPEAISKASSTTG**T*** QCDILTTNQAGR.R	45.4	50.2	0.0	3
S257	R.RL**S*** PIMQDYIAEEEEPLPPPQAR.V	67.4	49.2	16.5	3
S284	R.VIPQFP**S*** PRPHPPIAQSTGYR.A	49.8	47.2	12.8	2
S294	R.VIPQFPSPRPHPPIAQ**S*** TGYR.A	44.4	46.8	6.2	2
S345, S348	R.LGA**S*** PK**S*** PNPEPLRPIDNIGHAQSPNDISNASYK.Y	53.1	51.2	3.6	3
S348	R.LGASPK**S*** PNPEPLRPIDNIGHAQSPNDISNASYK.Y	54.7	49.8	5.2	3
S365	K.SPNPEPLRPIDNIGHAQ**S*** PNDISNASYK.Y	69.4	49.8	7.6	3
S370	K.SPNPEPLRPIDNIGHAQSPNDI**S*** NASYK.Y	62.4	50.4	0.4	3
S395	R.LLPEEQLEPVCPQ**S*** PMAATAPSPHIQLDLENIR.N	125.2	50.5	10.0	3

S403	R.LLPEEQLEPVCPQSPMAATAP**S***PHIQLDLENIR.N	72.7	50.1	3.5	3

Supplemental Table 1

In vitro and in vivo phosphorylated residues of Ana2.

(A) Bacterially-expressed GST-Ana2 was incubated with Plk4 1-317 and MgATP, then resolved by SDS-PAGE, and the excised Ana2 band processed for analysis by tandem mass spectrometry. Peptide sequences were identified with the Sequest algorithm. Confidence of the identification of the tryptic peptides was based primarily on XCorr scores; a positive identification required an Xcorr score >2.5 and >3.4 for doubly and triply charged peptides, respectively. Confidence of the peptide identification was further increased if the deltaCn score was >0.1. T69 is a lower confidence site because of the low XCorr score (which could be due, in part, to the relatively small size of this peptide). Phosphorylated residues are indicated with bold and large font and are followed with the (*) symbol. Total coverage was 85%; the first 64 residues of Ana2 were not recovered. No phosphorylated residues were observed in the control sample of Ana2 (i.e., GST-Ana2 incubated with only MgATP); total coverage was 85% for the control sample (the first 64 residues were not recovered).

(B and C) S2 cells were transfected with the GFP-Ana2 construct which was induced with 2 mM

$CuSO_4$. Cells were treated with 100 nM (final) okadaic acid (or the same volume of control DMSO), and then the GFP-Ana2 immunoprecipitated from cell lysates. Samples were resolved by SDS-PAGE and the GFP-Ana2 bands excised from the Coomassie-stained gels for processing in preparation for MS/MS analysis. Peptide sequences were matched to spectra using Mascot (MatrixScience). Coverage was 83% for B and 81% for C; the first 65 residues were poorly covered.

CHAPTER FOUR: FUTURE STUDIES AND CONCLUSIONS

4.1 Future Studies

My studies have led to the discovery of an interaction between 2 key centriolar proteins responsible for promoting procentriole assembly. First, in chapter 2 we discovered a centrosome interactome, identifying several centriole protein-protein interactions by yeast-2-hybrid. Several of these interactions were validated, including the Plk4-Ana2 interaction. In chapter 3, we discovered that Plk4 phosphorylates Ana2, which functions to both positively and negatively regulate centriole duplication. When we mutated the 3 N-terminal residues to mimic phosphorylation (T69ET159ET242E, 3E) we noticed a decrease in centriole numbers when replacing endogenous Ana2. We determined this was occurring because Plk4 could no longer bind Ana2, and subsequently no longer phosphorylate the key C-terminal residues required for Sas-6 recruitment to the centriole. Interestingly, we found that Ana2-3E was still able to localize to the centriole, even though it was no longer interacting with Plk4, negating the direct interaction of the two proteins being required for Ana2 localization at the centriole. Plk4 kinase activity, however is required for maintaining the human ortholog of Ana2, STIL, at the centriole. We thus concluded that Plk4 is phosphorylating a separate protein at the centriole to recruit Ana2. (Figure 1)

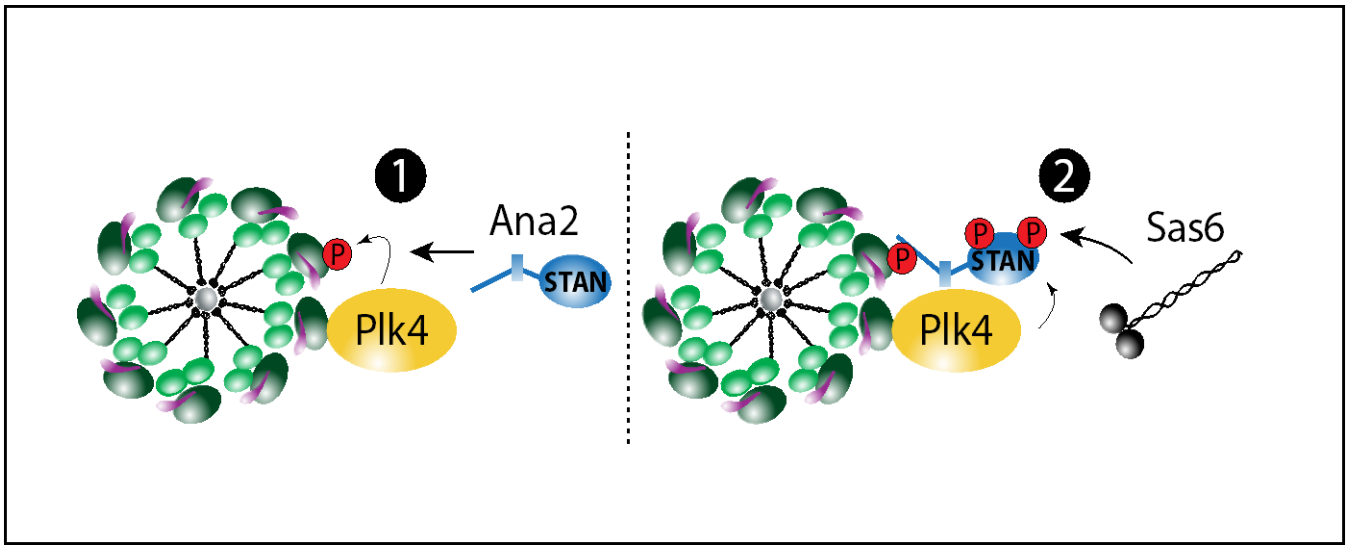

Figure 1: Assembly of centriole proteins.

(1) Plk4 localizes to the outer wall of the centriole, positioning it to phosphorylate a key centriole protein to recruit Ana2.

(2) Ana2 binds phosphorylated protein X and Plk4 is able to bind and phosphorylate Ana2 in mitosis to recruit Sas-6 and continue with centriole assembly.

To determine the centriole protein being phosphorylated by Plk4 to recruit Ana2, we hypothesized that the protein would need to be required for centriole assembly, as misregulation of this pathway would lead to a failure of centrioles to duplicate. Testing some key components of protein duplication, I was able to find 2 new interactors of Ana2, and several other proteins already known to interact with Ana2. (Figure 2)

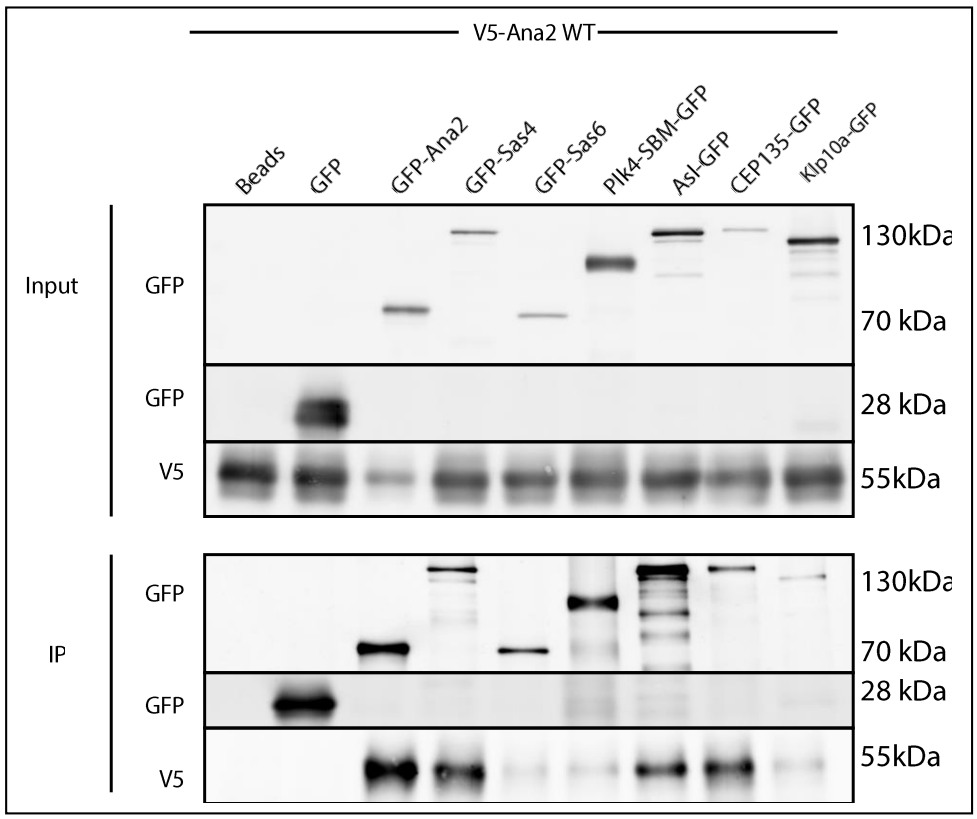

Figure 2. Ana2 interacts with several centriole proteins. Co-IP of V5-Ana2-WT with GFP-tagged centriole proteins were detected by western blot

4.1.1 Identify Plk4 dependent interactors of Ana2

In Drosophila S2 cells, we co-transfected V5-ana2 with several GFP-tagged centriole proteins and performed co-IPs. Both Asl and Cep135 are novel interactors of Ana2, and we were able to confirm that Ana2 interacts with Sas-4 and is able to self-interact. To test whether these proteins are able to recruit Ana2 to the centriole in a Plk4 dependent manner, we tested the overexpression of a non-degradable form of Plk4, Plk4-SBM-myc, versus the kinase dead form, Plk4-KD-myc, or no Plk4, with the expression of V5-Ana2 and 3 of the main centriole proteins, Sas-4, Asl, and Cep135. Notably, Sas-6 is already known to interact with Ana2 in a

phosphodependent manner. Co-transfection of the 3 proteins led to an increase in bound Ana2 in only one. Overexpression of Plk4-SBM led to a notable increase in the amount of Ana2 bound to Sas-4, a slight increase in Ana2 bound to Cep135, and no increase in Ana2 bound to Asl. (Figure 3 A, B, C, resp.) Furthermore, Sas-4 has a strong interaction with hyper-phosphorylated Ana2. As seen in Figure 3A, an approximate 2-fold increase in ana2 is bound to Sas-4 when Plk4-SBM is overexpressed compared to no Plk4 OE, and Plk4-KD OE. Interestingly, a higher band appears when Plk4, Ana2 and Sas-4 are all OE, indicating Ana2 is hyper-phosphorylated in the presence of excess Sas-4. This band also appears to bind preferentially to Sas-4 as indicated by co-IP in Figure 3A. The consequences of hyper-phosphorylation of Ana2 have not been elucidated, however, we believe it may aid in the recruitment of sas-6 to further centriole duplication.

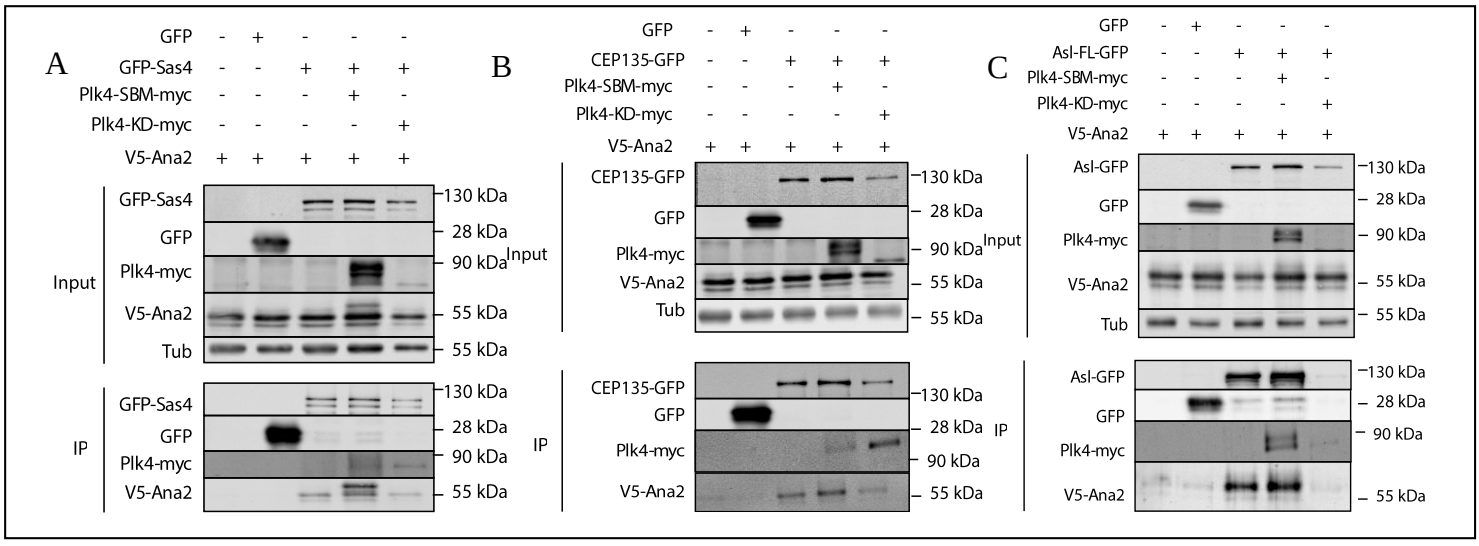

Figure 3. Ana2 associates with centriole proteins in a phosphor-dependent manner

(A) Co-transfection of V5-Ana2-WT, Sas4-GFP and either Plk4-SBM-myc or Plk4-KD-myc, into S2 cells, was followed by and anti-GFP IP and analysis by Western blot.

(B) Co-transfection of V5-Ana2-WT, Cep135-GFP and either Plk4-SBM-myc or Plk4-KD-myc, into S2 cells, was followed by and anti-GFP IP and analysis by Western blot.

(C) Co-transfection of V5-Ana2-WT, Asl-GFP and either Plk4-SBM-myc or Plk4-KD-myc, into S2 cells, was followed by and anti-GFP IP and analysis by Western blot.

We next tried to discover the region in Sas-4 necessary for this increase in ana2 binding. Previously, the crystal structure of Ana2 bound to Sas4-C, or the G-box domain, had been solved. We aimed to discover if this is the necessary interaction for binding of hyperphosphorylated Ana2. S2 cells were co-transfected with 3 truncated versions of Sas4-GFP, Sas4-A-GFP, Sas4-B-GFP and Sas4-C-GFP, and V5-Ana2 and either Plk4-SBM-myc or Plk4-KD-myc. We found that Sas4-C is sufficient to mediate hyperphosphorylation and increased binding of Ana2. (Figure 4)

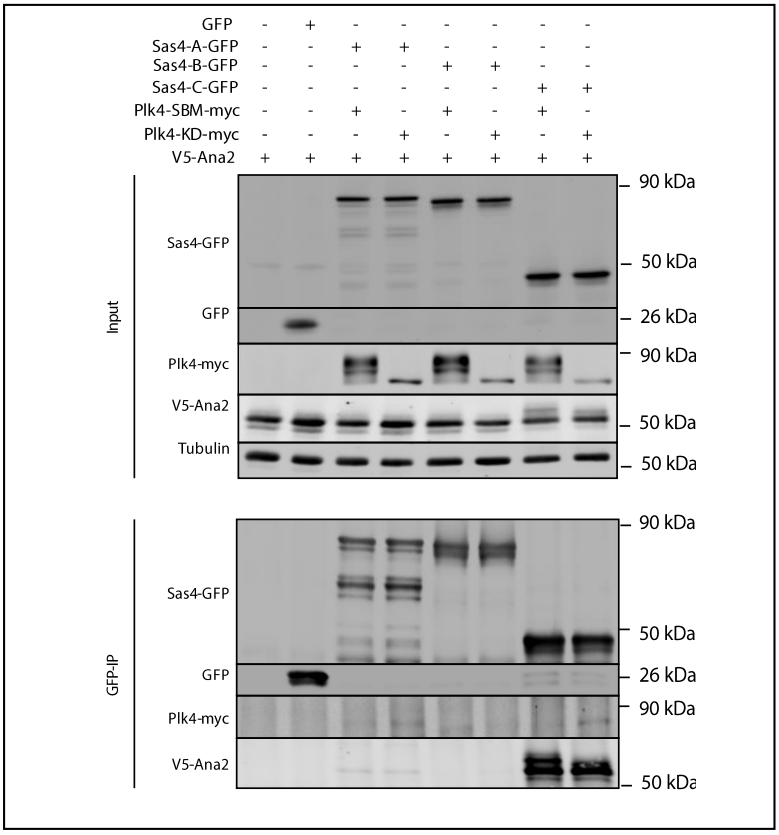

Figure 4. Hyper-phosphorylated Ana2 interacts with Sas4-C

(1) Co-transfection of V5-Ana2-WT, Sas4-A,B,C-GFP and either Plk4-SBM-myc or Plk4-KD-myc, into S2 cells, was followed by and anti-GFP IP and analysis by Western blot.

4.1.2 Identify centriolar targets of Plk4 phosphorylation

Importantly, all 3 of the proteins seen to interact with Ana2 in Figure 2 are substrates of Plk4. In an in vitro kinase assay, we looked at several possible substrates of Plk4 phosphorylation. Notably, Plk4 phosphorylates Ana2, as previously determined, but it does not phosphorylate Sas-6, indicating Plk4 is not a promiscuous kinase. (Figure 5)

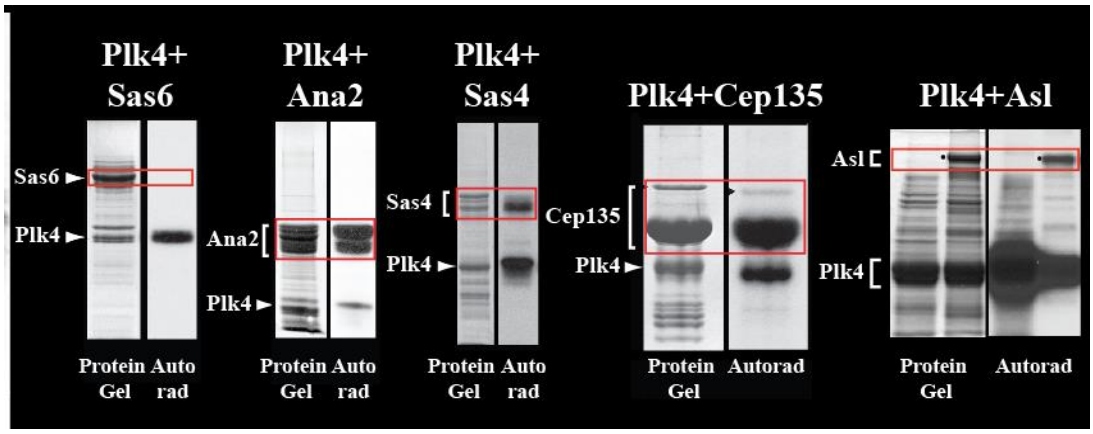

Figure 5. Centriolar substrates of Plk4 phosphorylation

In vitro kinase assays were performed on recombinant proteins purified from E. coli

We continued in this line of thought, and determined Sas-4 to be a good target for Plk4 based recruitment of Ana2 and hence the target for the initial licensing event of the mother centriole in preparation for centriole duplication.

Full-length Sas4 is phosphorylated by Plk4 both in vitro and in vivo. In order to narrow down the sites of phosphorylation, Sas-4 was cut up into 3 pieces termed Sas4-A, Sas4-B and Sas4-C. S2 cells were co-transfected with the Sas-4 construct tagged with GFP and either Plk4-SBM or Plk4-KD. Anti-GFP IPs were performed and the gel slice corresponding to the Sas-4 construct was analyzed by mass-spec. Concurrently, we performed in vitro kinase assays on purified recombinant Sas-4 constructs to determine locations of Plk4 phosphorylations. We found that Plk4 phosphorylates Sas-4 A, B, and c in vitro, and Sas-4 A, and B in vivo. (Figure 6A, C)

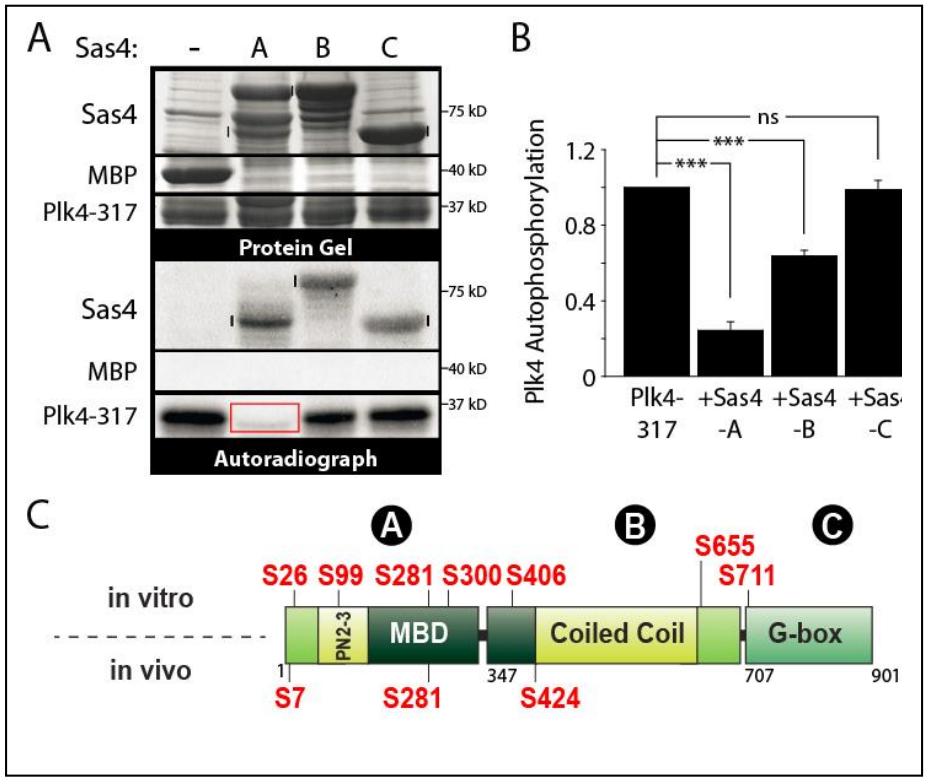

Figure 6. Plk4 phosphorylates Sas-4

(A) In vitro kinase assays performed on recombinant MBP-Sas4-A, B, C purified from E. coli.

(B) Graph depicting relative levels of autophosphorylation of Plk4 1-317-His in the presence of truncated MBP-Sas4.

(C) Mass spectrometry analysis of MBP-Sas4 truncated constructs incubated with Plk4 1-317-His

4.1.3 Sas-4 interacts with Plk4 and regulates kinase activity

Interestingly, we found that incubating Sas-4-A or Sas-4-B with Plk4 1-317 led to a decrease in Plk4 autophosphorylation (Figure 6B) This decrease in Plk4 autophosphorylation implies a possible direct interaction of Plk4 and Sas-4. Plk4 is a heavily phosphorylated protein, its autophosphorylation leading to its own destruction. Sas-4 binding to a heavily phosphorylated region of Plk4 and blocking the subsequent phosphorylation could be one mechanism by which Sas-4 diminishes Plk4's autophosphorylation capacity, without affecting kinase activity (as Sas-4-A, -B are still phosphorylated) Using recombinant sas-4 and Plk4 1-317 we looked into in vitro binding of sas-4 with plk4. We discovered that Sas-4-A, -B, and –C interact with Plk4. (Figure 7)

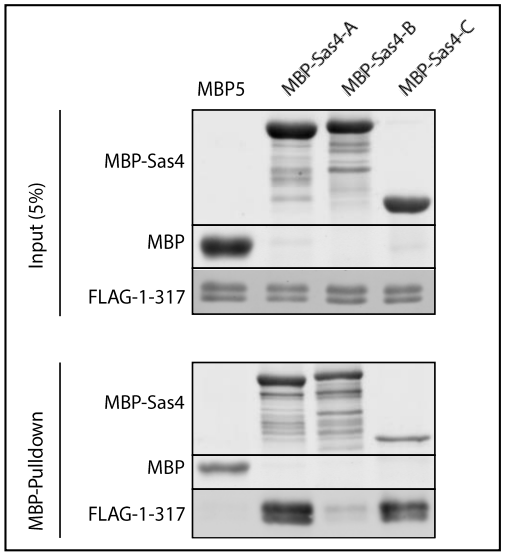

Figure 7. Sas4 directly interacts with Plk4.

Recombinant MBP-Sas4 and Plk4 1-317-His were incubated for 2 hours followed by an amylose resin pulldown. Analysis by Western blot followed.

It remains to be seen if Sas4-A is causing a decrease in autophosphorylation of Plk4 by blocking specific residues to be phosphorylated. Future experiments using recombinant Plk4 and Sas4 in vitro and mass spec can determine the phosphorylated residues of Plk4 in the presence and absence of Sas4. Notably, the truncated Sas4 constructs bind Plk4 in a region that regulates its destruction. In chapter 1, I discussed the regulatory mechanism of Plk4. In brief, Plk4 trans-autphosphorylates generating its own Slimb-binding phosphodegron. Should Sas4-A bind in this region, we would expect Plk4 to be stabilized, as its trans-autophosphorylation would be impaired and impede Slimb binding. Possibly, Sas4 competes with Slimb for binding as well. More research will need to be conducted to determine the effects of Sas4 binding to Plk4, however preliminary results indicate that Plk4 is not highly stabilized by overexpression of the Sas4 truncated constructs. Co-transfection of S2 cells with Sas4-A, -B, -C and Plk4 did not cause an amplification of centriole number, (data not shown) as one would expect for a stabilized Plk4.

4.1.4 Plk4 regulates Sas4-dependent microtubule polymerization

Sas4 is known to regulate microtubule assembly and has the ability to bind and sequester α/β tubulin. It is thought to control centriole assembly and elongation through assembling the centriole microtubules. [48,59–62,73,109,110] Furthermore, the human Sas4 orthologue, CPAP, regulates microtubule assembly at the centriole, a process that is governed by phosphorylation by Plk2. Plk2 is not conserved across species, thus we hypothesized that Plk4 might serve this

regulatory role in flies. Importantly, Plk4 phosphorylates Sas4 on three residues in the microtubule capping/binding domains (PN2-3, MBD) (figure 5C); one of these residues is conserved across species and phosphorylated by both Plk2 and Plk4 in CPAP.[60] In S2 cells co-transfected with Sas4 truncations and Plk4, I was able to determine the possible regulation of microtubule assembly by Plk4 and Sas4. Using a sedimentation assay, I found that a higher percentage of microtubules pelleted when in the presence of overexpressed Sas4-FL or Sas4-AB (containing the entire MBD) than compared to the GFP control. Overexpression of both Sas4 and Plk4 led to a dramatic decrease in the pelleted fraction of tubulin, with a shift to tubulin dimers in the supernatant fraction. This is indicative of Plk4 phosphorylating Sas4, increasing Sas4 affinity for the α/β tubulin dimer, leading to a decrease in polymerization of tubulin dimers and decreased microtubules in the pelleted fraction. (Data not shown) We can infer from studies in human cells that Sas4 is an important regulator of microtubule assembly at the centriole. In fact, Sas4-A and Sas4-B (regions containing the MBD and PN2-3) localize to microtubules when overexpressed in S2 cells depleted of endogenous Sas4. Importantly, the truncated mutants of Sas4 do not rescue centriole duplication. (Figure 8)

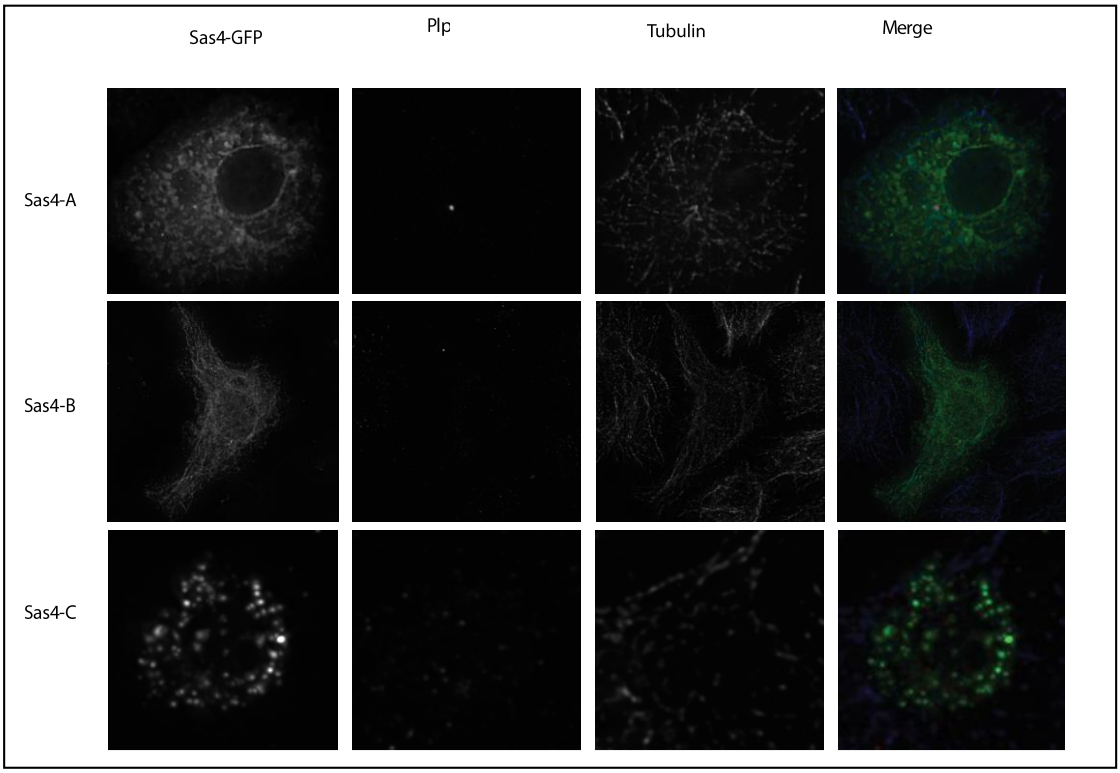

Figure 8. Localization of Sas4-A, -B, -C-GFP in S2 cells

S2 cells were transfected with Sas4-A,B,C-GFP constructs and analyzed by fluorescent microscopy.

A recent study by Sharma et al. was key to understanding the function of CPAP in centriole assembly. They determined that the conserved CPAP domain, PN2-3, caps microtubule plus ends and dampens their elongation, providing insight into why centrioles assemble microtubules slowly and achieve a specific length.[61] This study did not look at the effect of Plk4 phosphorylation of CPAP, but one can imagine that Plk4 phosphorylates CPAP/Sas4 causing decreased microtubule growth, limiting the length of the centriole.

4.1.5 Plk4 influences Sas4 aggregation

One long standing question in the field of centriole biogenesis is how Plk4 determines the spot on the mother centriole to be licensed. The centriole is a symmetric barrel-shaped structure with no known inherent asymmetries. How then is the site of the procentriole determined? Early research on Drosophila Plk4 indicated that it localized to asymmetrically to the outside wall of the mother centriole. More recently, human Plk4 was shown to localize to the mother centriole as either a ring or a spot, depending on the amount of STIL present. Importantly, in Drosophila, Ana2 localizes to a single spot in the lumen of the mother centriole, or to the site of daughter centriole assembly. There does not seem to be an asymmetric-like pattern to its localization. We discovered that Sas4 exhibits a dynamic localization at the centriole, often localizing to a ring around the mother centriole and a spot designating the site of procentriole assembly, as well as a spot in the lumen of the mother centriole. (Figure 9) How Sas4 attains this localization pattern is not fully understood. This protein could provide keen insights into the first event in centriole duplication, the licensing of the centriole.

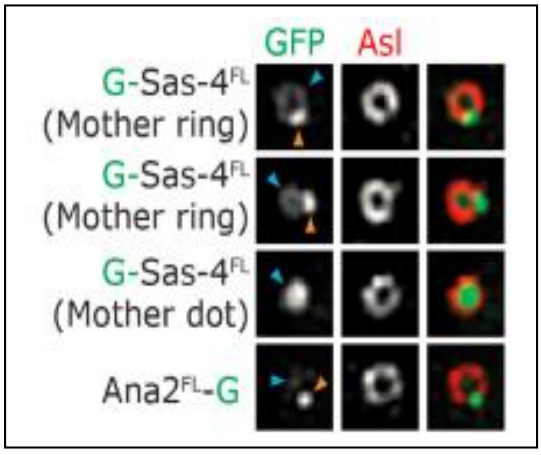

Figure 9. Sas4 is a dynamic centriolar protein.

S2 cells were transfected with Sas4-GFP or Ana2-GFP constructs and analyzed by fluorescent microscopy.

Sas4 consists of 4 distinct domains, a microtubule plus end capping region, PN2-3, a microtubule binding domain, MBD, a coiled coil domain, CCD, and a C-terminal glutamine rich G-box domain. The Sas4 GBox is essential for binding to Ana2 and localizing to centrioles. The crystal structure of the Gbox domain has revealed this important region forms an amyloid fibril

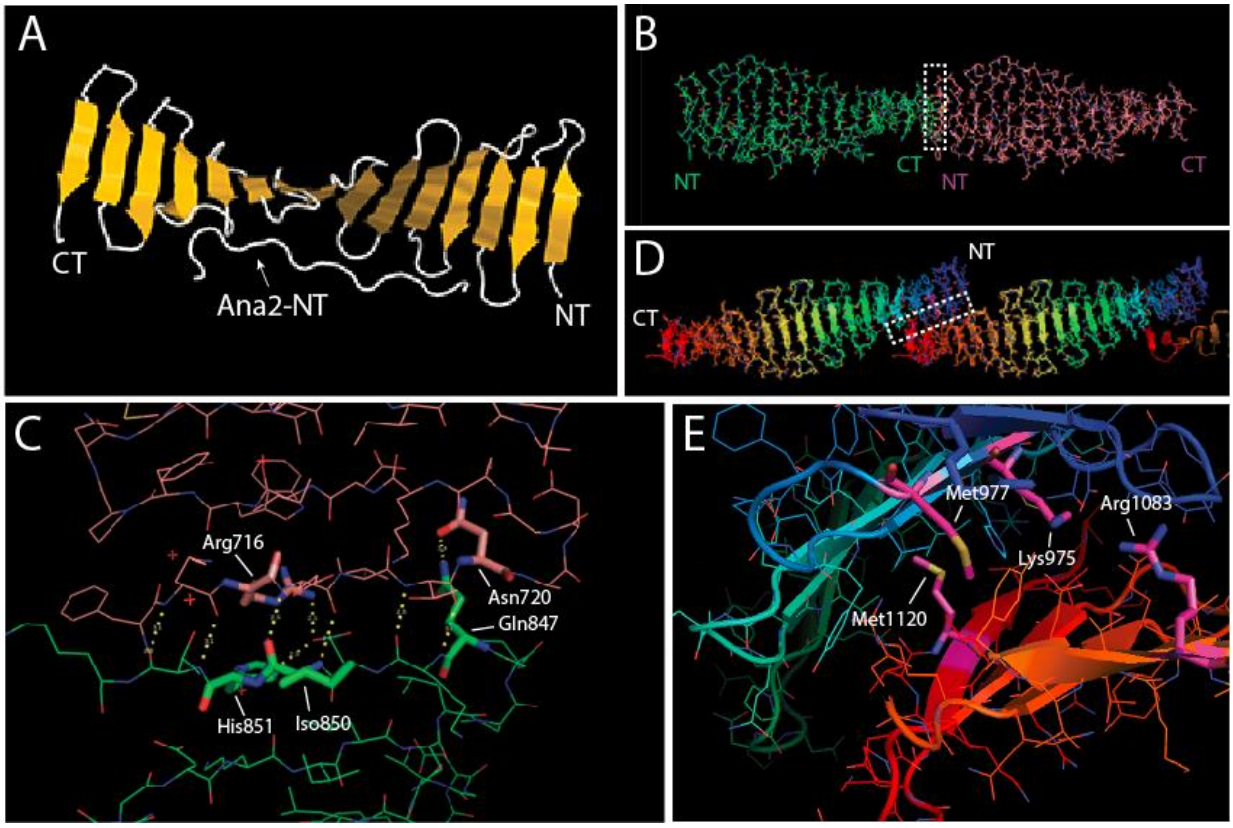

Figure 10. Crystal structure of Sas4 GBox.

at certain concentrations. An amyloid fibril is composed of normally soluble proteins assembling to form a more insoluble, degradation resistant aggregate. The amyloid fibril domain

of Sas4 consists of an organized structure of N-terminal to C-terminal interactions, forming either a head-to-tail structure, or a staggered head-to-tail structure, thus enabling the G-Box to aggregate.[111,112] We propose that Sas4 aggregation into a single spot may occur in a Plk4 dependent fashion. Plk4 phosphorylates Sas4 on one residue in the G-Box domain, inducing a possible conformational change that leads to aggregation in an amyloid-like manner. Prion promoted phosphorylation has been seen in yeast,[113] but is unstudied in Drosophila. In the future, I would like to discover the basis for phosphorylation promoting aggregation in Sas-4 as a mechanism for designing a scaffold to recruit and concentrate other centriolar proteins and designate the site of procentriole assembly on the parental centriole.

4.2 Conclusions

Our understanding of the field of centriole duplication has greatly expanded in recent years, along with our knowledge of the mechanisms regulating this process. Recent advances in experimental techniques (functional genomic RNAi-based screening and structured illumination microscopy, as examples) and the complete sequencing of the genomes of several model systems have greatly enhanced our abilities to analyze this set of complex events, and so further advances to our knowledge are emerging rapidly. Since many fundamentally important processes (like stem cell division, embryonic development and cell locomotion) depend on centrosome function, the motivation to understand when and how cells fail to properly maintain their centriole number is clear.

The pathways which regulate centriole biogenesis are complex, but likely as phylogenetically conserved as these organelles are themselves. Proper centriole number is necessary for proper

centriole function, and so cells and organisms are likely subjected to a substantial selective pressure to control centriole duplication. Since centrioles normally duplicate once and only once per cell cycle, it will be particularly instructive to study cell types (like multi-ciliated cells or cancer cells) that fail to follow this general rule. Knowledge of the safeguards and how they may fail could further our understanding of the etiology of diseases such as cancer, dwarfism, primary microcephaly, and polycystic kidney disease.

4.3 References

1. Delattre M, Canard C, Gonczy P. Sequential Protein Recruitment in C. elegans Centriole Formation. *Curr Biol*. 2006;16(18):1844-1849. doi:10.1016/j.cub.2006.07.059.
2. Nigg EA, Cajanek L, Arquint C. The centrosome duplication cycle in health and disease. *FEBS Lett*. 2014;588(15):2366-2372. doi:10.1016/j.febslet.2014.06.030.
3. Gönczy P. Towards a molecular architecture of centriole assembly. *Nat Rev Mol Cell Biol*. 2012;13(7):425-435. doi:10.1038/nrm3373.
4. Robbins E, Jentzsch G, Micali A. The centriole cycle in synchronized HeLa cells. *J Cell Biol*. 1968;36(2):329-339. doi:10.1083/jcb.36.2.329.
5. Avidor-Reiss T, Gopalakrishnan J. Building a centriole. *Curr Opin Cell Biol*. 2013;25(1):1-6. doi:10.1016/j.ceb.2012.10.016.
6. Tsou, Meng-Fu Bryan; Stearns T. Mechanism limiting centrosome duplication to once per cell cycle. http://www.nature.com/nature/journal/v442/n7105/pdf/nature04985.pdf.
7. Lingle WL, Barrett SL, Negron VC, et al. Centrosome amplification drives chromosomal instability in breast tumor development. *Proc Natl Acad Sci U S A*. 2002;99(4):1978-1983. doi:10.1073/pnas.032479999.

8. Negrini S, Gorgoulis VG, Halazonetis TD. Genomic instability--an evolving hallmark of cancer. *Nat Rev Mol Cell Biol*. 2010;11(3):220-228. doi:10.1038/nrm2858.

9. Ganem NJ, Godinho S a, Pellman D. NIH Public Access. 2010;460(7252):278-282. doi:10.1038/nature08136.A.

10. Lingle WL, Salisbury JL. Altered centrosome structure is associated with abnormal mitoses in human breast tumors. *Am J Pathol*. 1999;155(6):1941-1951. doi:10.1016/S0002-9440(10)65513-7.

11. Cunha-Ferreira I, Bento I, Bettencourt-Dias M. From zero to many: control of centriole number in development and disease. *Traffic*. 2009;10(5):482-498. doi:10.1111/j.1600-0854.2009.00905.x.

12. Bettencourt-Dias M, Hildebrandt F, Pellman D, Woods G, Godinho SA. Centrosomes and cilia in human disease. *Trends Genet*. 2011;27(8):307-315. doi:10.1016/j.tig.2011.05.004.

13. Zyss D, Gergely F. Centrosome function in cancer: guilty or innocent? *Trends Cell Biol*. 2009;19(7):334-346. doi:10.1016/j.tcb.2009.04.001.

14. Tsou MFB, Stearns T. Controlling centrosome number: Licenses and blocks. *Curr Opin Cell Biol*. 2006;18(1):74-78. doi:10.1016/j.ceb.2005.12.008.

15. Brownlee CW, Rogers GC. Show me your license, please: deregulation of centriole duplication mechanisms that promote amplification. *Cell Mol Life Sci*. 2013;70(6):1021-1034. doi:10.1007/s00018-012-1102-6.

16. Nigg E a, Stearns T. The centrosome cycle: Centriole biogenesis, duplication and inherent asymmetries. *Nat Cell Biol*. 2011;13(10):1154-1160. doi:10.1038/ncb2345.

17. Fujita H, Yoshino Y, Chiba N. Regulation of the centrosome cycle. *Mol Cell Oncol*. 2015;3556(August):00-00. doi:10.1080/23723556.2015.1075643.

18. Rodrigues-martins AA, Riparbelli M, Callaini G, Glover DM. Revisiting the Role of the Mother Centriole in Centriole Biogenesis. *Science*. 2007;316(5827):1046-1050.

19. Lopes CAM, Jana SC, Cunha-Ferreira I, et al. PLK4 trans-Autoactivation Controls Centriole Biogenesis in Space. *Dev Cell*. 2015;35(2):222-235. doi:10.1016/j.devcel.2015.09.020.

20. Gopalakrishnan J, Guichard P, Smith AH, et al. Self-assembling SAS-6 multimer is a core centriole building block. *J Biol Chem*. 2010;285(12):8759-8770. doi:10.1074/jbc.M109.092627.

21. Kitagawa D, Vakonakis I, Olieric N, et al. Structural basis of the 9-fold symmetry of centrioles. *Cell*. 2011;144(3):364-375. doi:10.1016/j.cell.2011.01.008.

22. Nakazawa Y, Hiraki M, Kamiya R, Hirono M. SAS-6 is a Cartwheel Protein that Establishes the 9-Fold Symmetry of the Centriole. *Curr Biol*. 2007;17(24):2169-2174. doi:10.1016/j.cub.2007.11.046.

23. Habedanck R, Stierhof Y-D, Wilkinson CJ, Nigg E a. The Polo kinase Plk4 functions in centriole duplication. *Nat Cell Biol*. 2005;7(11):1140-1146. doi:10.1038/ncb1320.

24. Wang W-J, Soni RK, Uryu K, Tsou M-FB. The conversion of centrioles to centrosomes: essential coupling of duplication with segregation. *J Cell Biol*. 2011;193(4):727-739. doi:10.1083/jcb.201101109.

25. Hatch EM, Kulukian A, Holland AJ, Cleveland DW, Stearns T. Cep152 interacts with Plk4 and is required for centriole duplication. *J Cell Biol*. 2010;191(4):721-729. doi:10.1083/jcb.201006049.

26. Blachon S, Gopalakrishnan J, Omori Y, et al. Drosophila asterless and vertebrate Cep152 are orthologs essential for centriole duplication. *Genetics*. 2008;180(4):2081-2094.

doi:10.1534/genetics.108.095141.

27. Kim T-S, Park J-E, Shukla A, et al. Hierarchical recruitment of Plk4 and regulation of centriole biogenesis by two centrosomal scaffolds, Cep192 and Cep152. *Proc Natl Acad Sci U S A*. 2013;110(50):E4849-E4857. doi:10.1073/pnas.1319656110.

28. Sonnen KF, Gabryjonczyk A-M, Anselm E, Stierhof Y-D, Nigg E a. Human Cep192 and Cep152 cooperate in Plk4 recruitment and centriole duplication. *J Cell Sci*. 2013;126(Pt 14):3223-3233. doi:10.1242/jcs.129502.

29. Cizmecioglu O, Arnold M, Bahtz R, et al. Cep152 acts as a scaffold for recruitment of Plk4 and CPAP to the centrosome. *J Cell Biol*. 2010;191(4):731-739. doi:10.1083/jcb.201007107.

30. Hatch EM, Kulukian A, Holland AJ, Cleveland DW, Stearns T. Cep152 interacts with Plk4 and is required for centriole duplication. *J Cell Biol*. 2010;191(4):721-729. doi:10.1083/jcb.201006049.

31. Dzhindzhev NS, Yu QD, Weiskopf K, et al. Asterless is a scaffold for the onset of centriole assembly. *Nature*. 2010;467(7316):714-718. doi:10.1038/nature09445.

32. Klebba JE, Galletta BJ, Nye J, et al. Two Polo-like kinase 4 binding domains in Asterless perform distinct roles in regulating kinase stability. *J Cell Biol*. 2015;208(4):401-414. doi:10.1083/jcb.201410105.

33. Dzhindzhev NS, Tzolovsky G, Lipinszki Z, et al. Plk4 Phosphorylates Ana2 to Trigger Sas6 Recruitment and Procentriole Formation. *Curr Biol*. 2014:1-7. doi:10.1016/j.cub.2014.08.061.

34. Rogers GC, Rusan NM, Roberts DM, Peifer M, Rogers SL. The SCF Slimb ubiquitin ligase regulates Plk4/Sak levels to block centriole reduplication. *J Cell Biol*.

2009;184(2):225-229. doi:10.1083/jcb.200808049.

35. Ohta M, Ashikawa T, Nozaki Y, et al. Plk4 directly interactes with STIL. *Nat Commun*. 2014;5:1-12. doi:10.1038/ncomms6267.

36. Zitouni S, Francia ME, Leal F, et al. CDK1 Prevents Unscheduled PLK4-STIL Complex Assembly in Centriole Biogenesis. *Curr Biol*. 2015:1127-1137. doi:10.1016/j.cub.2016.03.055.

37. Moyer TC, Clutario KM, Lambrus BG, Daggubati V, Holland AJ. Binding of STIL to Plk4 activates kinase activity to promote centriole assembly. *J Cell Biol*. 2015;209(6):863-878. doi:10.1083/jcb.201502088.

38. Kratz A-S, Bärenz F, Richter KT, Hoffmann I. Plk4-dependent phosphorylation of STIL is required for centriole duplication. *Biol Open*. 2015;4(3):370-377. doi:10.1242/bio.201411023.

39. Arquint C, Gabryjonczyk AM, Imseng S, et al. STIL binding to Polo-box 3 of PLK4 regulates centriole duplication. *Elife*. 2015;4(JULY2015):1-22. doi:10.7554/eLife.07888.

40. Gibbons IR, Grimstone A V. On flagellar structure in certain flagellates. *J Biophys Biochem Cytol*. 1960;7(4):697-716. doi:10.1083/jcb.7.4.697.

41. Hirono M. Cartwheel assembly. *Philos Trans R Soc Lond B Biol Sci*. 2014;369(1650):20130458 - . doi:10.1098/rstb.2013.0458.

42. Cottee MA, Muschalik N, Johnson S, Leveson J, Raff JW, Lea SM. The homo-oligomerisation of both Sas-6 and Ana2 is required for efficient centriole assembly in flies. *Elife*. 2015;4(MAY):1-65. doi:10.7554/eLife.07236.

43. Fong CS, Kim M, Yang TT, Liao JC, Tsou MFB. SAS-6 Assembly Templated by the Lumen of Cartwheel-less Centrioles Precedes Centriole Duplication. *Dev Cell*.

2014;30(2):238-245. doi:10.1016/j.devcel.2014.05.008.

44. Arquint C, Sonnen KF, Stierhof Y-D, Nigg E a. Cell-cycle-regulated expression of STIL controls centriole number in human cells. *J Cell Sci*. 2012;125(Pt 5):1342-1352. doi:10.1242/jcs.099887.

45. Arquint C, Nigg EA. STIL microcephaly mutations interfere with APC/C-mediated degradation and cause centriole amplification. *Curr Biol*. 2014;24(4):351-360. doi:10.1016/j.cub.2013.12.016.

46. Stevens NR, Dobbelaere J, Brunk K, Franz A, Raff JW. Drosophila Ana2 is a conserved centriole duplication factor. *J Cell Biol*. 2010;188(3):313-323. doi:10.1083/jcb.200910016.

47. Hilbert M, Noga A, Frey D, et al. SAS-6 engineering reveals interdependence between cartwheel and microtubules in determining centriole architecture. *Nat Cell Biol*. 2016;18(4):393-403. doi:10.1038/ncb3329.

48. Lin Y-NY-CY-NY-C, Chang C-W, Hsu W-B, et al. Human microcephaly protein CEP135 binds to hSAS-6 and CPAP, and is required for centriole assembly. *EMBO J*. 2013;32(8):1141-1154. doi:10.1038/emboj.2013.56.

49. Chang C, Hsu W, Tsai J, Tang CC, Tang TK. CEP295 interacts with microtubules and is required for centriole elongation. *J Cell Sci*. 2016;(May):2501-2513. doi:10.1242/jcs.186338.

50. Gudi R, Zou C, Li J, Gao Q. Centrobin-tubulin interaction is required for centriole elongation and stability. *J Cell Biol*. 2011;193(4):711-725. doi:10.1083/jcb.201006135.

51. Tang CJ, Fu RH, Wu KS, Hsu WB, Tang TK. CPAP is a cell-cycle regulated protein that controls centriole length. *Nat Cell Biol*. 2009;11(7):825-831. doi:10.1038/ncb1889.

52. Schmidt TI, Kleylein-Sohn J, Westendorf J, et al. Control of Centriole Length by CPAP and CP110. *Curr Biol*. 2009;19(12):1005-1011. doi:10.1016/j.cub.2009.05.016.

53. Sonnen KF, Schermelleh L, Leonhardt H, Nigg E a. 3D-structured illumination microscopy provides novel insight into architecture of human centrosomes. *Biol Open*. 2012;1(10):965-976. doi:10.1242/bio.20122337.

54. Conduit PT, Wainman A, Novak ZA, Weil TT, Raff JW. Re-examining the role of Drosophila Sas-4 in centrosome assembly using two-colour-3D-SIM FRAP. *Elife*. 2015;4(NOVEMBER2015):1-12. doi:10.7554/eLife.08483.

55. Novak ZA, Conduit PT, Wainman A, Raff JW. Asterless licenses daughter centrioles to duplicate for the first time in Drosophila embryos. *Curr Biol*. 2014;24(11):1276-1282. doi:10.1016/j.cub.2014.04.023.

56. Fu J, Lipinszki Z, Rangone H, et al. Conserved Molecular Interactions in Centriole-to-Centrosome Conversion. 2016;18(1):87-99. doi:10.1038/ncb3274.Conserved.

57. Hiraki M, Nakazawa Y, Kamiya R, Hirono M. Bld10p Constitutes the Cartwheel-Spoke Tip and Stabilizes the 9-Fold Symmetry of the Centriole. *Curr Biol*. 2007;17(20):1778-1783. doi:10.1016/j.cub.2007.09.021.

58. Izquierdo D, Wang WJ, Uryu K, Tsou MFB. Stabilization of cartwheel-less centrioles for duplication requires CEP295-mediated centriole-to-centrosome conversion. *Cell Rep*. 2014;8(4):957-965. doi:10.1016/j.celrep.2014.07.022.

59. Comartin D, Gupta GD, Fussner E, et al. CEP120 and SPICE1 cooperate with CPAP in centriole elongation. *Curr Biol*. 2013;23(14):1360-1366. doi:10.1016/j.cub.2013.06.002.

60. Chang J, Cizmecioglu O, Hoffmann I, Rhee K. PLK2 phosphorylation is critical for CPAP function in procentriole formation during the centrosome cycle. *EMBO J*.

2010;29(14):2395-2406. doi:10.1038/emboj.2010.118.

61. Sharma A, Aher A, Dynes NJ, et al. Centriolar CPAP/SAS-4 Imparts Slow Processive Microtubule Growth. *Dev Cell*. 2016;37(4):362-376. doi:10.1016/j.devcel.2016.04.024.

62. Tang C-JC, Lin S-Y, Hsu W-B, et al. The human microcephaly protein STIL interacts with CPAP and is required for procentriole formation. *EMBO J*. 2011;30(23):4790-4804. doi:10.1038/emboj.2011.378.

63. Franz A, Roque H, Saurya S, Dobbelaere J, Raff JW. CP110 exhibits novel regulatory activities during centriole assembly in Drosophila. *J Cell Biol*. 2013;203(5):785-799. doi:10.1083/jcb.201305109.

64. Spektor A, Tsang WY, Khoo D, Dynlacht BD. Cep97 and CP110 Suppress a Cilia Assembly Program. *Cell*. 2007;130(4):678-690. doi:10.1016/j.cell.2007.06.027.

65. Delgehyr N, Rangone H, Fu J, et al. Klp10A, a microtubule-depolymerizing kinesin-13, cooperates with CP110 to control drosophila centriole length. *Curr Biol*. 2012;22(6):502-509. doi:10.1016/j.cub.2012.01.046.

66. Saurya S, Roque H, Novak ZA, Wainman A, Mustafa G. Drosophila Ana1 is required for centrosome assembly and centriole elongation. 2016;(May):2514-2525. doi:10.1242/jcs.186460.

67. Fu J, Glover D. How the newborn centriole becomes a mother. *Cell Cycle*. 2016;4101(July):1-2. doi:10.1080/15384101.2016.1164566.

68. Fu J, Glover DM. Structured illumination of the interface between centriole and peri-centriolar material. *Open Biol*. 2012;2(8):120104. doi:10.1098/rsob.120104.

69. Lawo S, Hasegan M, Gupta GD, Pelletier L. Subdiffraction imaging of centrosomes reveals higher-order organizational features of pericentriolar material. *Nat Cell Biol*.

2012;12(1):308-317. doi:10.1038/ncb2591.

70. Mennella V, Keszthelyi B, McDonald KL, et al. Subdiffraction-resolution fluorescence microscopy reveals a domain of the centrosome critical for pericentriolar material organization. *Nat Cell Biol*. 2012;14(11):1159-1168. doi:10.1038/ncb2597.

71. Mennella V, Agard DA, Huang B, Pelletier L. Amorphous no more: Subdiffraction view of the pericentriolar material architecture. *Trends Cell Biol*. 2014;24(3):188-197. doi:10.1016/j.tcb.2013.10.001.

72. Gopalakrishnan J, Mennella V, Blachon S, et al. Sas-4 provides a scaffold for cytoplasmic complexes and tethers them in a centrosome. *Nat Commun*. 2011;2(May):359. doi:10.1038/ncomms1367.

73. Zheng X, Gooi LM, Wason A, et al. Conserved TCP domain of Sas-4/CPAP is essential for pericentriolar material tethering during centrosome biogenesis. *Proc Natl Acad Sci U S A*. 2014;111(3):E354-E363. doi:10.1073/pnas.1317535111.

74. Santamaria A, Wang B, Elowe S, et al. The Plk1-dependent phosphoproteome of the early mitotic spindle. *Mol Cell Proteomics*. 2011;10(1):M110.004457. doi:10.1074/mcp.M110.004457.

75. Conduit PT, Feng Z, Richens JH, et al. The centrosome-specific phosphorylation of Cnn by Polo/Plk1 drives Cnn scaffold assembly and centrosome maturation. *Dev Cell*. 2014;28(6):659-669. doi:10.1016/j.devcel.2014.02.013.

76. Lee K, Rhee K. PLK1 phosphorylation of pericentrin initiates centrosome maturation at the onset of mitosis. *J Cell Biol*. 2011;195(7):1093-1101. doi:10.1083/jcb.201106093.

77. Gomez-Ferreria MA, Bashkurov M, Helbig AO, et al. Novel NEDD1 phosphorylation sites regulate γ-tubulin binding and mitotic spindle assembly. *J Cell Sci*. 2012;125(Pt

16):3745-3751. doi:10.1242/jcs.105130.

78. Giansanti MG, Bucciarelli E, Bonaccorsi S, Gatti M. Drosophila SPD-2 Is an Essential Centriole Component Required for PCM Recruitment and Astral-Microtubule Nucleation. *Curr Biol*. 2008;18(4):303-309. doi:10.1016/j.cub.2008.01.058.

79. Dix CI, Raff JW. Drosophila Spd-2 Recruits PCM to the Sperm Centriole, but Is Dispensable for Centriole Duplication. *Curr Biol*. 2007;17(20):1759-1764. doi:10.1016/j.cub.2007.08.065.

80. Scrofani J, Sardon T, Meunier S, Vernos I. Microtubule nucleation in mitosis by a RanGTP-dependent protein complex. *Curr Biol*. 2015;25(2):131-140. doi:10.1016/j.cub.2014.11.025.

81. Choi YK, Liu P, Sze SK, Dai C, Qi RZ. CDK5RAP2 stimulates microtubule nucleation by the ??-tubulin ring complex. *J Cell Biol*. 2010;191(6):1089-1095. doi:10.1083/jcb.201007030.

82. Firat-Karalar EN, Rauniyar N, Yates JR, Stearns T. Proximity interactions among centrosome components identify regulators of centriole duplication. *Curr Biol*. 2014;24(6):664-670. doi:10.1016/j.cub.2014.01.067.

83. Rogers GC, Rusan NM, Roberts DM, Peifer M, Rogers SL. The SCF Slimb ubiquitin ligase regulates Plk4/Sak levels to block centriole reduplication. *J Cell Biol*. 2009;184(2):225-239. doi:10.1083/jcb.200808049.

84. Bettencourt-Dias M, Rodrigues-Martins A, Carpenter L, et al. SAK/PLK4 is required for centriole duplication and flagella development. *Curr Biol*. 2005;15(24):2199-2207. doi:10.1016/j.cub.2005.11.042.

85. Kleylein-Sohn J, Westendorf J, Le Clech M, Habedanck R, Stierhof Y-D, Nigg E a. Plk4-

induced centriole biogenesis in human cells. *Dev Cell*. 2007;13(2):190-202. doi:10.1016/j.devcel.2007.07.002.

86. Sillibourne JE, Bornens M. Polo-like kinase 4: the odd one out of the family. *Cell Div*. 2010;5:25. doi:10.1186/1747-1028-5-25.

87. Klebba JE, Buster DW, Nguyen AL, et al. Polo-like kinase 4 autodestructs by generating its slimb-binding phosphodegron. *Curr Biol*. 2013;23(22):2255-2261. doi:10.1016/j.cub.2013.09.019.

88. Holland AJ, Fachinetti D, Zhu Q, et al. The autoregulated instability of Polo-like kinase 4 limits centrosome duplication to once per cell cycle. *Genes Dev*. 2012;26(24):2684-2689. doi:10.1101/gad.207027.112.

89. Holland AJ, Lan W, Niessen S, Hoover H, Cleveland DW. Polo-like kinase 4 kinase activity limits centrosome overduplication by autoregulating its own stability. *J Cell Biol*. 2010;188(2):191-198. doi:10.1083/jcb.200911102.

90. Guderian G, Westendorf J, Uldschmid A, Nigg EA. Plk4 trans-autophosphorylation regulates centriole number by controlling betaTrCP-mediated degradation. *J Cell Sci*. 2010;123(Pt 13):2163-2169. doi:10.1242/jcs.068502.

91. Varmark H, Llamazares S, Rebollo E, et al. Asterless Is a Centriolar Protein Required for Centrosome Function and Embryo Development in Drosophila. *Curr Biol*. 2007;17(20):1735-1745. doi:10.1016/j.cub.2007.09.031.

92. Lee K, Rhee K. Separase-dependent cleavage of pericentrin B is necessary and sufficient for centriole disengagement during mitosis. *Cell Cycle*. 2012;11(13):2476-2485. doi:10.4161/cc.20878.

93. Tsou MFB, Wang WJ, George KA, Uryu K, Stearns T, Jallepalli P V. Polo Kinase and

Separase Regulate the Mitotic Licensing of Centriole Duplication in Human Cells. *Dev Cell*. 2009;17(3):344-354. doi:10.1016/j.devcel.2009.07.015.

94. Kim J, Lee K, Rhee K. PLK1 regulation of PCNT cleavage ensures fidelity of centriole separation during mitotic exit. *Nat Commun*. 2015;6:10076. doi:10.1038/ncomms10076.

95. J L, P H, V M, Khodjakov A. Control of Daughter Centriole assembly by the Pericantriolar Material. *Nat Cell Biol*. 2008;10(3):322-328. doi:10.1126/scisignal.2001449.Engineering.

96. Loncarek, J; Hergert, P; Khodjakov A. Centriole reduplication during prolonged interphase requires procentriole maturation governed by Plk1: *Curr Biol*. 2011;20(14):1277-1282. doi:10.1016/j.cub.2010.05.050.Centriole.

97. Pagan JK, Marzio A, Jones MJK, et al. Degradation of Cep68 and PCNT cleavage mediate Cep215 removal from the PCM to allow centriole separation, disengagement and licensing. *Nat Cell Biol*. 2015;17(1):31-43. doi:10.1038/ncb3076.Degradation.

98. Peel N, Stevens NR, Basto R, Raff JW. Overexpressing Centriole-Replication Proteins In Vivo Induces Centriole Overduplication and De Novo Formation. *Curr Biol*. 2007;17(10):834-843. doi:10.1016/j.cub.2007.04.036.

99. Zitouni S, Nabais C, Jana SC, Guerrero A, Bettencourt-Dias M. Polo-like kinases: structural variations lead to multiple functions. *Nat Rev Mol Cell Biol*. 2014;15(7):433-452. doi:10.1038/nrm3819.

100. Archambault V, Lépine G, Kachaner D. Understanding the Polo Kinase machine. *Oncogene*. 2015;(November 2014):1-9. doi:10.1038/onc.2014.451.

101. Slevin LK, Nye J, Pinkerton DC, Buster DW, Rogers GC, Slep KC. The structure of the Plk4 cryptic polo box reveals two tandem polo boxes required for centriole duplication.

Structure. 2012;20(11):1905-1917. doi:10.1016/j.str.2012.08.025.

102. Klebba JE, Buster DW, McLamarrah TA, Rusan NM, Rogers GC. Autoinhibition and relief mechanism for Polo-like kinase 4. *Proc Natl Acad Sci U S A*. 2015;112(7):E657-E666. doi:10.1073/pnas.1417967112.

103. Hutchinson D, Ho V, Dodd M, Dawson HN, Zumwalt AC, Colton CA. Direct Binding of SAS-6 to ZYG-1 Recruits SAS-6 to the Mother Centriole for Cartwheel Assembly. *Dev Cell*. 2013;148(4):825-832. doi:10.1038/jid.2014.371.

104. Puklowski A, Homsi Y, Keller D, et al. The SCF-FBXW5 E3-ubiquitin ligase is regulated by PLK4 and targets HsSAS-6 to control centrosome duplication. *Nat Cell Biol*. 2011;13(8):1004-1009. http://dx.doi.org/10.1038/ncb2282.

105. Strnad P, Leidel S, Vinogradova T, Euteneuer U, Khodjakov A, Gönczy P. Regulated HsSAS-6 Levels Ensure Formation of a Single Procentriole per Centriole during the Centrosome Duplication Cycle. *Dev Cell*. 2007;13(2):203-213. doi:10.1016/j.devcel.2007.07.004.

106. Khire A, Vizuet AA, Davila E, Avidor-Reiss T. Asterless Reduction during Spermiogenesis Is Regulated by Plk4 and Is Essential for Zygote Development in Drosophila. *Curr Biol*. 2015;25(22):2956-2963. doi:10.1016/j.cub.2015.09.045.

107. Galletta BJ, Jacobs KC, Fagerstrom CJ, Rusan NM. Asterless is required for centriole length control and sperm development. *J Cell Biol*. 2016;213(4):435-450. doi:10.1083/jcb.201501120.

108. Galletta BJ, Fagerstrom CJ, Schoborg TA, et al. *A Detailed Centrosome Interactome Provides Insight into Organelle Assembly and Human Disease*.

109. Kitagawa D, Kohlmaier G, Keller D, et al. Spindle positioning in human cells relies on

proper centriole formation and on the microcephaly proteins CPAP and STIL. *J Cell Sci*. 2011;124(Pt 22):3884-3893. doi:10.1242/jcs.089888.

110. Hsu W Bin, Hung LY, Tang CJC, Su CL, Chang Y, Tang TK. Functional characterization of the microtubule-binding and -destabilizing domains of CPAP and d-SAS-4. *Exp Cell Res*. 2008;314(14):2591-2602. doi:10.1016/j.yexcr.2008.05.012.

111. Hatzopoulos GN, Erat MC, Cutts E, et al. Structural analysis of the G-box domain of the microcephaly protein CPAP suggests a role in centriole architecture. *Structure*. 2013;21(11):2069-2077. doi:10.1016/j.str.2013.08.019.

112. Cutts EE, Inglis A, Stansfeld PJ, Vakonakis I, Hatzopoulos GN. The centriolar protein CPAP G-box: an amyloid fibril in a single domain. *Biochem Soc Trans*. 2015;43(5):838-843. doi:10.1042/BST20150082.

113. Zi Yang, David e Stone SWL. Prion promoted phosphorylation of heterologous amyloid is coupled with ubiquitin-proteasome system inhibition and toxicity. *Mol Microbiol*. 2014;93(5):1043-1056. doi:10.1111/mmi.12716.Prion.